Summer 8-3-2013

The Addition of Melatonin to 17beta-Estradiol and Progesterone Modulated Markers Relevant to Mammary Tumor Development and Modulated Steroid Receptors Relevant to Uterine Protection in a Mouse Model of Breast Cancer

Corry Dominic Bondi

THE ADDITION OF MELATONIN TO 17β-ESTRADIOL AND PROGESTERONE MODULATED MARKERS RELEVANT TO MAMMARY TUMOR DEVELOPMENT AND MODULATED STEROID RECEPTORS RELEVANT TO UTERINE PROTECTION IN A MOUSE MODEL OF BREAST CANCER

A Dissertation

Submitted to the Mylan School of Pharmacy

Duquesne University

In partial fulfillment of the requirements for

the degree of Doctor of Philosophy

By

Corry Dominic Bondi

August 2013

THE ADDITION OF MELATONIN TO 17β-ESTRADIOL AND PROGESTERONE MODULATED MARKERS RELEVANT TO MAMMARY TUMOR DEVELOPMENT AND MODULATED STEROID RECEPTORS RELEVANT TO UTERINE PROTECTION IN A MOUSE MODEL OF BREAST CANCER

By

Corry Dominic Bondi

Approved May 15, 2013

Paula Witt-Enderby, Ph.D.
Professor of Pharmacology
(Committee Chair)

David A. Johnson, Ph.D.
Associate Professor of Pharmacology
Division Head of Pharmaceutical Sciences
(Committee Member)

Jane Cavanaugh, Ph.D.
Assistant Professor of Pharmacology
(Committee Member)

Rehana Leak, Ph.D.
Assistant Professor of Pharmacology
(Committee Member)

J. Douglas Bricker, Ph.D.
Dean, Mylan School of Pharmacy
Professor of Pharmacology

Melissa Melan, Ph.D.
Division of Molecular Diagnostics
University of Pittsburgh Medical Center
(Committee Member)

ABSTRACT

THE ADDITION OF MELATONIN TO 17β-ESTRADIOL AND PROGESTERONE MODULATED MARKERS RELEVANT TO MAMMARY TUMOR DEVELOPMENT AND MODULATED STEROID RECEPTORS RELEVANT TO UTERINE PROTECTION IN A MOUSE MODEL OF BREAST CANCER

By

Corry Dominic Bondi

August 2013

Dissertation supervised by Paula Witt-Enderby, Ph.D.

The use of hormone replacement therapy (HRT) is important to relieve menopausal symptoms. However, HRT use declined after an increased risk of breast cancer was reported by the Women's Health Initiative. With the ultimate goal of developing a novel replacement therapy to relieve menopausal symptoms without increasing the risk of breast cancer, we postulated that a novel replacement therapy containing 17β-estradiol (E2) and half the recommended dose of progesterone (P4) along with nocturnal melatonin supplementation (EPMRT) would be protective against mammary tumor development. Previously, in a mouse model of HER2+ breast cancer, our laboratory demonstrated that EPMRT was protective against mammary cancer by increasing mammary tumor latency, decreasing tumor incidence and weight, and decreasing gross lung metastases while not increasing uterine weight. A pre-tumor study was conducted to gain insight into these protective effects. Randomized, non-ovariectomized, 60-day old female MMTV/unactivated *Neu* mice were provided therapies comprised of E2 and P4, with or without nocturnal melatonin supplementation, given continually for 30 days. To investigate actions on mammary tissues, whole mount, microarray, and real-time RT-PCR analyses were performed. To assess impact on the uterus, uterine wet weight, luminal epithelial height, estrogen receptor (ERα) and progesterone receptor (PR) expression, as well as Ki67 expression were performed. Tertiary side-branching, the initial step in the process of mammary ductal differentiation, was significantly increased by Melatonin and EPMRT as compared to Control. Also, EPMRT displayed significantly decreased expression of the cancer-related genes encoding amphiregulin and indoleamine 2, 3-dioxygenase. In the uterus, there were no differences detected in wet weight, luminal epithelial height, and proliferation. Also, there was no effect on serum E2 or P4 levels; however, EPMRT increased the time in estrus. Moreover, the increase in expression of aromatase mRNA by low dose P4 was abolished by increasing doses of P4 and by addition of melatonin. Overall, these data provide important insight into the protective actions of EPMRT on *Neu*-induced mammary cancer. These findings provide a rationale for future investigations with the ultimate goal of having women use this novel therapy to relieve menopausal symptoms while providing protective actions on the breast and the uterus.

DEDICATION

For Bianca Dominique – with love

Your Father

ACKNOWLEDGEMENT

My acknowledgement to the *Susan G. Komen for the Cure* for providing the financial resources that allowed me to explore the research questions. I want to thank, first and foremost, *Paula Witt-Enderby, Ph.D.* for her mentorship during this journey. My deepest gratitude. I want to extent my appreciation to my dissertation committee members: *David A. Johnson, Ph.D., Jane Cavanaugh, Ph.D., Rehana Leak, Ph.D., Melissa Melan, Ph.D.* for their active participation during and beyond the committee meetings. Also, I want to thank them for their thoughtful suggestions that improved my research. I enjoyed being your student. During my graduate years at Duquesne University, I received support from a number of talented individuals, from inside and outside the University, including: *Vicki Davis, Ph.D., Jose Sanchez-Barcelo, Ph.D., Mary Kotlarczyk, Ph.D., Bill Clafshenkel, Ph.D., Shalini Sethi, Ph.D., Bala Dodda, Ph.D., Katie Gallagher, Pharm.D, Jeffrey Barnes, Ph.D., Fredyne Springer, Peter White, Ph.D., David Newsom, Joseph McCormick, Ph.D., Faculty members of Duquesne University, and the Animal care staff.*

TABLE OF CONTENTS

LIST OF TABLES

LIST OF FIGURES

BACKGROUND

As a woman progresses through life, changes in her hormone levels, specifically estrogen, progesterone (P4), and melatonin, produce symptoms such as hot flashes, vaginal atrophy, sleep disturbances, anxiety, and depression [1, 2]. These symptoms can be debilitating and leads her to seek relief. A therapy prescribed to women for relief of these symptoms, especially hot flashes, is hormone replacement therapy (HRT). Clinically, HRT is used to restore the hormone balance lost during menopause, a state characterized by estrogen deficiency resulting from the loss of ovarian function. In addition to alleviating menopausal symptoms (i.e., hot flashes and vaginal atrophy), HRT is used to reduce the risk of heart disease, osteoporosis, and to improve mood, thereby, improving quality of life within this population [1].

As more and more women were taking HRT for relief of menopausal symptoms, a randomized, placebo-controlled study was established called the Women's Health Initiative (WHI) to investigate the health risks and benefits of HRT in postmenopausal women ages 50 to 79. This study used a common HRT, PREMPRO® (formally Wyeth Ayerst, Collegeville, PA), that contains conjugated equine estrogens (CEE) combined with medroxyprogesterone acetate (MPA). The results revealed that women taking PREMPRO® had an increased risk in developing breast cancer [3-5]. Following the initial reports from the WHI, the use of HRT declined dramatically in the United States [1] impacting negatively a menopausal woman's quality of life.

The increase risk of breast cancer with the combined therapy, that is HRT therapies containing both an estrogen and a progestogen, is controversial. The WHI revealed that PREMPRO® increased the risk of breast cancer [6]; however, the E3N prospective cohort study of postmenopausal, metropolitan French women revealed that 17β-estradiol (E2) plus P4 did not increase the risk of breast cancer. Moreover, the type of progestogen included along with E2 may be an important contributor to the increased risk of breast cancer. E2 plus dydrogesterone was not associated with an increase in risk of breast cancer; but, E2 plus other progestogens such as nomegestrol acetate and promegestone were associated with an increase in risk [7]. Also, in another study, combination therapies with norethindrone acetate increased the risk breast cancer as compared to MPA when used for more than 5 years [8]. In a postmenopausal primate model, E2 combined with micronized P4 did not increase Ki67 expression, an indicator of DNA synthesis, in lobular and ductal breast epithelium as compared to placebo; however, E2 combined with MPA increased Ki67 expression indicating an increase in DNA synthesis and cell proliferation [9]. Women taking PREMARIN® (CEE) demonstrated a decreased risk of breast cancer suggesting a possible association of progestogens in increasing this risk. However, the results of the WHI were in contrast to the E3n study that revealed a 1.3 fold increase in breast cancer risk associated with the use of E2 alone [7, 10, 11]. These studies suggest that the progestogen component of the HRT may be an important contributor to the associated increased the risk of breast cancer.

In addition to the type of hormones used in the HRT, the doses of these hormones, time of initiation of therapy, and length of exposure were found to be important as well. The authors of the Endocrine Society Scientific Statement urge that "continued research on the lowest doses … is necessary [1]." Thus, doses of HRT should be at the lowest effective dose that provides symptom relief. For example, 0.5mg of micronized oral E2 provided relief from hot flashes [12] so this low dose should be considered versus higher doses for menopausal symptom relief. The length of exposure and initiation of therapies were critical to the development of breast cancer. For example, P4 usage for five years or less, as a component of an HRT, may not increase breast cancer risk [13, 14]. However, women taking estrogen alone or E2 plus progestogen therapies closer to menopause had an increased risk of breast cancer compared to women with a longer gap time [14]. Moreover, women taking PREMPRO® who were closer to menopause (less than five years) were at a somewhat greater risk compared to women taking PREMPRO® who were more than five years after menopause [3]. Therefore, the timing of HRT use as it relates to menopause, the duration of usage, and the dose of HRT all seem to contribute to the risk of breast cancer, but the data are unclear.

With the ultimate goal of relieving menopausal symptoms without increasing the risk of breast cancer and offering uterine protection, we postulated that a novel, HRT containing E2 and half the recommended dose of P4 along with nocturnal melatonin supplementation (EPMRT) would not increase and could potentially decrease mammary tumor development and be uterine protective in a mouse model of HER2+ breast cancer. Half the clinically recommended dose of P4 was used to assess if the reduced dose would decrease mammary cancer development in our mouse model even though this P4 dose may not be sufficient to reduce E2-mediated uterine stimulation. However, because melatonin has both anti-estrogenic and anti-cancer actions in the body, it is hypothesized that nocturnal melatonin supplementation will prevent mammary tumor development and protect the uterus from excessive estrogen exposure.

In another study assessing the efficacy of EPMRT on mammary cancer in this same model, our laboratory demonstrated that EPMRT was protective against mammary cancer by increasing tumor latency, decreasing tumor incidence, decreasing tumor weight, and by decreasing gross lung metastases while remaining uterine protective [15]. Together, these results indicate that EPMRT provided a protective action in the mammary gland, as well as inhibited effects on the uterus even though half the recommended dose of P4 was used. The possible early events (i.e., pre-tumor) underlying the protective effects of EPMRT are unknown. Therefore, the results described herein may provide insight into the protective actions of EPMRT on mammary tumorigenesis and against excessive uterine proliferation in order to advance the future use of EPMRT in women experiencing menopausal symptoms.

HYPOTHESIS and SPECIFIC AIMS

Hypothesis

The addition of melatonin to 17β-estradiol and half the clinically recommended dose of progesterone will modulate markers relevant to mammary tumor development and uterine protection in female MMTV/unactivated *Neu* mice.

Specific Aim 1

To determine estrogen, progesterone, and/or melatonin effects on mammary ductal development and gene expression which are relevant to mammary tumor development in female MMTV/unactivated *Neu* mice.

Specific Aim 2

To determine estrogen, progesterone, and/or melatonin effects on uterine weight, cellular hypertrophy and proliferation, and ERα and PRA expression which are relevant to uterine protection in female MMTV/unactivated *Neu* mice.

INTRODUCTION

Cancer

Hippocrates used the word "Cancer" to describe diseases in which tissues grow and spread throughout the body. Cancer develops from disruptions in the homeostatic balance between the rate of cell division, and the rate of cell differentiation and loss possibly due to factors such as radiation or chemical exposures, heredity, and viruses. Therefore, the homeostatic balance is shifted toward greater cell division due to a loss of growth control that results in tumor formation. Malignant tumors (i.e., cancer) are life-threatening because tumor cells can invade surrounding tissues and metastasize to other parts of the body. Depending on the origin of the tumor cell type, cancers are categorized as carcinomas (originating from epithelial tissues), sarcomas (originating in supporting tissues of mesodermal origin), and lymphomas (originating from lymphatic and blood cells) [16].

Cellular proto-oncogenes (e.g., unactivated *Neu* in this study) are normal cellular genes that can be converted into oncogenes by various mechanisms including, but not limited to, mutations (e.g. point or frame deletions), amplification (i.e., an increase in gene copy number), insertional mutagenesis (e.g., an integrated retrovirus), DNA rearrangement, or chromosomal translocation. Therefore, the conversion of a proto-oncogene to an oncogene produces proteins that are structurally abnormal or over-expressed [16]. Oncogenes encode proteins involved in growth control, such as receptor tyrosine kinases (e.g., mouse ERBB2 receptor and human HER2/ERBB2 receptor). Through the expression of these proteins, oncogenes disrupt normal growth control by induction of cell proliferative, anti-apoptotic, and/or pro-survival pathways.

Breast cancer

According to the National Cancer Institute, breast cancer is defined as "cancer that forms in tissues of the breast, usually the ducts (tubes that carry milk to the nipple) and lobules (glands that make milk) [17]" with the former being the most prevalent. Ductal carcinoma in situ (DCIS) is the most common of the non-invasive cancers with 60,000 newly diagnosed cases each year at a rate of 1 out of every 5 cases. DCIS has not metastasized and originates from the epithelial tissue lining the milk ducts. However, invasive ductal carcinoma (IDC) is the most prevalent form of invasive breast cancer with 180,000 new diagnoses each year and is more common in women over 55 [18] .

Breast cancer statistics

Breast cancer is the most commonly diagnosed cancer and ranks second in overall cancer-related deaths of women in the United States [19]. During 2012, an estimated 226,870 women will be diagnosed with breast cancer (i.e., 26% of new cases each year) and 39,510 are expected to die from this malignancy. The median age at diagnosis is 61 years, and as of January 1, 2009, over 2.7 million women living in the U.S. have a history of breast cancer [19, 20]. With breast cancer having such a negative impact on national public health, scientific research into ways to reduce the development of this cancer is paramount.

The age-adjusted incidence for all races was 124.3 per 100,000 women per year with incidence ranked by race from highest to lowest: White > Black > Asian / Pacific Islander > American Indian / Alaska Native > Hispanic. The median age of death was 68 with the highest percentage of mortality between 55 to 84 years and the age-adjusted death rate of 23.0 per 100,000 women per year. For the years 2002 to 2008, the 5-year relative survival was 89.0%; however, the survival was greater for white women than black women (i.e., a difference of 12.6%) [20].

Early detection and diagnosis is important for an overall 5-year relative survival. The stage distribution and the 5-year relative survival by stage at diagnosis are as follows: 60% are diagnosed as Localized with a 98.4% survival; 33% are diagnosed as Regional (i.e., spread to regional lymph nodes) with a 83.9% survival; 5% are diagnosed as Distant (i.e., metastasized) with 23.8% survival; and 2% are diagnosed as Unknown with a 50.7% survival. The overall lifetime risk, as calculated from rates between 2007 to 2009, is 12.48%. Based on these data, 1 in 8 women born today will be diagnosed with breast cancer during their lifetime with the highest risk (i.e., 3.45% or 1 in 29) occurring from age 60 to 69 [20].

Risk factors

There are multiple risk factors that contribute to the development of breast cancer such as age, family history, lack of or late parity, age of first menarche, late menopause, and exogenous hormone exposures from HRT [21, 22]. Moreover, other exposures may include high fat diet, pharmaceuticals, food additives, and environmental pollutants [23-26]. Interestingly, a study investigating breast cancer development in identical twins suggests that 27% of breast cancer has a genetic component while 73% may result from unknown environmental exposures [27].

HER2+ breast cancer

In women, amplification of the *ERBB2* gene, which encodes the HER2 receptor that belongs to the epidermal growth factor receptor family, as well as increased HER2 receptor expression, is demonstrated in up to two-thirds of in situ ductal and one-third of invasive ductal breast cancers [28-31]. *ERBB2* amplification occurs in about 20% to 30% of primary breast cancers and subsequent HER2 receptor over-expression impacts negatively on prognosis [32]. Clinically, various methods are used to detect *ERBB2* amplification or HER2 receptor expression. Fluorescence in-situ hybridization (FISH) assesses *ERBB2* amplification and is considered the more precise, accurate, and reproducible test. The Dako "Herceptest," a semi-quantitative immunohistochemical test, assesses receptor over-expression based on intensity and completeness of membrane staining [33, 34].

Breast cancer treatments

The most common form of treatment for DCIS is a lumpectomy followed by radiation therapy; however, mastectomy or hormonal therapy may also be utilized for treatment. Treatments for IDC are broader based and include surgery (e.g., mastectomy), radiation, chemotherapy, anti-hormonal, and biopharmaceutical agents. Chemotherapies include various classes of antineoplastic agents such as alkylating (e.g., cyclophosphamide) and intercalating agents (e.g., doxorubicin and epirubicin) that inhibit DNA replication, antimetabolite and antifolate agents (e.g., capecitabine, 5-fluorouracil, and methotrexate) that inhibit RNA and DNA syntheses, as well as agents (e.g., docetaxel and paclitaxel) that inhibit microtubule disassembly leading to cell-cycle arrest [35]. Anti-hormonal therapies include selective estrogen receptor modulators (e.g., tamoxifen), aromatase inhibitors (e.g., anastrozole), estrogen receptor down-regulators (e.g., fulvestrant) and estrogen reducers (e.g., goserelin). Biopharmaceutical agents include targeting the HER2 receptor by use of monoclonal antibodies (e.g., trastuzumab), or by use of HER2 activated kinase inhibitors (e.g., lapatinib). The other therapies are directed towards the HER2/HER3 heterodimers (e.g., pertuzumab), or by inhibiting angiogenesis with VEGF inhibition (e.g., bevacizumab) [36].

Hormone replacement therapy

Hormone replacement therapy (HRT) is given clinically to women to replenish the hormone reduction that occurs during menopause. The rationale for using HRT is primarily to reduce menopausal symptoms of hot flashes and vaginal atrophy as well as to reduce the risk heart disease, colon cancer, and osteoporosis [1]. HRT consists of two main types: an estrogen alone replacement therapy or an estrogen plus progestogen replacement therapy. Even though the current consensus is that estrogen alone therapy reduces breast cancer risk, one problem with this therapy is the increased risk of endometrial hyperplasia and type I endometrial cancer [1, 6]; therefore, the addition of a progestogen counteracts the hyperplastic actions of estrogen resulting in no increased risk of endometrial cancer [1, 6, 37].

In the United States, the most widely prescribed progestogen, until recently, was the progestin, MPA [38] primarily as a combined therapy with CEE (i.e., PREMPRO®). Outside of the United States, other combinations of HRT are used; for example, in France, the estrogen component is predominately E2 combined with one of the various progestogens, such as P4 and dydrogesterone [7].

Women's Health Initiative and other studies

HRT has been used in clinical practice for many years and is known to be beneficial for cardiovascular health [39], prevention of osteoporosis [40] as well as for relief of menopausal symptoms [1]. Therefore, a definitive assessment of HRT was proposed under direct impetus of the late Dr. Bernadine Healy, then Director of the U.S.

National Institutes of Health [6]. In response, the WHI was established to conduct two large, full-scale, randomized, placebo-controlled trials in postmenopausal women aged 59 to 79 years with one study using PREMARIN® (i.e., estrogen-only replacement therapy) in postmenopausal women with a previous hysterectomy and the other study using PREMPRO® (i.e., estrogen-progestin combination therapy) in postmenopausal women with an intact uterus [6].

The randomized, placebo-controlled study with PREMPRO® was stopped after a mean of 5.6 years because health risks exceeded benefits. Moreover, this study revealed an increased risk of invasive breast cancer in addition to having a higher risks of heart disease, stroke, and blood clots [4, 5, 41]. However, the increased risk of breast cancer declined after discontinuing HRT [41, 42]. Follow-up results revealed that PREMPRO® increased mortality, invasive breast cancer incidence, and lymph node-positive cancers. In the Million Women Study, an increase in mortality in women diagnosed with breast cancer while using estrogen plus progestin therapy was observed [43]. However, it was also observed that a 40% reduction in mortality occurred in trials in which the mean age was less than 60 years and within ten years of menopause onset [1]. Furthermore, women taking PREMPRO® who were closer to menopause (less than five years) were at somewhat greater risk for breast cancer compared to women taking PREMPRO® who were five years or more since menopause [3]. A greater risk of developing breast cancer was also observed in the French E3N prospective cohort study as to the use of HRT closer to menopause [14].

Results from randomized clinical trials suggest that estrogen alone therapy reduces breast cancer incidence while estrogen plus progestin increases breast cancer incidence and death [6]. However, within the last decade, it was believed that estrogen alone therapy as well as estrogen plus progestin therapy increased the incidence of breast cancer; however, estrogen alone therapy required longer exposure than the combination [6]. In the WHI, estrogen-only therapy in postmenopausal women who had a hysterectomy resulted in a reduced risk of breast cancer [10], while many observational studies contradicted this finding [7, 43-47]. However, in the other arm of the WHI, women taking the combination therapy, PREMPRO®, had an increased risk of breast cancer [4]. In response to WHI findings, the use of PREMPRO® and PREMARIN® in the United States declined [48]. Even though HRT increased the risk of breast cancer [4, 5] and is classified as a known carcinogen based on the results of the WHI as well as in observational studies [49], HRT is beneficial for improving the quality of life of women suffering from hot flashes and vaginal atrophy. For example, a risk and benefit analysis revealed that there was a greater benefit achieved by use of this therapy compared to the relative risk. In this analysis, it was observed that per 1000 women per five years of HRT use, 800-900 women would receive benefit from an improvement in menopausal symptoms (i.e., hot flashes and vaginal atrophy, respectively) while approximately 7.5 women would be at risk for breast cancer [1].

Melatonin synthesis

Melatonin (i.e., N-acetyl-5-methoxytryptamine) is known to have important roles in entraining one's sleep/wake cycle, as well as having important roles in reproductive processes [50]. Melatonin is synthesized and secreted by the pineal gland in response to darkness with peak plasma levels occurring approximately at 02:00 hours (2 am) [51, 52]. In response to darkness, the retina, via the retino-hypothalamic tract, sends signals to the suprachiasmatic nucleus (SCN), the master biological clock. Activation of the neurons within the SCN results in the activation of the superior cervical ganglion that then sends signals to the pineal gland to initiate the synthesis of melatonin by inducing the rate-limiting enzyme, serotonin-N-acetyltransferase [53, 54].

The synthesis of melatonin is a two-step process with serotonin as a precursor. During the first step, serotonin, via N-acetylation by the enzyme serotonin-N-acetyltransferase, is converted to N-acetylserotonin. During the second step, N-acetylserotonin, via O-methylation by the enzyme hydroxyindole-O-methyltransferase, is converted to melatonin [54]. By contrast, melatonin synthesis is reduced in response to light via the depolarization of retinal ganglion cells that innervate the SCN thereby reducing sympathetic signaling [53], and light exposure at night inhibits the increase in plasma levels of melatonin through a suppression of the pineal gland [55].

Melatonin synthesis and secretion follows a diurnal rhythm whereby levels are highest during the hours of darkness and lowest during the hours of light. The release of melatonin begins at dusk and persists for eight to sixteen hours depending on the season. Summer months have the shortest duration of melatonin exposure whereas the winter months have the longest duration [56]. Therefore, melatonin receptors are exposed to melatonin for long periods of time during the hours of darkness and during the winter months that may lead to reduced cellular proliferation and enhanced cellular differentiation. For example, chronic exposure to melatonin, in vitro, modulates signaling cascades (i.e., cAMP-dependent or MAPK pathways) leading to reduced cellular proliferation and enhanced cellular differentiation [57-60].

Melatonin production is inhibited in middle and older aged adults to as much as one-eighth as that of young adults [61]. Also, as a woman ages, her levels of melatonin decline especially the nocturnal peak of melatonin. This decline in nocturnal melatonin levels may contribute the sleep disturbances and vasomotor symptoms (i.e., hot flashes) associated with menopause [2].

Melatonin pharmacokinetics

The following summary of information was obtained from Micromedex® 2.0 which compiled the information contained herein from a variety of sources. Melatonin is rapidly absorbed with peak serum levels occurring within one hour. Because of extensive hepatic first pass metabolism, the oral bioavailability is poor in humans (mean 33%), but is higher in rats (53%), dogs, and monkeys (both 100%). Because melatonin is highly lipophilic, it crosses the blood-brain barrier, as well as readily distributes to most tissues including the ovaries. After hepatic metabolism, the primary metabolite of melatonin is 6-hydroxymelatonin, with up to 85% of the given dose excreted in the urine as 6-hydroxymelatonin sulfate. The elimination half-life following an oral dose ranges from 30 to 50 minutes [62].

Melatonin receptors

Melatonin produces its effects independent of receptors via free radical scavenging or through up-regulation of anti-oxidant enzyme and/or in a receptor dependent manner through G-protein coupled receptors. There are two melatonin receptors, MT_1 and MT_2, that are seven transmembrane receptors belonging to the G-protein (i.e., guanine nucleotide-binding protein) coupled receptor family. The activation of melatonin receptors by melatonin results in an inhibition of adenylyl cyclase via pertussis toxin sensitive G-proteins [63]; this results in an inhibition of protein kinase A and the transcription factor, cAMP response element-binding (CREB), thereby reducing gene transcription [56, 64]. Additionally, an activated melatonin receptor may signal via Gq proteins to stimulate phospholipase C (PLC) leading to an increase in phosphoinositide hydrolysis resulting in an increase of intracellular calcium [65]. Also, melatonin, via the melatonin receptors, can activate the MAP kinase signal transduction pathway [58, 59, 66] through β-arrestin scaffolds [57, 60] producing effects on cell proliferation and differentiation.

Melatonin receptor expression

Melatonin receptors have been detected throughout the body including the brain, retina, cardiovasculature, kidney, gut, bone, reproductive organs, and mammary gland [67, 68]. With respect to each melatonin receptor subtype, some tissue specificity has been observed. For example, MT_2 receptors are expressed centrally in the SCN and cortex and peripherally in ovarian granulosa cells, kidney, adipocytes, retina, and blood vessels. MT_1 receptors are expressed centrally in the cerebellum, SCN, and pituitary gland as well as peripherally in ovarian granulosa cells, retina, kidney, pancreas, and blood vessels [68]. Furthermore, endogenous expression of melatonin receptors has been detected in various cell lines. For example, human breast cancer (MCF-7) cells, human prostate cancer (LNCaP) cells, mouse neuroblastoma (N1E-115) cells, as well as human embryonic kidney (HEK-293) cells, express MT_1 receptors while human choriocarcinoma (JAR) cells, various melanocytes and melanoma cells [68], and human adult mesenchymal stem hAMSC cells [58] express MT_2 receptors.

In vitro oncostatic effects of melatonin

Melatonin produces oncostatic effects in vitro and in vivo through multiple mechanisms including its free radical scavenging and antioxidant properties [69, 70], by inhibiting aromatase expression and activity [71], by inhibiting ER-mediated gene expression [72], and through its effects on MAPK signaling pathways. These actions of melatonin lead to a reduction in cellular proliferation [73-77] and an induction in cellular differentiation [59, 66, 78].

Most of the studies to date reveal that the oncostatic effects of melatonin are elicited mostly through anti-estrogen actions. Specifically, melatonin inhibits gonadal estrogen synthesis, down-regulates estrogen receptor (ER) expression, inhibits the binding of the E2-ERα complex to the estrogen response element (ERE), and inhibits aromatase expression and activity [71].

The anti-estrogenic actions result in decreases in cellular proliferation. For example, a physiological concentration of melatonin (1 nM) attenuates proliferation of MCF-7 breast cancer cells by inhibiting the binding of the E2-ERα complex to the ERE [79] resulting in a down-regulation of the cyclin D1 gene [72]. The mechanisms underlying melatonin-mediated inhibition of E2-ERα complex binding to ERE may be through receptor-independent and -dependent pathways. For example, melatonin inhibits the binding of the complex to EREs through an inhibition of calmodulin-sensitive adenylyl cyclases [50]. However, using dominant negative and positive G-proteins, it was found that the suppression of E2-induced ERα transcriptional activity by melatonin occurs through Gαi2 and not Gαq proteins [80]. Also, in serum-starved MCF-7 cells transiently expressing MT_1 receptors, melatonin attenuates E2-induced expression of

BRCA-1, *P53*, *P21(WAF)* and *c-MYC*, and this attenuation by melatonin is enhanced with increasing receptor expression [81].

In addition to blocking the E2-ERα complex to EREs, melatonin (1nM) attenuates aromatase expression and activity in MCF-7 cells [71]. This dose also inhibits steroid sulfatase and 17β-hydroxysteroid dehydrogenase type 1 but stimulates sulfotransferase [82] thereby reducing the conversion of sulfated metabolites to more potent non-sulfated forms of estrogens such as E2 and estrone (E1).

Besides MCF-7 cells, melatonin (100 pM to 100 nM) inhibits cellular proliferation in Chinese hamster ovary cells [73], human neuroblastoma SK-N-SH cells [74], rat hepatoma AH-130 cells [75], rat pheochromocytoma PC-12 cells [76], human mesenchymal stem hAMSC cells [58], mouse embryonic fibroblast NIH-3T3 cells [83], and mouse melanoma S-91 cells. Interestingly, in mouse melanoma S-91 cells, the potency of melatonin to inhibit cell proliferation increases 1000 fold (i.e., EC_{50} = 100 nM to EC_{50} = 100 pM) following stable expression of MT_1 receptors [77]. These studies demonstrate the importance of melatonin activation of melatonin receptors in the inhibition of cellular proliferation.

In many of the aforementioned studies, and concomitant to the anti-proliferative effects of melatonin, increases in cellular differentiation were demonstrated. For example, in Chinese hamster ovary (CHO) or B(E)2C cells, stably expressing melatonin receptors, or in cells endogenously expressing these receptors (e.g., N1E-115 and hAMSC), melatonin induces cellular differentiation as reflected by the induction of outgrowths or the differentiation of hAMSCs into osteoblasts [58, 59, 66, 78]. Also, melatonin (1 nM or 1 mM) induces the differentiation of 3T3-L1 mouse embryonic fibroblasts into an adipocyte-like phenotype [84].

Preclinical oncostatic effects of melatonin

Melatonin inhibits cellular proliferation and induces cellular differentiation in cancer cell in vitro models. Melatonin has also been demonstrated to protect against cancer in vivo using approaches that suppress endogenous melatonin production. Initial studies demonstrate that pinealectomy as well as constant light exposure enhanced chemically-induced mammary carcinogenesis, and exogenous administration of melatonin under the conditions attenuated these effects [85, 86]. Light exposure during the dark phase of the light:dark cycle promotes the uptake of linoleic acid and its metabolism to 13-hydroxyoctadecadienoic acid, a mitogenic signaling molecule, in rat hepatoma (7288CTC) cells and human breast xenographs thereby promoting tumor proliferation. Nocturnal supplementation with melatonin inhibits these processes through melatonin receptor-mediated mechanisms [87]. Furthermore, constant light (0.21 Lux) exposure during the dark phase of a 24-hour light:dark cycle increases the growth of dimethylbenzanthracene (DMBA)-induced mammary adenocarcinomas in female Sprague-Dawley rats; this increase in tumor growth rate was accompanied by lower survival. Examination into the potential mechanisms underlying the increase in tumor growth by constant light exposure at night suggests that low nocturnal melatonin levels and high E2 levels may be involved. In these mice exposed to light at night, levels of serum E2 were higher, vaginal cornification typical of persistent estrus was observed, and a lack of day-night rhythm of melatonin release occurred [88].

These data suggest that mammary tumor growth may be inhibited, in part, due to the anti-estrogenic effects of melatonin. For example, S-23478-1, a melatonin receptor agonist, suppressed N-nitroso-N-methyl-urea-induced mammary tumors in rats via attenuation of ERα expression and signaling [89]. In rats with E2-induced pituitary prolactin secreting tumors, melatonin administration (0.25 mg and 0.50 mg/day/rat for 97 days) inhibits proliferation as well as induces apoptosis [90].

Clinical oncostatic effects of melatonin

In 1978, Cohen, Lippman, and Chabner postulated a relationship between pineal function and estrogen responsive breast cancer [91]. For example, women shift workers exposed to light during the night reveal a higher incidence of breast cancer compared to non-shift workers [92-95]. By contrast, the degree of visual impairment has been correlates inversely with breast cancer incidence [96]; for example, blind women have a low incidence of breast cancer [97, 98]. Whether or not this is due to the oncostatic actions of melatonin alone, through anti-estrogenic actions of melatonin, or both still needs to be determined. However, due to its multiple anti-estrogenic actions, especially the ability to act as a selective estrogen enzyme modulator (SEEM), the use of melatonin as an adjuvant to existing therapies for preventing and treating breast cancer is warranted and is currently being tested clinically [99-101].

Action of melatonin on progesterone and 17β-estradiol

An inverse relationship between melatonin and E2 exists; that is, when melatonin levels are high, E2 levels are low and when melatonin levels are low, E2 levels are high [102]. Besides E2, melatonin also has a relationship with P4 except that levels of melatonin are positively correlated with P4 [102]. The mechanisms underlying the positive relationship between melatonin and P4 could be through the actions of melatonin on granulosa cells. For example, melatonin, at concentrations of 200 pg/mL and 100-400 pg/mL, directly stimulates the secretion of P4 from human and bovine granulosa cells in serum supplemented media, respectively [103]. Moreover, although melatonin exposure has no effect on basal P4 production in human granulosa-luteal cells, melatonin enhances human chorionic gonadotropin (hCG)-stimulated P4 production possibly through melatonin receptors coupled to the MAPK pathway [104]. In bovine granulosa cells, melatonin stimulates P4 production and inhibits E2 biosynthesis in a time-dependent manner [105]. Also, female Wistar rats, sacrificed two months after pinealectomy, have reduced serum levels of P4 and increased serum levels of E2 as well as decreases in progesterone receptor (PR) expression in the ovaries[106]. Finally, in women, melatonin administration (3 mg/day at 22:00 h) during the luteal phase of the menstrual cycle increases serum P4 concentrations [107].

METHODS

Drugs

Progesterone [57-83-0] (#57830), 17β-estradiol [50-28-2] (#2758) and melatonin [73-31-4] (#5250) were purchased from Sigma-Aldrich (St. Louis, MO).

Rationale for use of model

The use of transgenic mouse models has revealed that transgenes participate and activate oncogenic pathways involved in neoplastic progression. The key features are summarized by these five rules as directly quoted from Cardiff: 1) "Mammary development is related to the type and amount of transgene expressed;" 2) "dysplasias and tumors develop from secondary mutations;" 3) "the transgenes determine tumor phenotype;" 4) "transgenes may activate dominant oncogenic pathways;" and 5) "the oncogenic pathway determines prognosis [108]."

The mouse mammary tumor virus (MMTV) belongs to the *Retroviridae* family. A retrovirus (i.e., RNA virus) encodes the enzyme, reverse transcriptase, which catalyzes the synthesis of DNA from an RNA template resulting in the formation of a provirus. The provirus is integrated into the host's genome and replicated. In mice, the MMTV replicates in the alveolar epithelial cells of the mammary gland [109]. In MMTV/unactivated *Neu* transgenic mice, rat *Neu* transcripts, in addition to the mammary gland, are also detected in the salivary glands, spleen, thymus, and lungs [110].

MMTV mouse models are relevant for the study of breast cancer because of the latency, histology, and invasiveness of the mammary tumors. Sacco et al. 2003 presented an eloquent description of the relevance of one of the MMTV models (i.e., the MMTV/activated *Neu*) to human breast cancer. Taking the liberty of quoting directly;

"Breast tumors in MMTV-*Neu* mice occur spontaneously, over-express the *Neu* oncogene, escape the immune system, grow in situ and adapt to the microenvironment, recruit vessels, invade the tissues, penetrate the vasculature, and give rise to distant metastases [111]."

The FVB/N strain of mice are descendants of an outbred colony of Swiss mice N:GP (i.e., NIH general purpose mouse) established in 1935. The FVB/N are favorable for transgenic generation because of large litter size (e.g., mean 9.5), large and prominent pronuclei of the zygote that facilitates microinjection of DNA, as well as a high percentage (i.e., 74%) of embryo survival after injection resulting in an increased birth number compared with other mouse strains [112]. FVB/N mice do not form spontaneous tumors and at 24 months of age have no detectable mammary carcinomas [112, 113]. However, transgenic FVB/N female mice, expressing the rat *Neu* proto-oncogene under the transcriptional control of the MMTV promoter, demonstrate decreased mammary tumor latencies compared to transgenic C56BL/6 females expressing the same transgene under the control of the MMTV promoter (i.e., between 7 to 12 months compared to > 18 months) [114].

The *Neu* (i.e., *Erbb*2) proto-oncogene encodes a 185 kDa receptor tyrosine kinase (i.e., ERBB2 receptor) belonging to the epidermal growth factor receptor family. Amplification and over-expression of the human homologue of the *Neu* proto-oncogene (i.e. *ERBB2* gene) is demonstrated in up to two-thirds of *in situ* ductal and one-third of invasive ductal breast cancers [28-31] and is correlated with poor prognosis [32]. An earlier transgenic mouse model was developed that utilized an oncogenic form of the rat *Neu* (i.e., activated) gene under the transcriptional control of the MMTV promoter that results in the expression of activated ERBB2 receptors in the mammary epithelia. Activation of these ERBB2 receptors results from a valine to glutamic acid substitution in the transmembrane domain. Even though this mutation has been observed in chemically-induced neuroblastomas, analyses of breast cancer biopsies have not detected this mutation in the transmembrane domain of ERBB2, thus suggesting an involvement of receptor over-expression rather than the activated receptor [32, 115, 116]. Therefore, to investigate the role of receptor over-expression in mammary carcinogenesis, a transgenic mouse model [FVB/N-Tg(MMTVneu)202Mul/J] was developed containing the rat *Neu* proto-oncogene (i.e., unactivated) under the transcriptional control of the MMTV promoter [110]. The use of the rat *Neu* transgene allows for the identification and characterization of effects as compared to the endogenous mouse gene.

This transgenic model mimics the stochastic nature of breast cancer and develops focal mammary adenocarcinomas (i.e., carcinoma of glandular tissue), surrounded by hyperplastic mammary epithelia, by four months of age with an average latency of about seven months (mean onset of 205 days). Metastasis to the lungs is common with 72% of tumor-bearing mice living to an age of eight months or older develop metastatic disease. Histological examination reveals multiple foci of metastatic mammary adenocarcinomas in the pulmonary vessels [110]. Also, tumor formation is not pregnancy dependent [110]. The role of estrogen in tumor development has been suggested because ovariectomy, as well as tamoxifen administration, prevents mammary tumor development [117, 118]. No amplification of either the rat *Neu* transgene or endogenous mouse *Neu* (i.e., *Erbb2*) gene has been detected in these tumors, unlike in human breast tumors. However, over-expression of the transgene and the ERBB2 receptors exhibiting intrinsic tyrosine kinase activity has been detected suggesting an increase in transcription rate or RNA stability [110].

The elevated tyrosine kinase activity may be mediated by receptor over-expression as well as by somatic mutations that promote catalytic activation through homo- and heterodimerization. Specifically, PCR analysis reveals that 65% of tumors, but not adjacent mammary epithelia, express ERBB2 receptors containing deletions of 7 to 12 amino acids (i.e., from in-frame deletions of 21 to 36 base pairs) located in the extracellular domain. Moreover, there is no difference between the transcript levels of the altered and unactivated transgenes [119]. The expression of the altered *Neu* cDNAs in Rat-1 fibroblasts results in tyrosine-phosphorylated ERBB2 receptors suggesting oncogenic activation of ERBB2 receptors [119]. Therefore, the deletion of these amino acids in the extracellular domain may contribute to the formation of disulfide-linked receptor dimers through a favorable particular spatial arrangement between the cysteines [120]. The activation of ERBB2 may involve signaling through c-SRC because mammary tumor extracts contain higher levels of c-SRC kinase activity without an increase in the level of c-SRC, and the activation of c-SRC results from direct interaction of the SH2 domain with the activated ERBB2 receptor [121].

In postmenopausal women with breast cancer, tumors that are ER negative confer a poorer prognosis than tumors that are ER positive [122]. Tumors in the MMTV/unactivated *Neu* mice are characterized by low ER expression (i.e., 10 fmol/mg protein) with PR expression even lower, and tumors are classified as two subtypes, ER+, PR- and ER-, PR- [123]. Normal and abnormal hyperplastic ducts of pubertal mice demonstrate about 75% of ERBB2-positive epithelial cells are ERα negative [124].

Tumor-derived cell lines exhibit expression of mouse ERBB3 receptors and ERβ but not ERα [125]. Tumors also exhibit increased expression of activated ERBB2, ERBB3, SRC, GAB2, SHC, Rb, ERK, and AKT as well as express higher levels of EGFR, ERBB4, Cyclin D1, p15, p27, and GLUT1 [126].

Description of model

All animal care was reviewed and approved by The Duquesne University Institutional Animal Care and Use Committee (IACUC) according to institutional guidelines following the National Institutes of Health guidelines for humane use. All female mice were obtained from in-house breeding of wild-type FVB/N females (Jackson Laboratory, Bar Harbor, ME) with dizygous males (FVB/N-Tg(MMTVneu)202Mul/J) carrying the unactivated (i.e., proto-oncogene), rat *Neu* transgene under transcriptional control of the MMTV promoter (Jackson Laboratory) [110].

Experimental design

The animal colony was maintained under a 12:12 light-dark cycle and allowed access to isoflavone-free diet and water, *ad libitum*. The isoflavone-free diet (i.e., the Control diet) was the Harlan-Tekland AIN-93G diet modified with corn oil providing 3713 kcal/kg with a nutrient content of 20% casein protein, 16% fat, and 64% carbohydrate (Harlan Laboratories Inc., USA) [127]. The focus of the pre-tumor study was to gain insight into the protective actions of the treatments on mammary carcinogenesis; therefore, this investigation used the same treatment conditions as in the long-term tumor study, Control, Melatonin, EPRT, EPMRT [15]. At weaning, female mice were randomly assigned to these four groups as shown in Table 1.

	Isoflavone-free Diet (Continuous)	Isoflavone-free Diet containing 0.5 mg E2 + 50 mg P4 (Continuous)
Water containing Vehicle (Night only)	**Control**	**EPRT**
Water containing Melatonin (Night only)	**Melatonin**	**EPMRT**

Table 1. Treatment groups

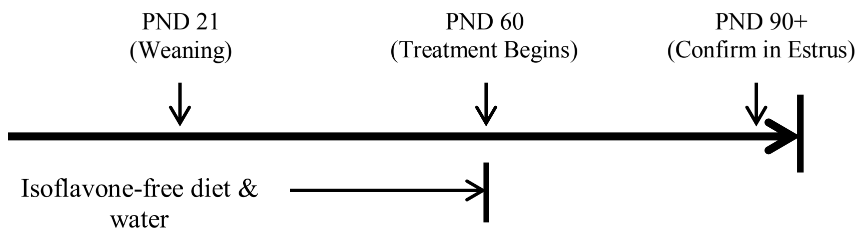

Diagram 1. Experimental timeline

All mice were maintained on isoflavone-free diet and water, *ad libitum*, until postnatal day 60 (See Diagram 1). At postnatal day 60 (i.e., two months of age), the mice began exposure to the treatment conditions. Depending on the experimental group, nocturnal melatonin supplementation (final concentration of 15 mg/L) was delivered in the drinking water during the hours of darkness. This supplementation was prepared daily by dissolving melatonin in 95% ethanol and then diluting this stock solution with water to a final concentration of 15 mg/L. Mice in the melatonin group were given melatonin in the drinking water between the hours of 18:00 to 06:00 (i.e., 6 p.m. to 6 a.m.) each day for 30 days. Each mouse in the Melatonin and EPMRT groups would be consuming approximately 52.5 μg of melatonin per period of darkness based on the measured mean nightly consumption of 3.5 mL of water. The melatonin dose is approximately equivalent to 5 mg of melatonin consumed by an adult woman per night.

Mice not consuming the nocturnal melatonin supplementation were provided water containing a final ethanol concentration of 0.03% (i.e., vehicle water).

Depending on the experimental group, mice were provided a combination of 17β-estradiol (E2) and progesterone (P4) in the isoflavone-free diet. The hormones were blended into the diet by the supplier. The isoflavone-free diet containing the hormones was provided, *ad libitum,* to the EPRT and EPMRT groups beginning at postnatal day 60 and continuing until postnatal day 90, or after, until the mouse was in estrus, as confirmed by visualization of the vaginal smear. The dose of E2 (0.5 mg) or P4 (50 mg) was added to 1800 kcal of diet, the average daily caloric intake of a woman [128], to account for the metabolic differences between mice and humans. Therefore, the final daily hormonal doses consumed by the mice eating 18 kcal or approximately 4 g of diet would be 5 μg of E2 and 500 μg of P4. Following completion of the experimental timeline, the mice were euthanized by carbon dioxide inhalation, and tissues were collected and frozen immediately or processed as described below.

Tissue collection and processing

Mammary gland collection: The left upper and inguinal mammary glands were fixed with cold 4% paraformaldehyde for 24 hours before storage at room temperature in 70% ethanol. The right inguinal mammary glands were cut into four transverse sections, frozen immediately in liquid nitrogen, and stored at -80^{o}C.

Serum collection: Whole blood was obtained via cardiac puncture and transferred to ice-cold Serum Gel S/1.1 tubes (#41.1387.005, Sarstedt Inc., Newton, NC). Tubes were placed on ice, and blood was allowed to clot before centrifugation at 16,500 g for five minutes, and then stored at -20^{o}C.

Ovary and uterus collection: Ovaries were frozen immediately in liquid nitrogen and stored at -80°C. The whole uterus was weighed and then cut into transverse sections (i.e., cross-sections), fixed in cold 4% paraformaldehyde for 24 hours, and stored at room temperature in 70% ethanol. Alternatively, after sectioning, some sections were frozen immediately with liquid nitrogen and stored at -80°C.

Radioimmunoassay

To assess the effect of the treatments on E2 and P4, the serum levels of E2 were assessed using the Double Antibody Estradiol kit (Diagnostic Products Corp., Los Angeles, CA) according to manufacturer's protocol. Briefly, a standard curve was generated with the provided standards. To 200 µL of serum sample, 100 µL of "Estradiol Antiserum" was added, vortexed, and incubated at room temperature for two hours. After incubation, 100 µL of [^{125}I] estradiol was added to all sample tubes, vortexed, and incubated at room temperature for one hour. After incubation, 1.0 mL of cold Precipitating Solution was added to all sample tubes, vortexed, and incubated at room temperature for 10 minutes. After incubation, all sample tubes were centrifuged at 3,000 g for 15 minutes. The supernatant was removed, and the precipitated pellet was retained for counting. Tubes containing the precipitated pellet were counted for five minutes each with a Packard Cobra II Gamma Counter. Serum levels of E2 were determined using the standard curve.

Serum levels of P4 were assessed with the Coat-A-Count® Progesterone kit (Diagnostic Products Corp, Los Angeles, CA) according to manufacturer's protocol. Briefly, a standard curved was generated with the provided standards. To 100 µL of serum sample, 1.0 mL of [^{125}I] progesterone was added, vortexed, and incubated at room temperature for three hours. After incubation, the tubes were decanted thoroughly, and tubes were counted for five minutes each with a Packard Cobra II Gamma Counter. Serum levels of P4 were determined with the standard curve.

Vaginal smear cytology

To assess whether or not the treatments regulated the estrous functioning of the female mice, vaginal smears were performed daily for 30 days in the morning by vaginal lavage. The vaginal canals were washed gently three times with sterile 0.9% NaCl solution delivered by a dropper. After the third wash, a drop of lavage fluid was placed onto a glass slide and allowed to air dry. These slides were stained using the Diff Quick Stain Kit (Imeb, Inc, San Marcos, CA). Briefly, the slides were immersed by dipping 15 times into 100% methanol, 15 times into Solution B (i.e., eosin and xanthene dye), and 15 times into Solution C (i.e., azure dye). The slides were rinsed with deionized water and allowed to air dry. Imaging was accomplished with a Nikon Eclipse E400 phase contrast microscope with an attached QImaging MicroPublisher 5.0 RTV camera (QImaging, Canada). Electronic images were captured using QCapture software (QImaging, Canada). The stage of the estrous cycle (i.e., proestrus, estrus, metestrus, or diestrus) for each day was determined by light microscopy at 400x after observation of three independent fields per smear by the investigator "blinded" to the treatment groups. To determine the stage of the estrous cycle, the investigator utilized criteria reported previously [129, 130]. Figure 1 depicts representative photos of each stage of the estrous cycle. Proestrus was identified by predominance of nucleated epithelial cells; estrus was identified by predominance of irregular, keratinized squamous epithelial cells with no visible nuclei; metestrus was identified by a mix of cell types with a predominance of leukocytes along with the keratinized epithelial cells; diestrus was identified by the predominance of leukocytes with the absence of keratinized epithelial cells [129]. An overall mean +/- SEM for various estrous cycling parameters was calculated for each treatment group.

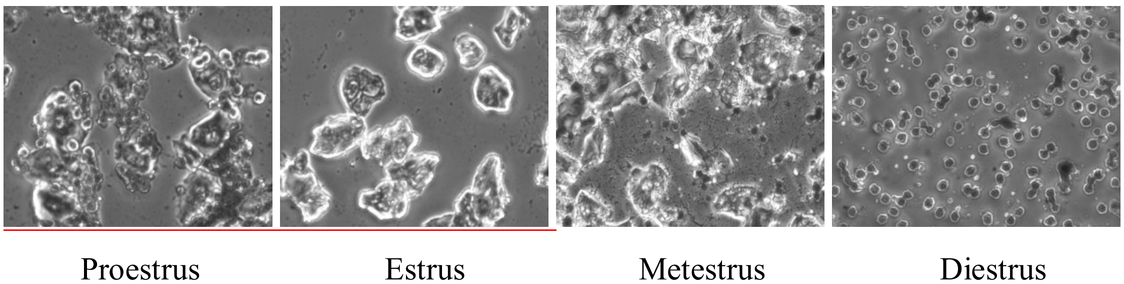

Figure 1. Representative images of each stage of the estrous cycle

Mammary morphology

To assess whether or not melatonin, HRT, or the combination therapy induced any morphological changes including effects on ductal elongation and mammary ductal differentiation, mammary whole mount analysis was performed on left inguinal mammary glands. Carmine alum stain (1 g Carmine alum and 2.5 g Aluminum potassium sulfate, added to 500 mL deionized water and boiled for 20 minutes) was prepared. After boiling, the volume was adjusted to 500 mL with deionized water, filtered, a crystal of thymol added, and then stored at 4^{o}C. The mammary glands were placed into cassettes and washed at room temperature for 15 minutes with 70% ethanol and then washed at room temperature for five minutes with deionized water. Each mammary gland was then incubated at 4^{o}C overnight carmine alum stain. The next day, each mammary gland was washed at room temperature for 15 minutes each in a graded series of ethanol (i.e., 70%, 95%, and 100%). Next, each mammary gland was incubated for at least 40 minutes with toluene to defat and clear the glands. Each mammary gland was then stored at room temperature in methyl salicylate (Sigma Aldrich) until imaging analysis. For imaging, each mammary gland was placed into a glass petri dish and immersed with methyl salicylate. Imaging was accomplished with a Nikon SMZ 800 dissecting microscope with an attached Olympus DP70 camera. Electronic images were captured using DP control software (Olympus Optical Co. LTD. 2002), and these images were saved by DP Manager. Measurements were calibrated with a metric ruler, and the parameters were quantified by the investigator "blinded" to the treatments groups using Image J software. Figure 2 depicts how ductal elongation and the number of tertiary side branches were quantified. Specifically, the elongation of the ducts into the mammary fat pad (depicted by black arrow labeled "A") and the overall length of the mammary fat pad (depicted by black arrow labeled "B") were determined by measurement from the center of the lymph node to the farthest terminal duct or the leading edge of the gland, respectively. An overall mean +/- SEM was calculated for each treatment group. Tertiary branching was determined by quantifying the number of tertiary branches per mm^2 (depicted by black box labeled "C") in three separate distal ductal containing areas of the gland. The mean number of tertiary branches per mm^2 was determined for each mammary gland per mouse in each treatment group. An overall mean +/- SEM was calculated for each treatment group.

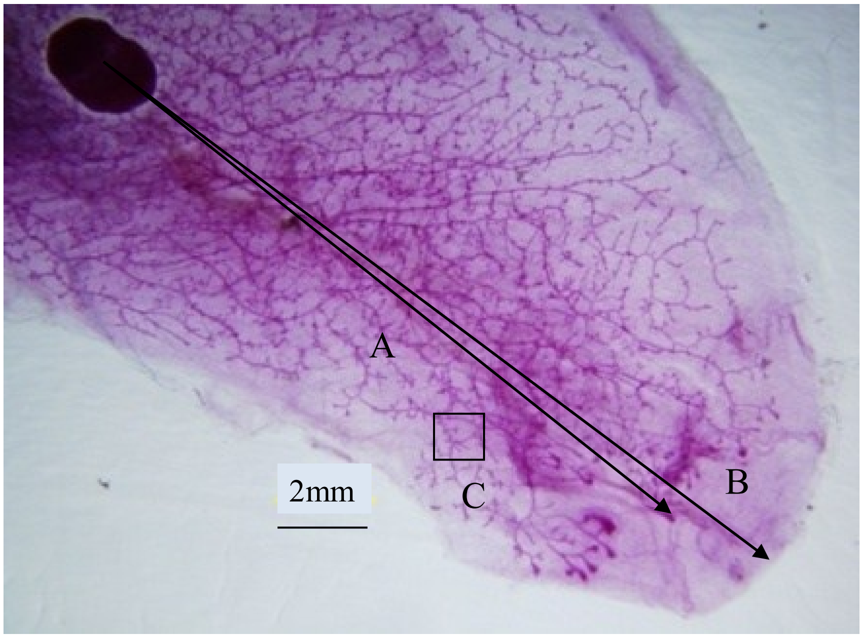

Figure 2. Representative image of a mammary gland depicting how the duct and mammary gland lengths and number of tertiary branches were measured. The large nodule is the mammary lymph node.

Total binding assay

To determine whether or not melatonin receptors are expressed in mammary tissue, total 2-[^{125}I] iodomelatonin binding analysis was determined in inguinal mammary glands of Control mice. Briefly, membranes were prepared from frozen cross-sections of inguinal mammary glands of Control mice through homogenization of the tissue in 1 mL of Tris buffer (50 mM Tris-HCl, pH 7.4) containing protease inhibitors. Homogenates were then centrifuged at 20,000 g for 30 minutes. Membranes were resuspended in 1 mL of ice-cold Tris buffer (pH 7.4) and then vortexed gently to resuspend the membranes. Aliquots of these membrane homogenates were either subjected to protein analysis using the Bradford method according to manufacturer's protocol or total binding analysis using 2-[^{125}I] iodomelatonin radioligand (PerkinElmer, Waltham, MS). Briefly, membrane aliquots of 200 μL were added to tubes containing 1 nM 2-[^{125}I] iodomelatonin in the absence (i.e., Total binding) or presence of 1 μM melatonin (i.e., Non-specific binding). Tubes were incubated at room temperature for one hour and then filtered using a Brandel harvester through Whatman GF/B Paper (FP-100) filter strips presoaked in 0.5% polyethylenimine (PEI) to reduce non-specific binding. Radioactivity was counted for five minutes with a Packard Cobra II Gamma Counter. Data were expressed as fmoles of 2-[^{125}I] iodomelatonin per mg of protein and then a mean was calculated.

RNA isolation

To ascertain the effect of the various treatments on gene expression, microarray and real-time RT-PCR analysis was performed with RNA prepared from central sections of frozen right inguinal mammary gland. RNA was isolated from tissues weighing between 30-90 mg using the Absolutely RNA® Miniprep Kit (Stratagene, La Jolla, CA) according to the manufacturer's protocol. Briefly, the gland was placed into a 1.5 mL microfuge tube and homogenized in lysis buffer containing β-mercaptoethanol with a disposable RNase-free plastic douncer. The homogenate was frozen at -20^{o}C. Once frozen, the homogenate was then thawed at room temperature. To the Prefilter Spin Cup, 700 μL of homogenate was added, centrifuged at 15,000 g for five minutes, and the filtrate was retained. To the filtrate, an equal volume of 70% ethanol was added and vortexed thoroughly. To the RNA Binding Spin Cup, 700 μL of mixture was added, centrifuged at 15,000 g for one minute, and the filtrate was discarded. To the RNA Binding Spin Cup, the remaining 700 μL of mixture was added, centrifuged at 15,000 g for one minute, and the filtrate was discarded. To the RNA Binding Spin Cup, 600 μL of 1x Low-Salt Wash Buffer was added, centrifuged at 15,000 g for one minute, and filtrate was discarded. An additional centrifugation was performed for two minutes. To the RNA Binding Spin cup, 55 µL of DNase solution was added directly to the filter matrix and incubated at 37^{o}C for 15 minutes. After incubation, 600 µL of 1x High Salt Buffer was added, centrifuged at 15,000 g for one minute, and filtrate was discarded. Then, 600 µL of 1x Low-Salt Wash Buffer was added, centrifuged at 15,000 g for one minute, and the filtrate was discarded. Next, 300 µL of 1x Low-Salt Wash Buffer was added, centrifuged at 15,000 g for two minutes, and filtrate was discarded. The RNA Binding Spin Cup was transferred to a 1.5 mL microfuge tube and 40 µL of pre-warmed (i.e., 60^{o}C) Elution Buffer was added gently onto the center of the filter matrix. The microfuge tube was incubated at room temperature for two minutes and centrifuged at 15,000 g for one minute. The elution step was repeated to maximize RNA yield. The RNA quantities and purities were determined by UV spectrophotometry (Beckman DU® 530 Life Sciences UV/Vis spectrophotometer). RNA dilutions were prepared with RNase-free water. The RNA quantities were calculated using the equation: Concentration = A_{260nm} x dilution factor x 0.4 µg/µL. The RNA purities were determined by calculating the 260 nm / 280 nm ratio where ratios between 1.8 and 2.0 were considered as pure preparations. The purified RNA was stored in -80^{o}C until analysis.

Microarray

Microarray analysis was performed with the isolated RNA by the Biomedical Genomics Core of The Research Institute at Nationwide Children's Hospital, Columbus, Ohio. Arrays were scanned with the Affymetrix GeneChip Scanner 3000 7G and information extracted from image data by GeneChip Operating Software (GCOS) version 1.4., and then analyzed in-house with the R-software environment for statistical computing and graphics. These scripts utilize several Bioconductor packages which provide tools for the analysis and comprehension of genomic data [131]. Genes were identified if the fold change was less than or equal -1.5 or greater than or equal to 1.5 of the Control samples.

RT-PCR reactions

Based on the findings from the microarray analysis, genes were further analyzed by real-time RT-PCR analysis to confirm the results. Candidate genes were selected for further analysis if the genes were hormone-regulated, growth-promoting, related to cell differentiation, or involved in tumorigenesis. Genes were also selected to serve as controls for the amount of mammary epithelial tissue (e.g., *Krt18*), lymph-node and lymphocyte contamination (e.g., *Ms4a1*) and the rat *Neu* (e.g., *Erbb2*) regulation. Using the isolated RNA, 250 ng of total RNA was reversed transcribed into cDNA using the qScript™ cDNA Synthesis Kit (Quanta BioSciences, Inc., Gaithersburg, MD). Briefly, a mixture containing 19 µL of total volume was prepared by adding qScript™ Nuclease Free Water, qScript™ Reaction Mix, and isolated RNA into a thin-walled PCR tube, vortexed, and centrifuged at low gravitational force. To this tube, 1 µL of qScript™ Reverse Transcriptase was added, inverted gently to mix, and centrifuged at low gravitational force. Another mixture containing 19µL of total volume was prepared by adding qScript™ Nuclease Free Water, qScript™ Reaction Mix, and isolated RNA, but without the addition of qScript™ Reverse Transcriptase enzyme. An Eppendorf Mastercycler Ep*gradient* (Eppendorf AG, Hamburg, Germany) was used to generate the cDNA. The cDNA samples generated for each mouse were stored at -20^{o}C.

Real-time RT-PCR

The cDNA samples from the RT-PCR reactions were used for real-time analysis. cDNA products were analyzed using primers designed for detection of: *Adra1a* (adrenergic receptor, alpha 1a) *F*: 5'-TGG GCG CTT TCC TTG GTC ATC TC-3' and *R*: 5'-TAC GGT GGA TAC GGA GCG TCA-3'; *Akr1c14* (aldo-keto reductase family 1 member C14) *F*: 5'-GGA ACC ACT GTG CCC GAT AAG G-3' and *R*: 5'-TGG CCT GGC CTA CTT CCT CTT CT-3'; *Areg* (amphiregulin) *F*: 5'-CTT TGT CTG TGC CAT CAT CC-3' and *R*: 5'-TCC CTG AAG TAT CGT TTC CA-3'; *Csn1s2a* (casein alpha s2-like) *F*: 5'-CAG AGC AGT GTG AAC CAG TG-3' and *R*: 5'-GGT ATC TGG GGA TGA AGA GC-3'; *Duox1* (dual oxidase 1) *F*: 5'-ACC ATT TCC ATC ATG GGG TTC CA-3' and *R*: 5'-GGG GGT TAG GCA GGT AGG GTT C-3'; *Erbb2* (v-erb-b2 erythroblastic leukemia viral oncogene homolog 2) *F*: 5'-TGG ATG TAC CTG TAT GAG ACG-3'and *R*: 5'-GGA TTC AAG CAG CAA GGA AAG-3'; *Esr1* (estrogen receptor 1, alpha) *F*: 5'-TAT GCC TCT GGC TAC CAT TAT-3' and *R*: 5'- CAT CAT GCC CAC TTC GTA AC-3'; *Figf* (c-fos induced growth factor or vascular endothelial growth factor D, VEGF-D) *F*: 5'-GGA GAT CTC ATT CAG CAC CCG GA-3'and *R*: 5'-TGG GCC CTT GTC TCC TTT GGA A-3'; *Greb1* (gene regulated by estrogen in breast cancer protein) *F*: 5'-CCT CCA CCA TGC AGC CCA TAT C-3' and *R*: 5'-AGC GTA GGA AGA TCT GCT CCA GG-3'; *Ido1* (indoleamine 2,3-dioxygenase 1) *F*: 5'-GTT CTC ATT TCC TGG TGG GGA CT-3' and *R*: 5'-AGC TAT GTC GTG CAG TGC CT-3'; *Krt18* (keratin 18) *F*: 5'-TTG CGA ATT CTG TGG ACA AT-3' and *R*: 5'-TTC CAC AGT CAA TCC AGA GC-3'; *Lcn2* (lipocalin 2) *F*: 5'-CAA TGT CAC CTC CAT CCT GGT CA-3' and *R*: 5'-CAG CCC TGG AGC TTG GAA CAA AT-3'; *Ms4a1* (membrane spanning 4-domains, subfamily A, member 1 or B-lymphocyte antigen CD20) *F*: 5'-TGC CTT CTT CCA GAA ACT TG-3' and *R*: 5'-TTG GTT GGG AAG ATA CTC CA-3'; <u>*Mtnr1a*</u> (melatonin receptor 1A) *F*: 5'-GCA ACA AGA AGC TCA GGA AC-3' and *R*: 5'-ATG TCA GCA CCA AGG GAT AA-3'; <u>*Mtnr1b*</u> (melatonin receptor 1B) *F*: 5'-GTC TGG CTC CTC ACT CTG GT-3' and *R*: 5'-AGG AAT AGA TGC GTG GAT CA-3'; <u>*Per2*</u> (period homolog 2, Drosophila) *F*: 5'-CTG ACG CAC ACA AAG AAC TG-3' and *R*: 5'-TCA TTA GCC TTC ACC TGC TT-3'; <u>*Pgr*</u> (progesterone receptor) *F*: 5'-GGC AAA TCC CAC AGG AGT TTG-3' and *R*: 5'-AGA CAT CAT TTC CGG AAA TTC-3'; <u>*Pgr(A)*</u> (progesterone receptor A) *F*: 5'-AG TGG TGG ATT TCA TCC ATG-3' and *R*: 5'-CTT CCA GAG GGT AGG TG-3'; <u>*Ptprd*</u> (protein tyrosine phosphatase receptor type D) *F*: 5'-TTC GCC GTG TCC CAC CAA GA-3' and *R*: 5'-GGC TTG GGT AAG GCT TTG ACA GT-3'; <u>*Slc24a3*</u> (solute carrier family 24 member 3 sodium/potassium/calcium exchanger) *F*: 5'-CGC TGT CTG TGG TCG CAC TC-3' and *R*: 5'-GAT CAC GGA CGC TTT GCG GT-3'; <u>*St3gal5*</u> (ST3 beta-galactoside alpha-2,3-sialytransferase 5) *F*: 5'-CTA GCA TGC ACA CAG AGG CGG T-3' and *R*: 5'-GTG AAC TCA CTT GGC ATT GCT CG-3'; <u>*Ppia*</u> (peptidylprolyl isomerase A or cyclophilin A) *F*: 5'-AGG TGA AAG AAG GCA TGA AC-3' and *R*: 5'-ACA GTC GGA AAT GGT GAT CT-3'.

The primers were designed to span at least one intron / exon boundary, whenever possible, to ensure that the amplification was from cDNA and not genomic DNA. All primers were purchased from Integrated DNA Technologies, Inc. (Coralville, IA). The efficiencies of the primers were tested before use to insure the primers are appropriate. To a PCR microfuge tube, 5 μL of diluted primers and 12.5 μL of B-R SYBR® Green

SuperMix for iQ (Quanta BioSciences, Inc., Gaithersburg, MD) were added. To a second PCR microfuge tube, 1 μL of the cDNA sample (from prior RT-PCR reaction) and 6 μL of UltraPure Distilled DNase- RNase-Free Water (Invitrogen Corp., Grand Island, NY) were added. To a third PCR microfuge tube, 1 μL of the no reverse transcriptase containing mixture (from prior RT-PCR reaction) and 6 μl UltraPure Distilled DNase-RNase-Free Water were added. Into each well of an ABgene® plate (Thermo Fisher Scientific, UK), 18 μL of the primer mix and 7 μL of the template mix or the no reverse transcripase mix were added. All samples were performed in duplicate. In addition to the no reverse transcriptase wells, wells containing water only (i.e., no template) were analyzed to detect amplification of contaminants. The plates were sealed and spun before placement into the Bio-Rad iCycler iQ™ real-time system set for SYBR green detection.

The real-time conditions were designated for enzyme activation at 95°C for three minutes followed by 50 cycles of 15 seconds each at 95°C for denaturing and 45 seconds each at 60°C for annealing/extension. To assess the quality of product, melt curves were generated to ensure a single product in each cDNA sample as well as comparison to the no reverse transcriptase samples. Data was expressed as the change in threshold cycle value (ΔCt), whereby the lower the ΔCt value the higher the relative mRNA level contained in the sample. The ΔCt value of each sample was calculated by subtracting the Ct of *Ppia* (i.e., cyclophilin A) from the Ct value of the candidate gene for each mouse in each treatment. An overall mean ΔCt +/- SEM was calculated for each treatment group. Fold change of gene expression as compared to Control were determined for each treatment with the $2^{-\Delta\Delta Ct}$ method [132].

Immunohistochemistry

To assess whether or not the treatments affected uterine weight, luminal epithelial height, and proliferation, fixed uteri from each of the groups were processed with a Shandon Pathcentre® Tissue Processor/Embeddor and then manually embedded in paraffin using a Shandon Histocentre 2® with a paraffin temperature of 64.5°C to avoid antigen degradation. Cross-sections of 5 μm were generated using a Microm HM 325 microtome. The cross-sections were allowed to float on water warmed to 37°C before placement on ProbeOn slides (Fisher Scientific, Pittsburgh, PA).

Each section was deparaffinized with three changes of mixed xylenes of five minutes each and then hydrated by a graded series of diluted ethanol concentrations (100% 2x, 90% 2x, 70% 2x, and 50% 1x) for 5 minutes each. Each section was washed two times for five minutes each with tap water. Antigen retrieval was performed using boiling citrate buffer (0.1 M Citric acid and 0.1 M sodium citrate dehydrate, pH 6.0) for 15 minutes. After boiling, each section remained in the citrate buffer and was allowed to cool on ice until buffer obtained room temperature. Each section was washed four times for five minutes each with PBS (0.58 M sodium phosphate dibasic, 0.17 M sodium phosphate monobasic, and 0.68 M NaCl, pH 7.4). Each section was then incubated in 0.6% hydrogen peroxide (1:5 dilution of 3% hydrogen peroxide to 100% methanol) for eight minutes to quench endogenous peroxidase activity. Each section was washed three times for five minutes each with 1x PBS. A hydrophobic barrier was first created around the tissue sections using a PAP pen followed by incubation at room temperature for 15 minutes with 150 μL of anti-goat blocking serum (1 drop goat serum to 3.33mls PBS as indicated in protocol by Vector Laboratories). Blocking serum was removed by capillary action using a Kimwipe™, and then each section was incubated at room temperature for one hour with 150 µL of rabbit polyclonal Ki67 antigen antibody (VPK451; Vector Laboratories, Inc., Burlingame, CA) at a dilution of 1:1,000. For negative controls, each section was incubated at room temperature for one hour with 150 µL of rabbit anti-serum without primary antibody. After incubation, each section was washed three times for five minutes each with 1x PBS, and then each section was incubated at room temperature for 30 minutes with diluted ABC biotinylated secondary antibody solution (1 drop to 10mls PBS, Vector protocol). Each section was then washed three times for five minutes each with 1x PBS and was incubated at room temperature for 30 minutes with VECTASTAIN elite ABC reagent (2 drops reagent A + 2 drops reagent B to 5 mL of 1x PBS, 30 minutes before addition to sections, Vector protocol). Sections were then washed three times for five minutes each with 1x PBS. To each section, diaminobenzidine (DAB) (Vector kit SK-4100) was applied and incubated for one minute until a pale brown color was visible and then immersed in deionized water and washed by constant flow with deionized water. Next, sections were immersed for two seconds into Mayer's hematoxylin QS (Sigma Aldrich) and washed briefly in deionized water. After washing, each section was immersed for one minute in Scott's tap water substitute (3.5 g sodium bicarbonate and 20 g magnesium sulfate/1L) to blue the nuclei. Each section was dehydrated for one minute each in a graded series of increasing ethanol concentrations (95% 2x and 100% 2x). Each section was then immersed with three changes for one minute each of p-xylene. Permount was applied to each section before the addition of a coverslip. After drying, each slide was observed at 300x with the Olympus BX 41 microscope attached to an Olympus DP70 camera. Images were captured using DP control software and electronic images saved by DP Manager. Figure 3 displays a representative photo depicting how the luminal columnar epithelial height was quantified. Measurements were calibrated using a grid from a hemacytometer. Luminal columnar epithelial height (as depicted by vertical black line) was determined by an investigator "blinded" to the treatment groups using Image J software. Measurements were performed in triplicate for each cross-section, and an overall mean +/- SEM was calculated for each treatment group.

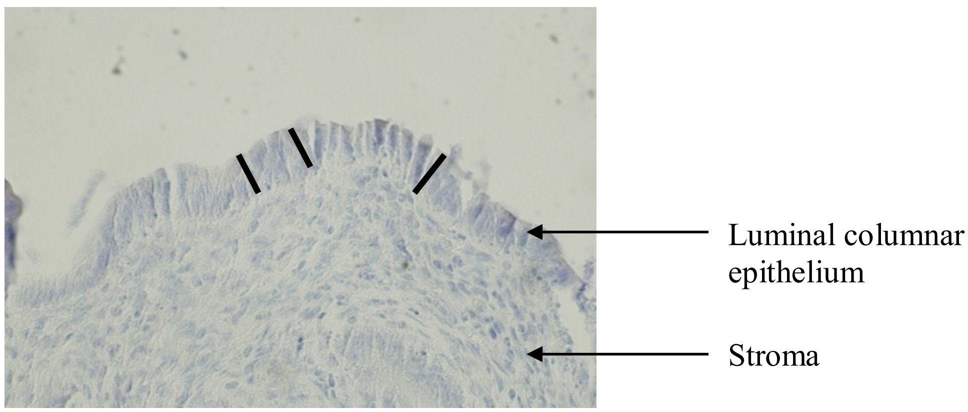

Figure 3. Representative image of a uterine cross-section depicting how luminal columnar epithelial height was measured.

Li-Cor Odyssey® with secondary infrared dyes

The effect of the treatments on uterine proliferation was assessed by quantifying Ki67 expression. Briefly, uterine cross-sections were obtained as described previously and then subjected to immunohistochemical analysis using 150 µL of rabbit polyclonal Ki67 antigen antibody (VPK451; Vector Laboratories, Inc., Burlingame, CA) at a dilution of 1:1,000. Tissue sections were incubated for one hour at room temperature. For negative controls, each section was incubated at room temperature for one hour with 150 µL of rabbit anti-serum without primary antibody. After incubation, each section was washed three times for five minutes each with 1x PBS. Each section was incubated at room temperature in the dark for 30 minutes with goat anti-rabbit secondary IRDye®

800 CW (Li-Cor Biosciences, Lincoln, NE - #827-08365) at a dilution of 1:1,000. Each section was allowed to air-dry. After drying, each section was imaged with the Li-Cor Odyssey® Infrared Imaging System and images were saved electronically. The intensity of Ki67 expression was determined in the luminal columnar epithelium and stroma by the investigator "blinded" to the treatment group using Image J software. Measurements were performed in triplicate for each cross-section, and an overall mean +/- SEM was calculated for each treatment group.

Cytosol and nuclear preparation

Cytosol and nuclear preparation were performed according a protocol provided online by Millipore (Billerica, MA). Frozen uterine cross-sections were homogenized with a Kontes Dounce Tissue Grinder that is designed to retain intact nuclei and dounced with ice-cold 400 µL RIPA buffer without detergents [50 mM Tris-HCl (pH 7.4), 140 mM NaCl, 1 mM EGTA (pH 8.0), 1 mM PMSF, 1 µg/mL aprotinin, 1 µg/mL leupeptin, 1 mM Na_3VO_4, 50 mM NaF, and 1 mM DTT]. The homogenates were centrifuged at 2,900 g for 20 minutes at 4^oC. The supernatant (i.e., cytosolic and membrane fractions) was removed and then centrifuged at 29,000 g for 45 minutes at 4^oC. The supernatant from this centrifugation (i.e., cytosolic fraction) was removed and immediately stored at -20^oC. To the pellet obtained from the first centrifugation (i.e., the nuclear fraction), 250 µL of ice-cold RIPA buffer containing 1% NP-40 was added. The pellet was disrupted using a pipette tip, vortexed, and stored at -20^oC.

Western blot

The cytosolic and nuclear fractions from uterine tissues were thawed on ice. Cytosolic fractions were centrifuged at 10,000 g for two minutes to remove insoluble proteins. A BioRad DC Protein Assay (BioRad Laboratories, Hercules, CA) was performed according to manufacturer's protocol. An equal volume of Laemmli sample buffer (BioRad Laboratories) containing β-mercaptoethanol was added to each fraction and boiled in a water bath for ten minutes. Proteins were separated using 7.5% Tris-HCl Ready Gels (BioRad Laboratories) submerged in running buffer (192 mM Glycine, 50 mM Trizma Base, and 0.1% SDS). Proteins were transferred to a PVDF membrane (BioRad Laboratories) submerged in ice-cold transfer buffer (192 mM Glycine, 25 mM Trizma Base, and 10% Methanol) at 90 V for 40 minutes. The membrane was submerged in 100% methanol for 10 seconds, air-dried, and then incubated at 37^{o}C for ten minutes. After incubation, the membrane was submerged in 100% methanol for ten seconds and then in Nanopure water for one minute. To reduce non-specific binding, each membrane was blocked at room temperature for one hour with blocking buffer (1x PBS, pH 7.4: 11.5 g Na_2HPO_4, 2.96 g NaH_2PO_4, and 5.84 g NaCl, 0.1% Tween 20 and 4% nonfat milk) and then incubated at 4^{o}C overnight with rocking in primary antibody containing either rabbit anti-estrogen receptor alpha (polyclonal estrogen receptor alpha; ab75635; Abcam; Cambridge, MA) or mouse anti-progesterone receptor (monoclonal PR-AT 4.14 to progesterone receptor; ab2764; Abcam) at a dilution of 1:8,000 (in 1x PBS containing 1% ECL Advance blocking agent; BioRad Laboratories). The next day, the membrane was washed four times for five minutes each in 1x PBS. The membrane was then incubated at room temperature for one hour with rocking in secondary antibody containing either ECL Anti-rabbit IgG, Horseradish peroxidase for ERα or ECL Anti-mouse IgG, Horseradish peroxidase for PR (GE Biosciences UK limited, United Kingdom) at a dilution of 1:16,000 (in 1x PBS with 0.1% Tween 20 and 4% nonfat milk).

After incubation, the membrane was washed four times for five minutes each with 1x PBS. In the dark, the blot was exposed to ECL Advance Western Blotting Detection System (GE Biosciences) diluted to 5% with water. Protein bands were visualized with Amersham Hyperfilm ECL (GE Biosciences) at various time intervals (10 seconds to five minutes). The protein bands were scanned electronically and quantified for mean intensity with Image J software. Cytosolic proteins were normalized to GAPDH (rabbit polyclonal GAPDH; ab9485; Abcam). An overall mean +/- SEM was calculated for each treatment group.

Statistical analysis

Body weights, serum levels of E2 and P4, estrous cycling, mammary morphology, whole uterine wet weight, luminal columnar epithelial height, expression of Ki67 in luminal columnar epithelium and stroma, and ERα and PRA localization were analyzed by one-way analysis of variance (ANOVA) followed by Newman-Keuls multiple comparison post-hoc test with GraphPad Prism 5 software (GraphPad Software Inc., La Jolla, CA). Significance was defined as $p < 0.05$ where (A), (B), and (C) represent significance as compared to Control, Melatonin, and EPRT, respectively.

Real-time RT-PCR results were analyzed by an unpaired Student's t-test or one-way analysis of variance (ANOVA) followed by Dunnett's multiple comparison post-hoc test or Newman-Keuls post-hoc test with GraphPad Prism 5 software. If the homogeneity of variances assumption was violated, a Dunnett's C post-hoc follow-up test was performed with IBM Statistical Package for the Social Sciences (SPSS) version 20. If the one-way ANOVA detected significant differences in both Melatonin and EPMRT groups, then a two-way ANOVA was performed using SPSS version 20 to investigate the main effects of melatonin and E2 and P4. Significance was defined as $p < 0.05$, $p < 0.01$, and $p < 0.001$ where (*), (**), and (***) represent significance to Control, respectively.

RESULTS

EPMRT and other treatments did not affect body weight

Each mouse was weighed before necropsy to determine if the treatments affected body weight. The assessment of body weight is important to determine if the treatments affected food consumption or growth of the mice. Moreover, melatonin has been demonstrated to reduce overall body weight in female BALBc and MMTV/activated *Neu* mice [117, 133]. Additionally, body weight was assessed as a means to standardize the uterine wet weight. The results are presented in Figure 4. Body weight was measured in grams. Statistical analysis detected no significant differences among the four treatments suggesting that none of the treatments affected body weight.

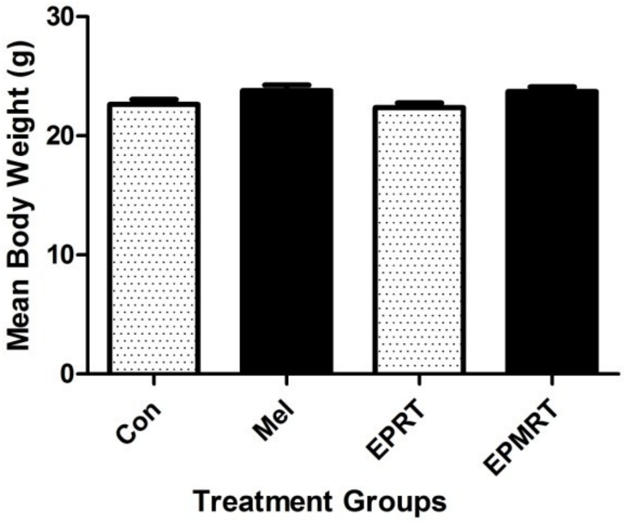

Figure 4. Treatment effects on body weight. No significant differences were detected. Each bar represents mean ± SEM values from n = 18 - 19 mice per treatment group. Data were analyzed by one-way ANOVA with significance defined as $p < 0.05$.

EPMRT and the other treatments did not affect serum levels of E2 and P4

The pre-tumor study was conducted to gain insight into the anti-tumor effects of EPMRT [15]. Because E2 and P4 were blended into the food pellets, it was essential to determine if the treatments affected serum levels of E2 and P4. The alterations in serum levels of E2 and P4 would provide an indication into the hormone environment of the mice which is necessary to understand and explain the findings from the tumor and pre-tumor studies. The results are presented in Figure 5. Serum levels of E2 (in pg/mL) (Fig 5A) and P4 (in ng/mL) (Fig 5B) were assessed in the three month old mice in estrus after one month of treatment. Statistical analysis detected no significant differences among the four treatments for serum levels of E2 and P4 suggesting that none of the treatments affected the serum levels of E2 and P4.

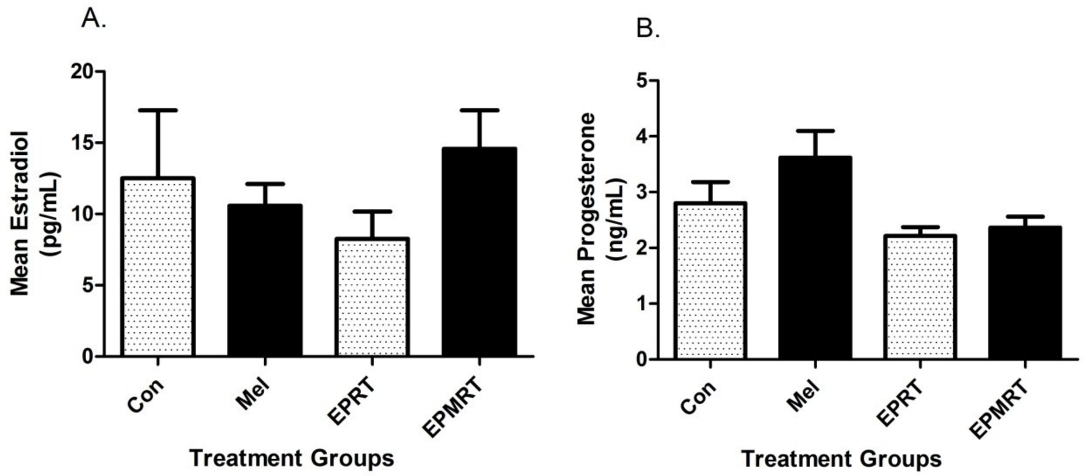

Figure 5. Treatment effects on serum levels of E2 and P4. None of the treatments affected serum levels of (A) E2 and (B) P4. Each bar represents the mean ± SEM values from n = 4 - 6 mice per treatment group for E2 and n = 7 - 8 mice per treatment group for P4 serum measurements. Data were analyzed by one-way ANOVA with significance defined as $p < 0.05$.

EPMRT and EPRT increased the days in estrus and within an estrous cycle

Even though the treatments did not affect the serum hormone levels of E2 and P4, the estrous cycling of the mice was measured as it may be more sensitive to subtle changes in serum E2 and P4 levels. Additionally, the assessment of alterations in estrous cycling may be used to predict if the uterine microenvironment is being exposed to conditions that may lead to uterine proliferation. In the tumor study, mice consuming EPRT had increases in uterine wet weight which was attenuated with the addition of melatonin (EPMRT). Therefore, the assessment of estrous cycling may provide information about the early effects contributing to the increase in uterine wet weight observed in the tumor study. To determine if the treatments altered estrous cycling, vaginal smears were performed daily for the 30 days of treatment. The results are presented in Figure 6. Treatment effects on estrous cycling were measured as: A) the number of days in estrus over a 30-day period, B) the number of days in estrus per estrous cycle, C) the length of each estrous cycle, and D) the number of complete estrous cycles over a 30-day period. Mice treated with EPRT or EPMRT had more days in estrus over 30 days (Fig 6A) as well as within a cycle (Fig 6B) as compared to Control and Melatonin-treated mice. However, no differences occurred in the length of each estrous cycle (Fig 6C) or the total number of estrous cycles over a 30-day period (Fig 6D). These results suggest that the hormone treatments, especially the E2 component, influenced the uterine environment of the mice.

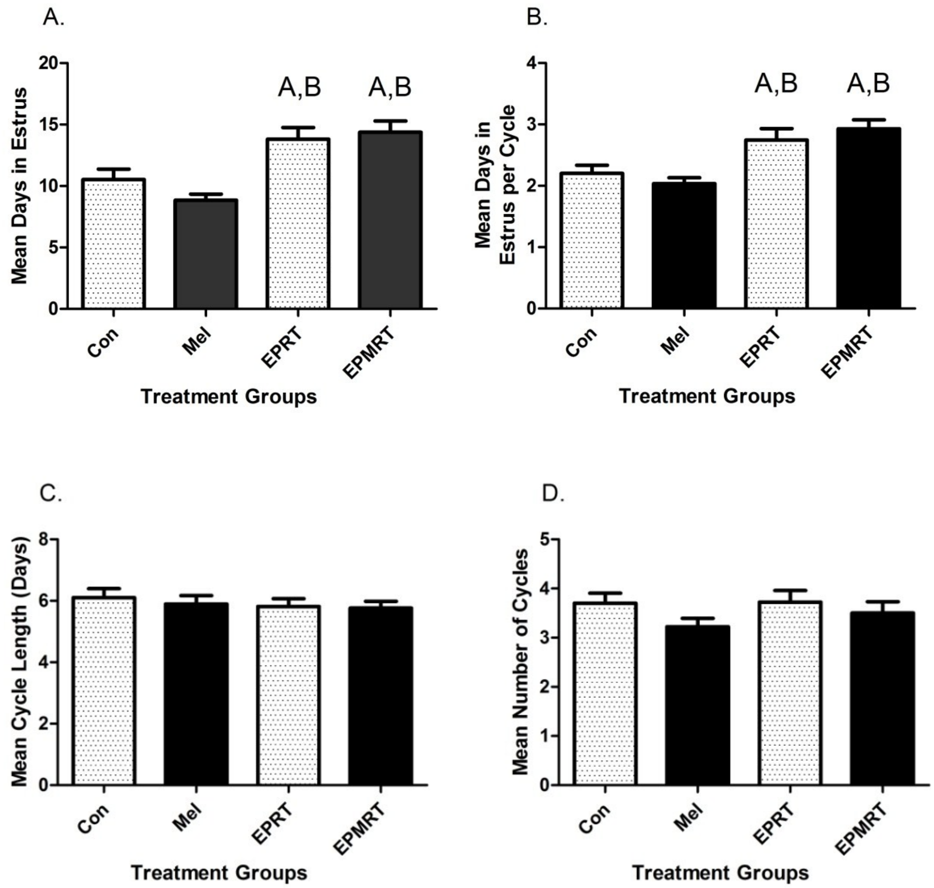

Figure 6. Treatment effects on estrous cycling. Mice given either EPRT or EPMRT demonstrated increases (A) in the days in estrus over a 30-day period, and (B) in the number of days in estrus per estrous cycle compared to Control and Melatonin-treated mice. However, no changes (C) in the length of each estrous cycle or (D) in the total number of estrous cycles over a 30-day period were detected. Each bar represents the mean ± SEM from n = 18 - 20 mice per treatment group. Data were analyzed by one-way ANOVA followed by Newman-Keuls post-hoc test with significance defined as $p < 0.05$. A = $p < 0.05$ compared to Control; B = $p < 0.05$ compared to Melatonin.

EPMRT and the other treatments did not affect ductal elongation

Beginning at about four weeks of age, the mammary gland is exposed to a surge of ovarian hormones to develop the mammary ductal network. The rudimentary ductal tree begins to elongate into the fat pad, and this process is mediated by E2 actions at ERα [134-136]. To assess the extent of ductal elongation into the mammary fat pad, various measurements were performed on whole mounts of the inguinal mammary glands stained with carmine alum (see Figure 2). Treatment effects on ductal elongation were measured as: A) the length to end of gland (in mm) from the center of the lymph node and B) the length to end of duct (in mm) from the center of the lymph node. Using these measurements, the extent of ductal elongation into the mammary fat pad was determined. The results are presented in Figure 7. Statistical analysis detected no significant differences among the four treatments suggesting the extent of ductal elongation was similar for all the groups. The ductal trees elongated into over 80% of the fat pat which is representative of a fully elongated ductal network.

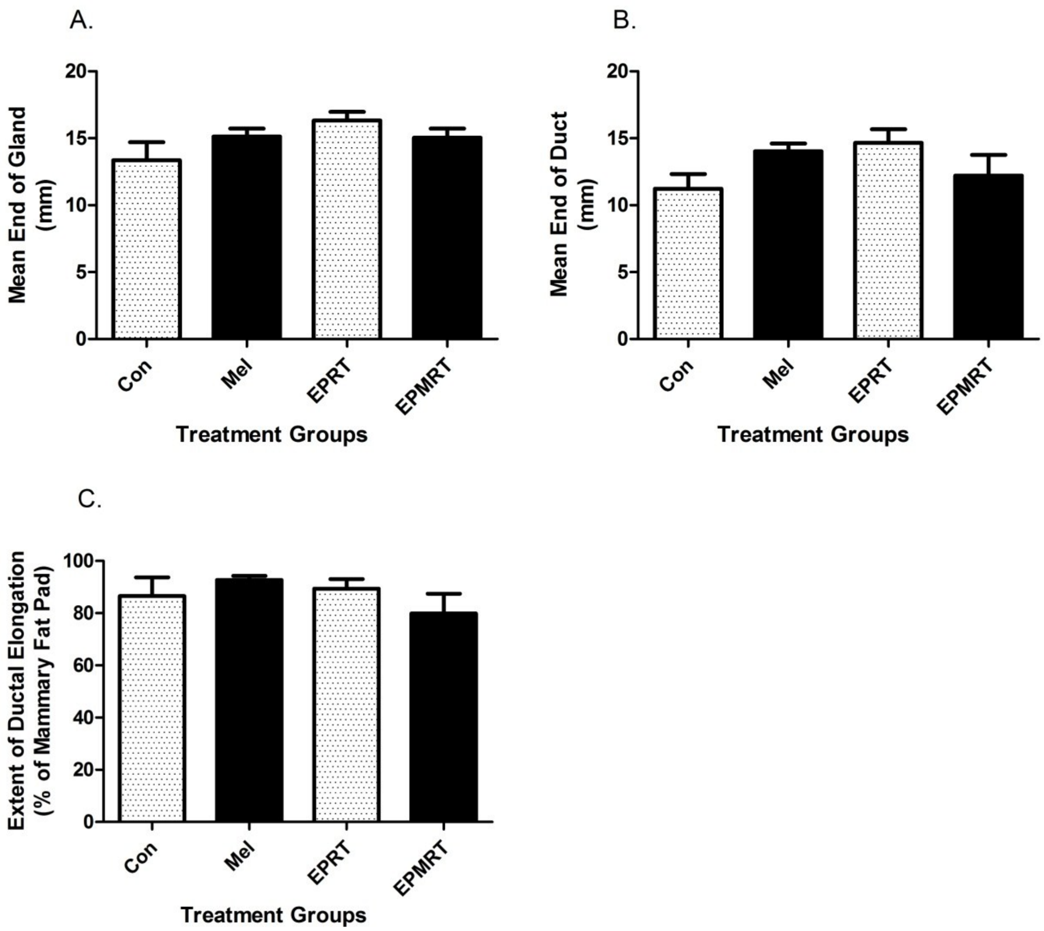

Figure 7. Treatment effects on ductal elongation into the mammary fat pad. No significant differences in (A) mammary gland length, (B) ductal length, and (C) the extent of ductal elongation into the fat pad were detected. Each bar represents the mean ± SEM values from n = 6 - 7 mice per treatment group. Data were analyzed by one-way ANOVA with significance defined as $p < 0.05$.

EPMRT and Melatonin induced tertiary side-branching

As revealed in the tumor study, EPMRT increased tumor latency and decreased tumor incidence and weight when compared to Control [15]. Previous work by Russo and Russo 1998 demonstrated that mammary gland differentiation reduces the risk of breast cancer [137]. The initial stage in mammary gland differentiation is the formation of tertiary-side branches, and this process is mediated by P4 actions at PRA [136, 138-140]. If EPMRT induces the formation of tertiary side-branching earlier in the process of ductal development, this may be a possible explanation for its protective actions against mammary cancer. Figure 8A, B, C, and D display representative images of mammary gland whole mounts. Qualitative increases in tertiary side-branching were observed in mammary glands from mice treated with EPMRT or Melatonin. Therefore, we investigated whether or not these treatments induced tertiary side-branching compared to Control by quantifying the number of tertiary side-branches (per mm^2) in mammary gland whole mounts stained with carmine alum. The results are presented in Figure 8E. Statistical analysis detected significant increases in tertiary side-branching in mice treated with EPMRT or Melatonin with melatonin having a main effect indicating that melatonin is inducing tertiary side-branching. The protective actions of EPMRT against mammary cancer may be through promoting the initial stage of mammary differentiation earlier in the process of ductal development.

A. Control

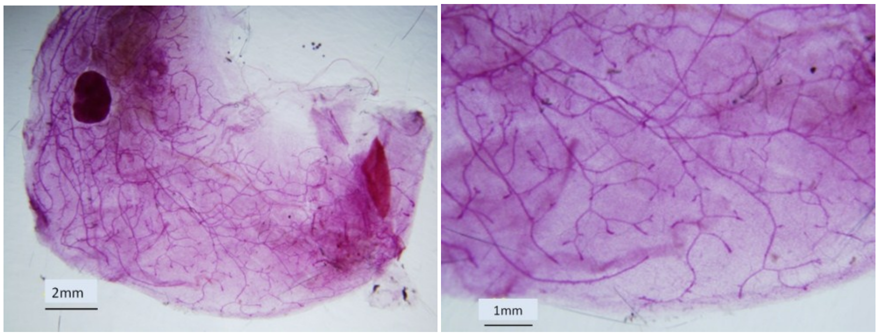

B. Melatonin

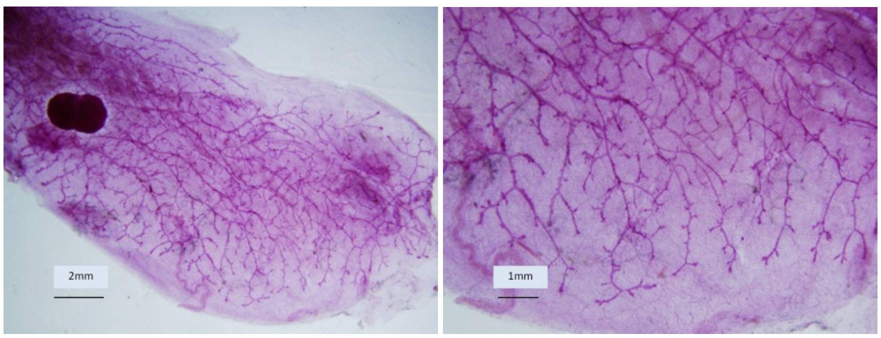

C. EPRT

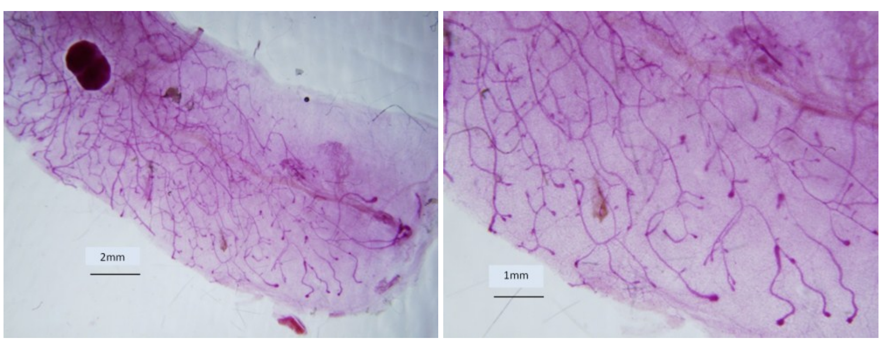

D. EPMRT

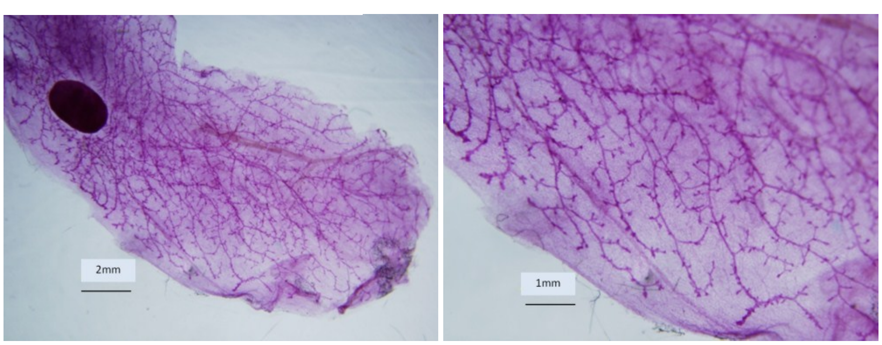

E.

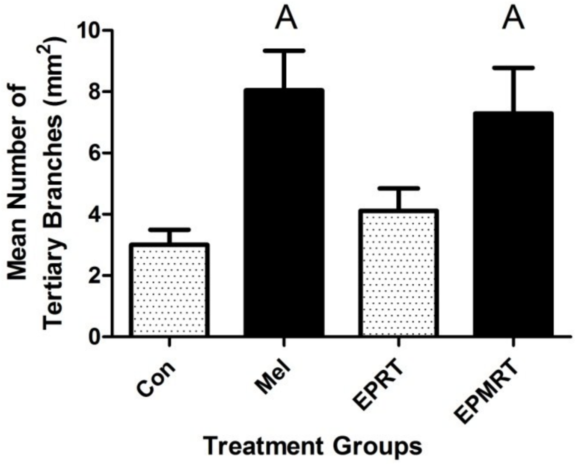

Figure 8. Treatment effects on tertiary branching in mammary glands. Representative images of mammary gland whole mounts displaying the extent of tertiary branching for each group: A) Control, B) Melatonin, C) EPRT, and D) EPMRT. (E) Quantification of stained glands for tertiary branching was performed for each group. Mammary ducts of mice treated with EPMRT or Melatonin had significantly more tertiary side-branches as compared to the Control group. Each bar represents the mean ± SEM values from n = 6 - 7 mice per treatment group. Data were analyzed by one-way ANOVA followed by Newman-Keuls post-hoc test with significance defined as $p < 0.05$. Two-way ANOVA revealed a significant main effect for melatonin, $p < 0.001$, but not for E2 and P4, $p = 0.88$. A = $p < 0.05$ compared to Control. Scale bar set at 2 mm (left panels, magnification = 13x) and at 1 mm (right panels, magnification = 26x).

Detection of melatonin receptors in mammary glands of Control mice

Because melatonin induced tertiary side-branching, investigations were performed to assess if the mammary gland expresses melatonin receptors. Melatonin can produce effects through melatonin receptor subtypes, MT_1 and MT_2, and can also elicit actions independent of these receptors. Therefore, the detection of melatonin receptor expression is important to help determine if the effects of melatonin may be occurring through melatonin receptor-dependent pathways. To determine if melatonin receptors are present in the mammary tissue, total binding assays were performed using the 2-[^{125}I] iodomelatonin radioligand in Control mice. The results are presented in Table 2. Mammary tissues of Control mice expressed low levels of receptor, 7.8 ± 2.8 fmoles/mg protein. Because of the non-selective nature of the radioligand, real-time RT-PCR was performed to assess for levels of melatonin receptor mRNA. The determination of melatonin receptor protein expression by western blot analysis or tissue distribution (i.e., epithelial or adipose) by immunohistochemisty could not be performed due to lack of a well-characterized and field-accepted primary antibodies for these receptors. The results of the real-time RT-PCR analysis indicated that MT_2 receptor mRNA (i.e., *Mtnr1b*) was detected in the mammary tissue in four of the six mice tested; however, no MT_1 receptor mRNA (i.e., *Mtnr1a*) was detected. In contrast to the real-time RT-PCR data, the results of the microarray analysis may suggest the presence of *Mtnr1a* mRNA. These data indicate that the expression of the melatonin receptors is low, and, in the mammary glands, the MT_2 receptor is the primary melatonin receptor subtype expressed. However, the possibility of MT_1 receptor expression was not excluded. These results suggest that the protective actions of EPMRT on mammary tumorigenesis and the effects of melatonin on mammary differentiation may be attributed, in part, to the actions of melatonin at MT_2 receptors in the mammary gland.

[redacted]

Microarray results

Official Symbol	**Accession #**	**Title (Designation)**	**Entrez Gene ID**	**FcMel**	**FcEPRT**	**FcEPMRT**
Mtnr1a	NM_008639	melatonin receptor 1A	17773	1.185	1.11	1.41
Mtnr1b	NM_145712	melatonin receptor 1B	244701	-1.10	-1.11	-1.00

Table 2. Expression of melatonin receptors in mammary tissue of Control mice. Melatonin receptor expression was assessed using 500pM 2-[^{125}I] iodomelatonin on membrane preparations from Control mammary tissue (n = 8). RNA was prepared from mammary tissues from six Controls and subjected to microarray and real-time RT-PCR analyses. Real-time RT-PCR analysis detected MT_2 but not MT_1 receptor mRNA. However, microarray analysis may indicate a presence of MT_1 receptor mRNA. Fc = fold change versus Control where as positive number indicates an increase in melatonin receptor mRNA expression while a negative number indicates a decrease in mRNA expression.

EPMRT synergistically altered gene expression in the mammary gland

To investigate if the protective actions of EPMRT on mammary tumorigenesis may occur through alterations in gene expression, microarray analysis was used to identify those genes differentially expressed in the mammary gland following EPMRT treatment compared to the Control group. To address this question, three pools of total RNA (i.e., two mice per pool from each group) from mammary tissue for each treatment group (Control, Mel, EPRT, and EPMRT) were subjected to microarray analysis. Genes induced by ≥ 1.5 fold or repressed by ≤ -1.5 fold compared to Control were considered as potential candidates to be further analyzed by real-time RT-PCR. The results are presented in Figure 9. Melatonin induced 14 genes, EPRT induced 123 genes, and EPMRT induced 204 genes. Also, Melatonin repressed 16 genes, EPRT repressed 10 genes, and EPMRT repressed 713 genes. EPMRT altered gene expression to a greater extent as compared to the other groups with most of the actions of EPMRT being through gene repression. These results suggest that melatonin in combination with E2 plus P4 (EPMRT) synergistically altered gene expression in the mammary gland.

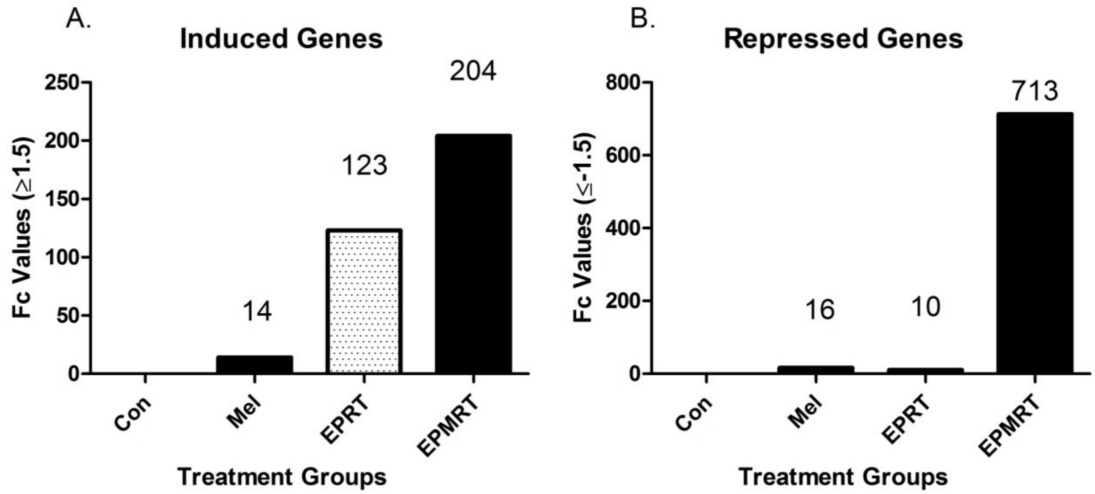

Figure 9. Treatment effects on gene expression in mouse mammary glands. Fold change (Fc) values are expressed by treatment group and compared to Control. EPMRT altered gene expression to a greater extent as compared to the other groups with most of the actions of EPMRT being through gene repression. Data are expressed as total number of genes induced (Fc values ≥ 1.5) or repressed (Fc values ≤ -1.5) for each treatment, n = 3 pools per treatment group.

Venn diagram of the genes with altered expression

To further identify those genes with expression uniquely altered by EPMRT compared to Melatonin or EPRT, a Venn diagram was created to assess the relationships of these genes for each of the treatments. The results are presented in Figure 10. EPMRT altered exclusively 827 genes and co-regulated 69 and 13 genes with EPRT and Melatonin, respectively. These genes may underlie the protective actions of EPMRT on mammary tumorigenesis.

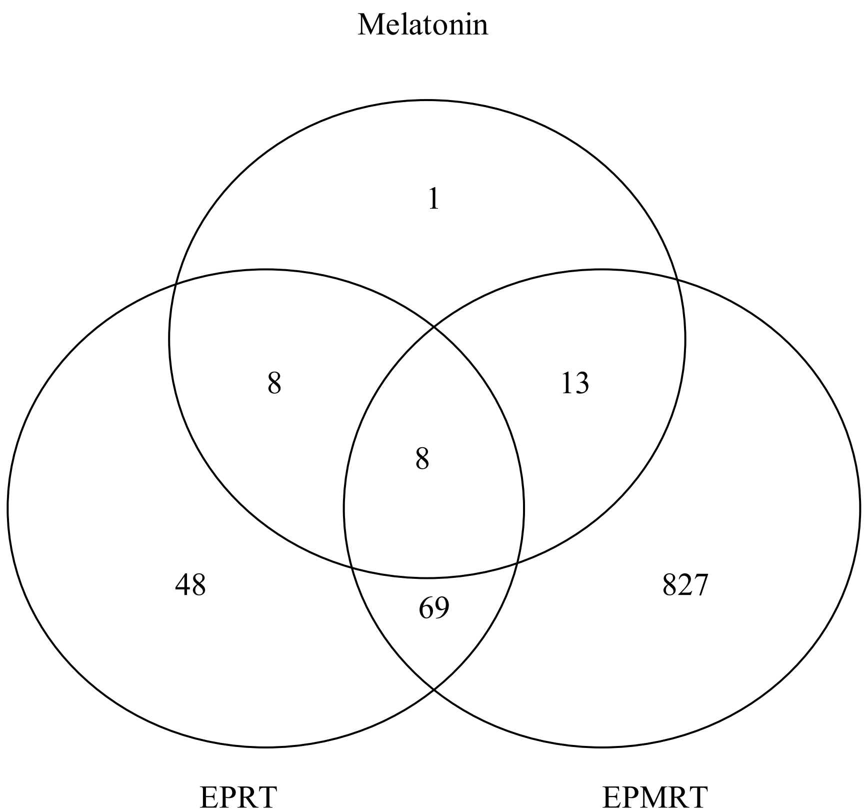

Figure 10. Venn diagram displaying the number of genes with altered expression for each of the treatments. EPMRT altered exclusively 827 genes and co-regulated 69 and 13 genes with EPRT and Melatonin, respectively. Data expressed in the Venn diagram represent the total number of genes with altered expression that were induced (Fc values ≥ 1.5) or repressed (Fc values ≤ -1.5) compared to Control with $n = 3$ [3 pools; 2 mice per pool per treatment group].

EPMRT and the other treatments did not alter the expression of rat *Erbb2*, *Krt18*, and *Ms1a4* mRNA

Before beginning the process of confirming the microarray data by real-time RT-PCR, tissue samples were analyzed to confirm that the samples were from epithelial-enriched regions of the mammary gland and free of lymph node contamination. Moreover, it was important to assess if the treatments did not influence the expression of the rat *Erbb2* transgene which could affect tumorigenesis by regulation at the MMTV promoter. To determine if the selected tissue samples were from epithelial-enriched regions and not from adipose-enriched areas, the levels of *Krt18* mRNA, a gene encoding the epithelial cell marker, keratin 18, were assessed. To determine if the RNA samples were free of lymph node contamination, levels of *Ms1a4* mRNA, the gene encoding B-lymphocyte antigen CD20, were assessed. This assessment was important to ensure that the mRNA in the sample was not diluted by the mRNA from the lymph node, thereby affecting the mRNA levels of the candidate genes. Treatment effects were assessed by determining the change in threshold cycle (ΔCt). A higher ΔCt value indicates lower gene expression and a lower ΔCt value indicates higher gene expression. The results are presented in Figure 11. Statistical analysis detected no significant differences among the four treatments suggesting that the tissue samples expressed similar levels of rat *Erbb2*, *Krt18*, and *Ms4a1* mRNA among the treatments. Because a higher ΔCt value indicates lower gene expression and a lower ΔCt value indicates higher gene expression, the results suggest that the tissue samples were from epithelial-enriched regions and did not contain lymph node tissue. The results also suggest that the levels of transgene mRNA were not altered by the treatments.

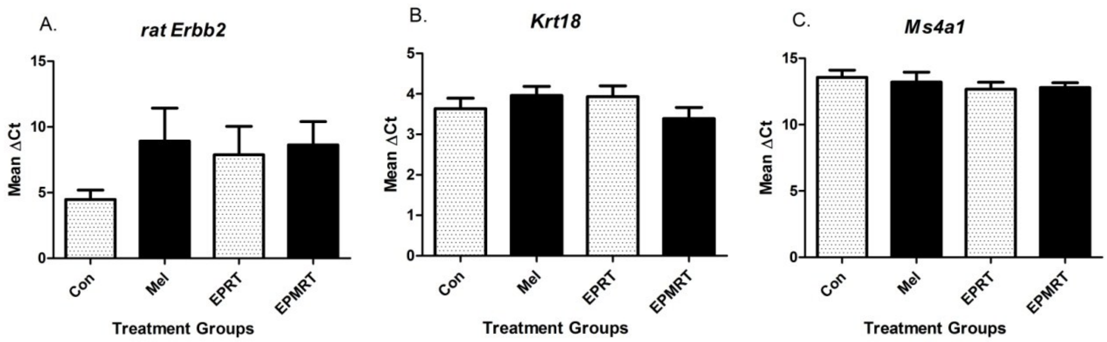

Official Symbol	Accession #	Title (Designation)	Entrez Gene ID
Erbb2	NM_001003817	v-erb-b2 erythroblastic leukemia viral oncogene homolog 2	24337
Krt18	NM_010664	keratin 18	16668
Ms4a1	NM_007641	membrane spanning 4-domains, subfamily A, member 1, B-lymphocyte antigen CD20	12482

Figure 11. Treatment effects on the expression of rat *Erbb2*, *Krt18*, and *Ms4a1 mRNA*. Analysis revealed that the tissue samples expressed similar levels of (A) rat *Erbb2*, (B) *Krt18*, and (C) *Ms4a1* mRNA among the groups. Each bar represents the mean ΔCt ± SEM values from n = 5 - 7 mice per treatment group. Data were analyzed by one-way ANOVA with significance defined as $p < 0.05$.

Selection of candidate genes

To select candidate genes for further investigation by real-time RT-PCR, the Entrez Gene summaries were visually scrutinized for each gene regulated by EPMRT. A list of candidate genes was compiled based on if the genes were hormone-regulated, growth-promoting, related to cell differentiation, or involved in tumorigenesis, in general. The candidate genes are presented in Table 3. The final selection of candidate genes included hormone regulated genes, *Areg*, *Esr1*, *Greb1*, *Per2*, and *Pgr;* growth-promoting genes, *Adra1a*, *Akr1c14*, *Areg*, *Esr1*, *Figf*, *Greb1*, and *Pgr;* genes involved with cell differentiation, *Csn1s2a, Esr1*, *Pgr*, and *St3gal5*; and genes involved with tumorigenesis, *Duox1*, *Figf*, *Greb1*, *Ido1*, *Lcn2*, *Per2*, *Ptprd*, and *Slc24a3*.

Official Symbol	Accession #	Title (Designation)	Entrez Gene ID
Adra1a	NM_013461	adrenergic receptor, alpha 1a	11549
Akr1c14	NM_134072	aldo-keto reductase family 1, member C14	105387
Areg	NM_009704	amphiregulin	11839
Csn1s2a	NM_007785	casein alpha s2-like	12993
Duox1	NM_001099297	dual oxidase 1	99439
Esr1	NM_007956	estrogen receptor 1, alpha	13982
Figf	NM_010216	c-fos induced growth factor vascular endothelial growth factor D (VEGF-D)	14205
Greb1	NM_015764	gene regulated by estrogen in breast cancer protein	268527
Ido1	NM_008324	indoleamine 2, 3-dioxygenase 1	15930
Lcn2	NM_008491	lipocalin 2	16819
Per2	NM_011066	period homolog 2, Drosophila	18627
Pgr	NM_008829	progesterone receptor	18667
Pgr [Pgr(A)]		progesterone receptor A	
Ptprd	NM_001014288	protein tyrosine phosphatase, receptor type D	19266
Slc24a3	NM_053195	solute carrier family 24 member 3 sodium/potassium/calcium exchanger	94249
St3gal5	NM_011375	ST3 beta-galactoside alpha -2, 3-sialyltransferase 5	20454

Table 3. Selected candidate genes for real-time RT-PCR analysis.

Functional annotation clustering of selected candidate genes

The online Database for Annotation, Visualization and Integrated Discovery (DAVID) Bioinformatics Resources 6.7 was used to generate a comprehensive clustering set of functional annotations (i.e., biological functions) to provide an understanding of the biological meaning behind the candidate genes. The hypothesis behind the grouping algorithm is that similar annotations should have similar gene members. Therefore, functional annotation clustering was performed to group these similar annotations together to determine the role of the genes in biological functions. The results of the clustering are presented in Table 4. An annotation cluster consisted of a grouping of biological functions due to sharing similar genes. The genes were grouped into seven clusters [141, 142].

Annotation Cluster 1	Genes	Count
Branching involved in mammary gland duct morphogenesis	*Areg, Esr1, Pgr*	3
Mammary gland duct morphogenesis	*Areg, Esr1, Pgr*	3
Mammary gland morphogenesis	*Areg, Esr1, Pgr*	3
Female sex differentiation	*Areg, Esr1, Pgr*	3
Gland morphogenesis	*Areg, Esr1, Pgr*	3
Mammary gland development	*Areg, Esr1, Pgr*	3
Branching morphogenesis of a tube	*Areg, Esr1, Pgr*	3
Epithelial tube morphogenesis	*Areg, Esr1, Pgr*	3
Morphogenesis of a branching structure	*Areg, Esr1, Pgr*	3
Sex differentiation	*Areg, Esr1, Pgr*	3
Tube morphogenesis	*Areg, Esr1, Pgr*	3
Morphogenesis of an epithelium	*Areg, Esr1, Pgr*	3
Gland development	*Areg, Esr1, Pgr*	3
Tissue morphogenesis	*Areg, Esr1, Pgr*	3
Reproductive developmental process	*Areg, Esr1, Pgr*	3
Tube development	*Areg, Esr1, Pgr*	3
Epithelium development	*Areg, Esr1, Pgr*	3
Annotation Cluster 2		
Response to organic substance	*Adra1a, Areg, Duox1, Esr1, Ido1*	5
Response to hormone stimulus	*Adra1a, Areg, Esr1*	3
Response to endogenous stimulus	*Adra1a, Areg, Esr1*	3
Growth	*Adra1a, Areg, Esr1*	3
Annotation Cluster 3		
Glycoprotein	*Adrala, Areg, Figf, Esr1, Lcn2, Ptprd, Slc24a3, St3gal5*	8
Disulfide bond	*Areg, Figf, Csn1s2a, Lcn2, Ptprd, Slc24a3*	6
Glycosylation site: N-linked (ClcNAc…)	*Adra1a, Areg, Figf, Lcn2, Ptprd, Slc24a3, St3gal5*	7
Annotation Cluster 4		
Signal	*Areg, Figf, Csn1s2a, Lcn2, Ptprd, Slc24a3*	6
Signal peptide	*Areg, Figf, Csn1s2a, Lcn2, Ptprd, Slc24a3*	6
Extracellular region	*Areg, Figf, Csn1s2a, Lcn2*	4
Secreted	*Figf, Csn1s2a, Lcn2*	3
Annotation Cluster 5		
Regulation of cell proliferation	*Figf, Esr1, Ido1, Pgr*	4
Transition metal ion binding	*Duox1, Esr1, Ido1, Pgr*	4
Metal ion binding	*Duox1, Esr1, Ido1, Pgr, Slc24a3*	5
Cation binding	*Duox1, Esr1, Ido1, Pgr, Slc24a3*	5
Ion binding	*Duox1, Esr1, Ido1, Pgr, Slc24a3*	5
Metal-binding	*Esr1, Ido1, Pgr*	3
Annotation Cluster 6		
Rhythmic process	*Esr1, Per2, Pgr*	3
Transcription regulation	*Esr1, Per2, Pgr*	3
Transcription	*Esr1, Per2, Pgr*	3
Regulation of transcription, DNA-dependent	*Esr1, Per2, Pgr*	3
Regulation of RNA metabolic process	*Esr1, Per2, Pgr*	3
Regulation of transcription	*Esr1, Per2, Pgr*	3
Nucleus	*Esr1, Per2, Pgr*	3

Annotation Cluster 7		
Transmembrane	*Adra1a, Areg, Duox1, Greb1, Ptprd, Slc24a3, St3gal5*	*7*
Transmembrane region	*Adra1a, Areg, Greb1, Ptprd, Slc24a3, St3gal5*	*6*
Membrane	*Adra1a, Areg, Duox1, Greb1, Ptprd, Slc24a3, St3gal5*	*7*
Integral to membrane	*Adra1a, Areg, Duox1, Greb1, Ptprd, Slc24a3, St3gal5*	*7*
Intrinsic to membrane	*Adra1a, Areg, Duox1, Greb1, Ptprd, Slc24a3, St3gal5*	*7*
Topological domain: Cytoplasmic	*Adra1a, Ptprd, Slc24a3, St3gal5*	*4*
Topological domain: Extracellular	*Adra1a, Ptprd, Slc24a3*	*3*
Not Clustered		
Cell proliferation	*Areg, Esr1, Figf*	*3*
Oxidation reduction	*Akr1c14, Duox1, Ido1*	*3*
Receptor	*Adra1a, Esr1, Pgr, Ptprd*	*4*
Phosphoprotein	*Adra1a, Csn1s2a, Esr1, Per2, Pgr, Ptprd, St3gal5*	*7*
Plasma membrane	*Adra1a, Esr1, Slc24a3*	*3*

Table 4. Functional annotation clustering of the genes. A DAVID analysis was conducted on the selected candidate genes to determine the functional annotation clustering of the genes. An annotation cluster consisted of a grouping of biological functions due to sharing similar genes. The genes were grouped into seven clusters.

EPMRT decreased expression of *Areg*, *Ido1*, and *Pgr(A)* mRNA

Based on the results of the tumor study, and the effects on gene expression by EPMRT, real-time RT-PCR analysis was performed on the selected candidate genes to confirm whether or not EPMRT altered the expression of these genes compared to Control. Real-time RT-PCR is a method used to validate results obtained from microarray analysis by quantifying changes in gene expression. Treatment effects were assessed by determining the change in threshold cycle (ΔCt). A higher ΔCt value indicates lower gene expression and a lower ΔCt value indicates higher gene expression. The results are presented in Figure 12. Statistical analysis detected significant decreases in the levels of *Areg*, *Ido1*, and *Pgr(A)* mRNA compared to Control. *Areg* encodes amphiregulin, an epidermal growth factor receptor 1 (ERBB1) ligand; *Ido1* encodes indoleamine 2, 3-dioxygenase, an immunosuppressive enzyme that impairs antigen-dependent T-cell activation thereby promoting tumor tolerance; and *Pgr(A)* encodes PRA, a receptor involved in mammary epithelial cell proliferation and differentiation. By contrast, a trend towards a significant increase was detected for *Csn1s2a*, $p = 0.06$. *Csn1s2a* encodes casein alpha s2-like, a marker of ductal differentiation. Therefore, these results suggest that EPMRT significantly modulated genes in a manner that may be protective against mammary cancer.

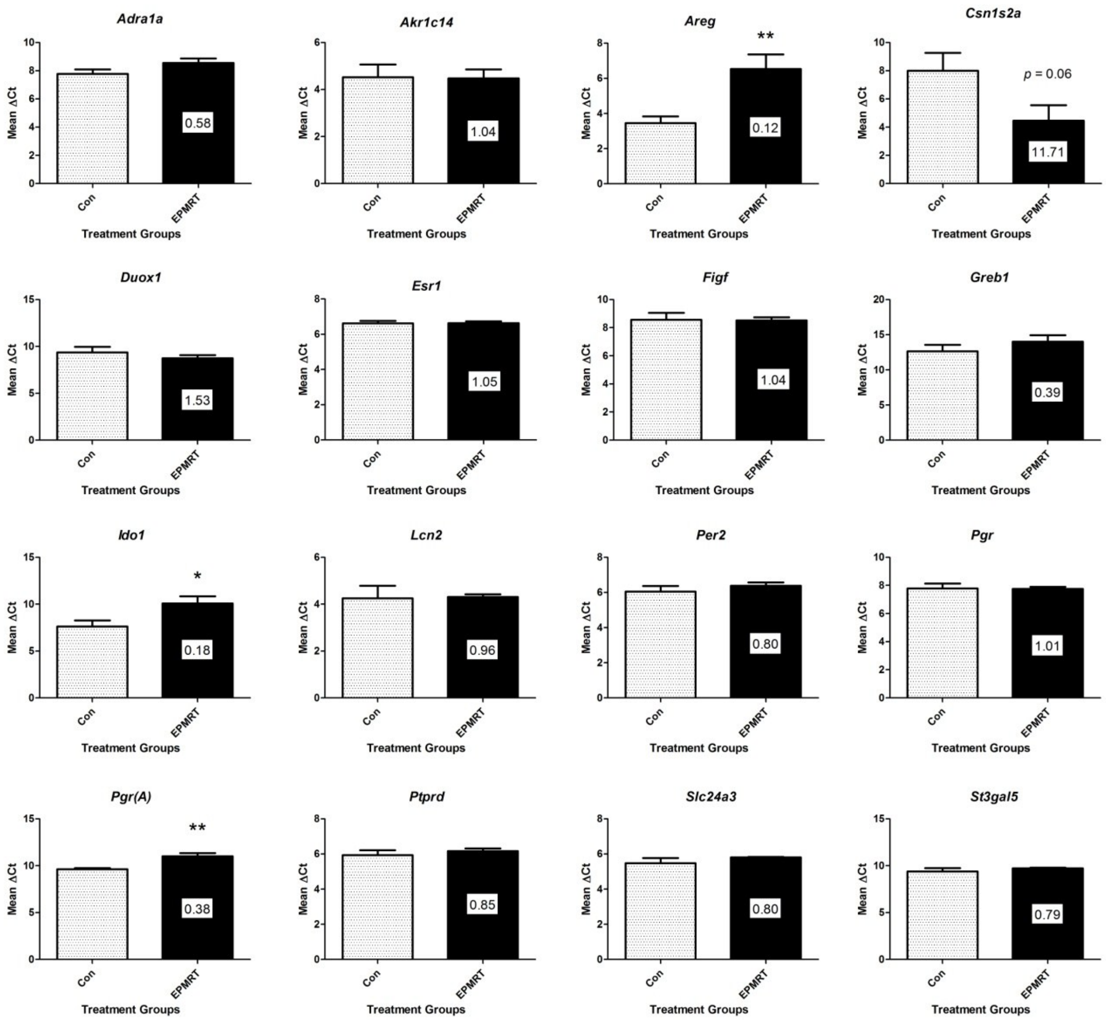

Figure 12. The effect of EPMRT on expression of selected candidate genes in mammary tissue compared to Control. The levels of *Areg*, *Ido1*, and *Pgr(A)* mRNA were significantly decreased compared to Control. A trend towards a significant increase was detected for *Csn1s2a*, $p = 0.6$. Each bar represents the mean ΔCt ± SEM values from n = 5 - 7 mice in Control or EPMRT groups. Value inside the bar represents fold change of expression as determined by the $2^{-\Delta\Delta Ct}$ method. Data were analyzed by unpaired Student's t-test with significance defined as $p < 0.05$ with (*) = $p < 0.05$ and (**) = $p < 0.01$. A higher ΔCt value indicates lower mRNA expression.

Treatments decreased expression *Areg, Ido1, and Pgr(A)* mRNA

In order to ascertain whether the decreases in the levels of *Areg*, *Ido1*, and *Pgr(A)* mRNA following EPMRT exposure were unique to EPMRT, real-time RT-PCR analysis was performed using mammary tissue samples from the Melatonin and EPRT groups. Treatment effects were assessed by determining the change in threshold cycle (ΔCt). A higher ΔCt value indicates lower gene expression and a lower ΔCt value indicates higher gene expression. The results are presented in Figure 13. Statistical analysis detected significant differences among the four treatments for these genes. Mammary tissue from mice treated with Melatonin or EPMRT had significantly decreased levels of *Areg* and *Pgr(A)* mRNA compared to Control (Figs. 13A and 13C) with further analysis indicating a significant main effect for melatonin. The levels of *Ido1* mRNA were significantly decreased in mammary tissue from mice given EPMRT compared to Control (Fig 13B) suggesting that melatonin in combination with E2 plus P4 repressed gene expression.

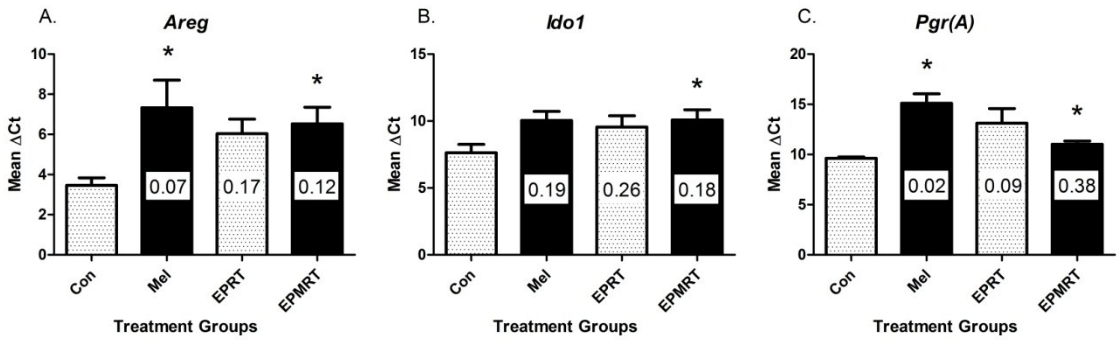

Figure 13. Treatment effects on the expression of *Areg*, *Ido1*, and *Pgr(A)* mRNA in mammary tissue. (A) The levels of *Areg* mRNA were significantly decreased in mammary tissue from mice given Melatonin or EPMRT compared to Control. (B) The levels of *Ido1* mRNA were significantly decreased in mammary tissue from mice given EPMRT compared to Control. (C) The levels of *Pgr(A)* mRNA were significantly decreased in mammary tissue from mice given Melatonin or EPMRT compared to Control. Each bar represents the mean ΔCt ± SEM values from n = 5 - 7 mice per treatment group. Value inside the bar represents fold change of expression as determined by the $2^{-\Delta\Delta Ct}$ method. Data were analyzed by one-way ANOVA followed by Dunnett's post-hoc test (A and B) or by Dunnett's C (C) with significance defined as $p < 0.05$ with (*) = $p < 0.05$. (A and C) Two-way ANOVA revealed a significant main effect for melatonin, $p < 0.05$, but not for E2 and P4, $p = 0.31$ and $p = 0.72$, respectively. A higher ΔCt value indicates lower mRNA expression.

Predicted protein association networks for amphiregulin and indoleamine 2, 3-dioxygenase

The online database resource Search Tool for the Retrieval of Interacting Genes (STRING) 9.05 was used to generate predicted protein – protein interactions of amphiregulin and indoleamine 2, 3-dioxygenase in the mouse. The STRING 9.05 database consists of known and predicted proteins derived from a variety of sources and then quantitatively integrates interaction data to generate an association network. These protein networks provide an opportunity to view a genome more dynamically as compared to a collection of functions. [143, 144].

Predicted protein – protein interactions of amphiregulin

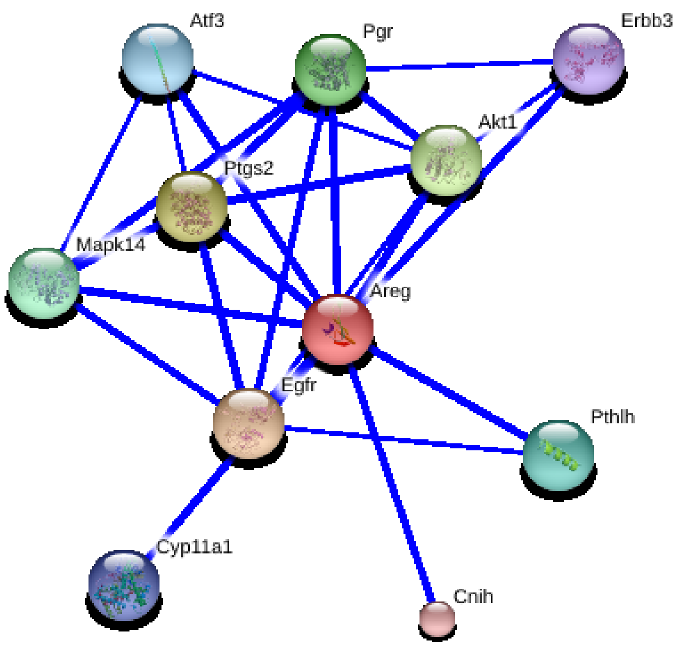

Egfr	epidermal growth factor receptor
Ptgs2	prostaglandin-endoperoxide synthase 2
Akt1	thymoma viral proto-oncogene 1
Pgr	progesterone receptor
Mapk14	mitogen-activated protein kinase 14
Pthlh	parathyroid hormone-like peptide
Atf3	activating transcription factor 3
Cyp11a1	cytochrome P450, family 11, subfamily a, polypeptide 1
Errb3	v-erb-b2 erythroblastic leukemia viral oncogene homolog 3 (avian)
Cnih	cornichon homolog (Drosophila)

Figure 14. Predicted protein – protein interactions of amphiregulin. The online database resource STRING 9.05 was used to generate predicted protein – protein interactions of AREG. STRING quantitatively integrates interaction data to generate an association network.

Predicted protein – protein interactions of indoleamine 2, 3-dioxygenase

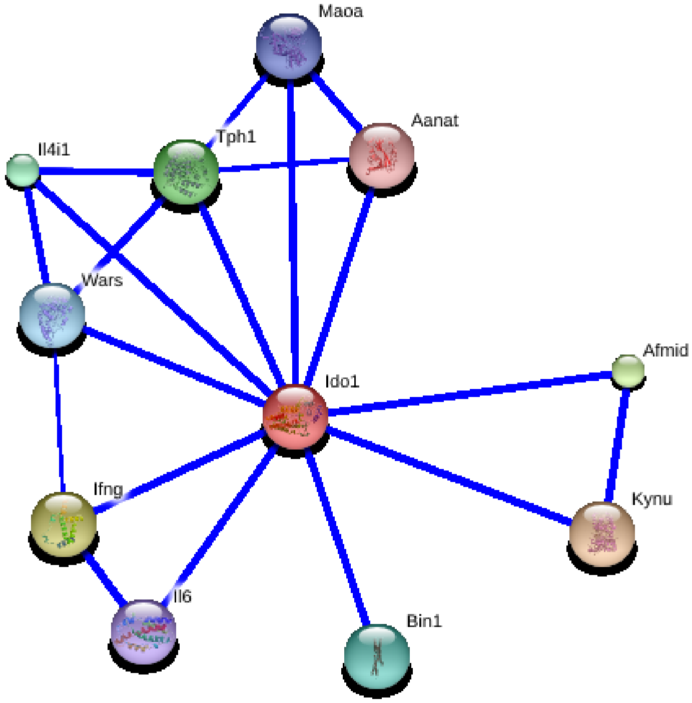

Kynu	kynureninase (L-kynurenine hydrolase)
Ifng	interferon gamma
Afmid	arylformamidase
Tph1	tryptophan hydroxylase 1
Il4i1	interleukin 4 induced 1
Bin1	bridging integrator 1
Wars	tryptophanyl-tRNA synthetase
Maoa	monoamine oxidase A
Il6	interleukin 6
Aanat	arylalkylamine N-acetyltransferase

Figure 15. Predicted protein – protein interactions of indoleamine 2, 3-dioxygenase. The online database resource STRING 9.05 was used to generate predicted protein – protein interactions of IDO1. STRING quantitatively integrates interaction data to generate an association network.

EPMRT and EPRT did not affect uterine wet weight

In the long-term tumor study, mice treated with EPRT, beginning at two months of age and continuing until 14 months of age, resulted in an increase in uterine wet weight. This finding was expected because of the lower dose of P4; therefore, the anti-proliferative actions of P4 on E2-mediated endometrial proliferation would be attenuated. We hypothesized that the addition of melatonin to EPRT would provide uterine protection through changes in P4 and PR levels. To attempt to explain why EPRT increased uterine wet weight while EPMRT had no effect, mice were exposed to these same treatments for 30 days, and the effects on the uterus were assessed. Specifically, treatment effects on uterine wet weight, luminal epithelial cell height, and endometrial proliferation were examined. Uterine wet weight was standardized to body weight (mg/g). The results are presented in Figure 16. Statistical analysis revealed no significant differences among the four treatments suggesting that, unlike the results from the tumor study, EPRT did not promote an increase in uterine wet weight following 30 days of treatment.

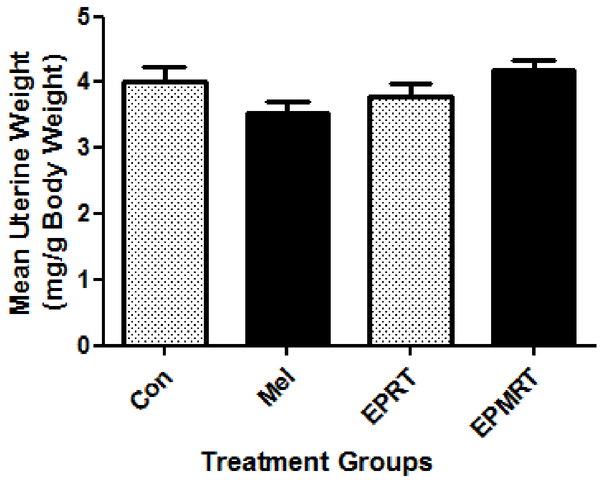

Figure 16. Treatment effects on uterine wet weight standardized to body weight. No significant differences were detected. Each bar represents the mean ± SEM values from n = 13 - 15 mice per treatment group. Data were analyzed by one-way ANOVA with significance defined as $p < 0.05$.

EPRT did not induce hypertrophy of the luminal columnar epithelium

In this 30 day pre-tumor study, mice treated with either EPRT or EPMRT demonstrated an increase in the number of days in estrus and the number of days in estrus per estrous cycle compared to Control. An increase in estrus may indicate an increase in E2 exposure on uterine tissues that may increase the E2-mediated proliferative effects in the endometrium, as well as induce hypertrophy of the luminal epithelium. Assessments of the hormones known to influence the uterus may help to explain the tumor study findings demonstrating that female mice given EPRT for one year had enlarged uteri and when melatonin was added in combination with E2 plus P4 this enlargement was attenuated. Figures 17A, B, C, and D display representative images of uterine cross-sections, and the black arrows denote the luminal columnar epithelium in each image. No increases in luminal epithelial height were qualitatively observed in the uterine cross-sections. In order to determine whether or not the treatments, especially EPRT, resulted in uterine epithelial cell hypertrophy, measurements of the luminal columnar epithelial height were performed on uterine tissue cross-sections taken from mice in estrus per treatment group. The results are presented in Figure 17E. Statistical analysis detected no significant differences among the four treatments suggesting that the treatments did not induce hypertrophy of the luminal epithelium beyond what occurs in mice during in estrus.

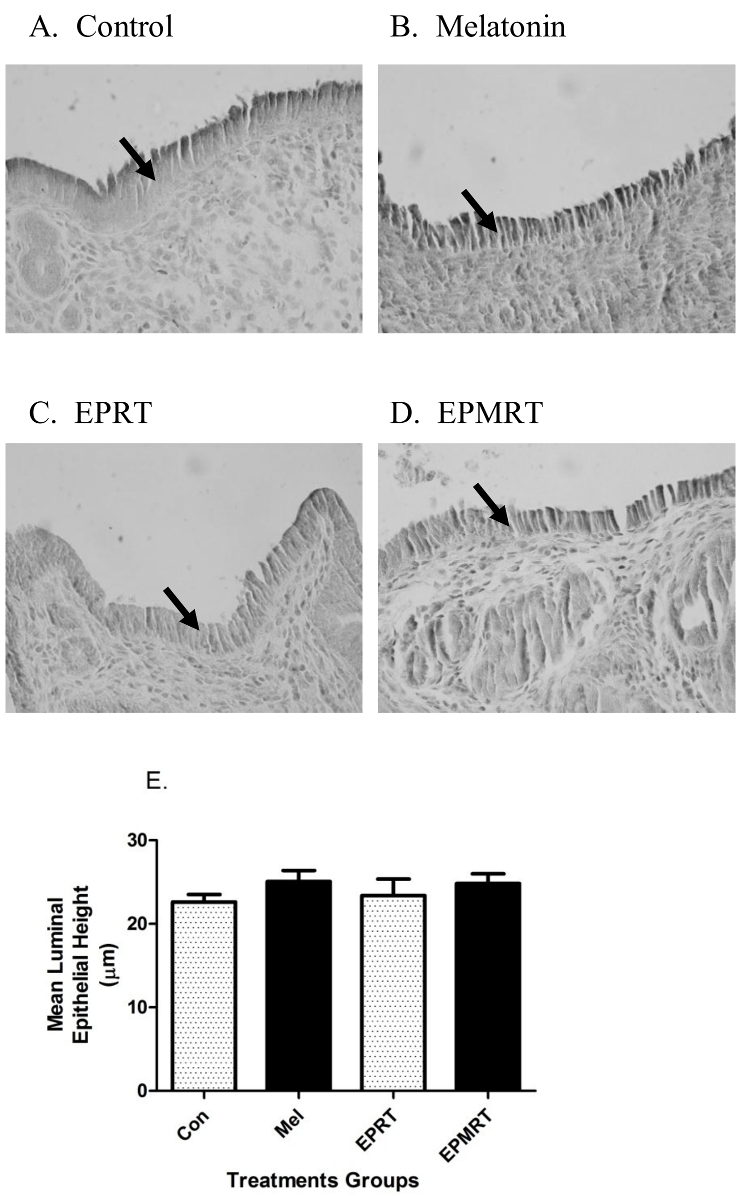

Figure 17. Treatment effects on hypertrophy of the luminal columnar epithelium. Representative images of uterine cross-sections for each group: A) Control, B) Melatonin, C) EPRT, and D) EPMRT. Black arrows denote the luminal columnar epithelium in each image. (E) No significant differences were detected. Each bar represents the mean ± SEM values from n = 6 - 9 mice per treatment group. Data were analyzed by one-way ANOVA with significance defined as $p < 0.05$.

EPRT did not increase endometrial proliferation

Even though mice treated with either EPRT or EPMRT for 30 days demonstrated no changes in uterine wet weight, the length of time in estrus was increased in mice exposed to these treatments. Because estrus is characterized by increased estrogen levels, this may enhance excessive endometrial proliferation. To investigate if EPRT or EPMRT induced excessive endometrial proliferation, uterine cross-sections from each of the four groups were probed with an antibody against Ki67, a protein marker of DNA synthesis. The intensity of Ki67 expression was assessed in both regions comprising the uterine endometrium (i.e., luminal epithelium and stroma). The results are presented in Figure 18. Statistical analysis detected no significant differences among the four treatments for Ki67 expression in the luminal epithelium or stroma suggesting that neither EPRT nor EPMRT increased endometrial proliferation during the 30 days of treatment even though these mice spent more time in estrus.

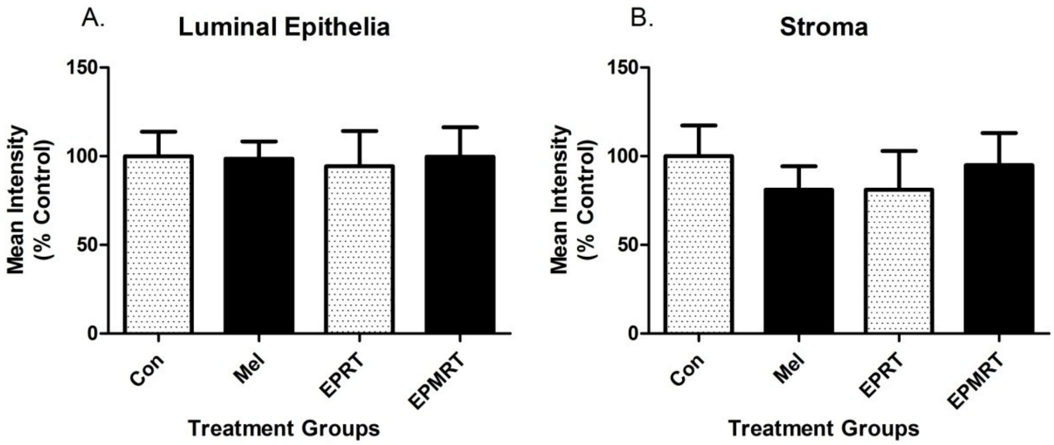

Figure 18. Treatment effects on endometrial proliferation. The intensity of Ki67 expression in the (A) luminal epithelia and (B) stroma was determined. No significant differences were detected. Each bar represents the mean ± SEM from n = 7 - 10 mice per treatment group. Data were analyzed by one-way ANOVA with significance defined as $p < 0.05$.

Melatonin increased uterine expression of ERα and PRA

Modulations of ERα and PRA expression in the uterus by the treatments may provide important early molecular indicators as to why EPRT treatment for over one year increases uterine weight, and how the addition of melatonin blocks this from occurring. In this study, cellular fractions were obtained from uterine cross-sections in order to assess the expression levels of ERα and PRA by western blot analysis. The results are presented in Figure 19. Statistical analysis detected significant differences among the four treatments. Mice treated with Melatonin had significantly increased nuclear expression of ERα and cytosolic expression of PRA in the uterus. The expression levels of these receptors were unchanged in the other groups compared to Control; however, the cytosolic expression of PRA remained elevated in mice treated with EPMRT.

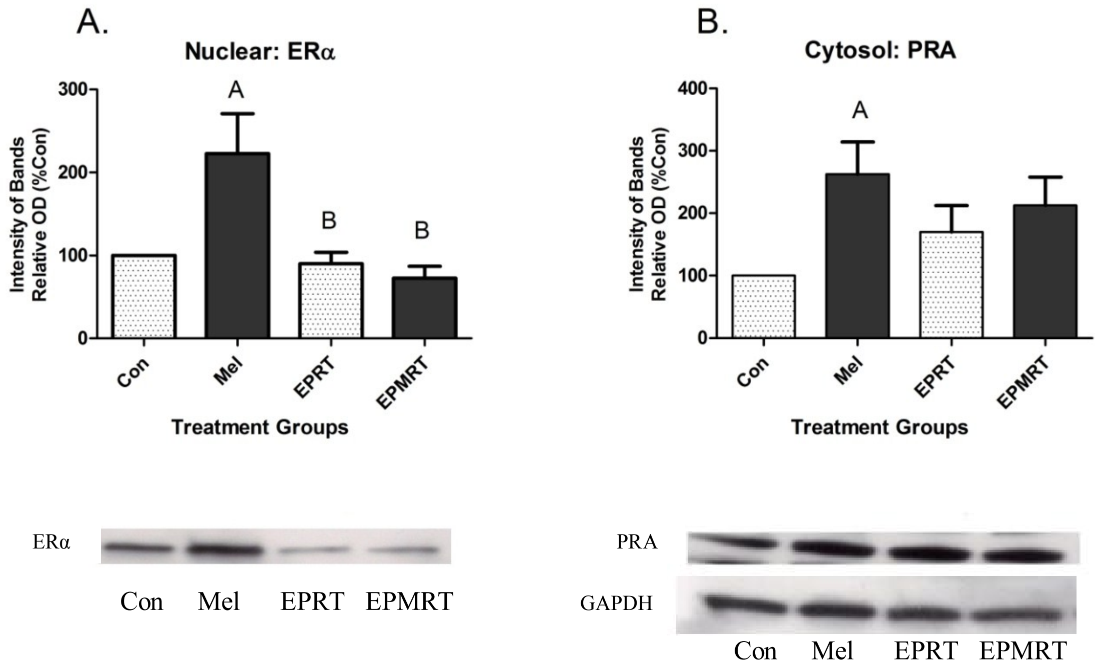

Figure 19. Treatment effects on uterine expression of ERα and PRA. Mice treated with Melatonin had significantly increased (A) nuclear expression of ERα and (B) cytosolic expression of PRA in the uterus. The expression levels of these receptors were unchanged in the other groups compared to Control; however, the cytosolic expression of PRA remained elevated in mice treated with EPMRT. Each bar represents the mean ± SEM from n = 4 - 7 mice per treatment group. Data were analyzed by one-way ANOVA followed by Newman-Keuls post-hoc test with significance defined as $p < 0.05$. A = $p < 0.05$ compared to Control; B = $p < 0.05$ compared to Melatonin.

DISCUSSION

The results of this 30-day pre-tumor study provide important insight into the protective actions of EPMRT against the development, growth, and progression of mammary cancer while protecting the uterus from excess estrogen exposure in the MMTV/unactivated *Neu* mouse model. Because novel HRTs need to be developed for women experiencing menopausal symptoms without increasing their risk of breast cancer, these studies are imperative in order to advance the future use of EPMRT in this population.

In this study, we demonstrated that EPMRT had no effect on body weight and serum levels of P4 and E2. In the mammary gland, specific melatonin binding sites were detected by radioligand binding analysis, and real-time RT-PCR analysis detected expression of MT_2 receptor mRNA. The ductal trees of the mammary glands were fully elongated in all groups; but, melatonin induced tertiary side-branching, an initial stage of ductal differentiation. Moreover, EPMRT differentially regulated gene expression in a synergistic manner compared to Control, and further analysis by real-time RT-PCR revealed decreases in expression of *Areg*, *Ido1*, and *Pgr(A)* mRNA. EPMRT increased the number of days in estrus as well as increased the number of days in estrus per estrous cycle without affecting the length and number of estrous cycles. However, these increases by EPMRT produced no changes in uterine wet weight, luminal epithelial height and endometrial proliferation. Moreover, treatments containing melatonin increased cytosolic localization of the PRA which may protect the uterus from excessive estrogen exposure over time.

The WHI demonstrated that PREMPRO® increased the risk of breast cancer [6, 10] suggesting that the progestogen component of the replacement therapy contributed to the increase in breast cancer and mortality [41]. Our approach was to lower the daily dose of P4 from the clinically recommended dose of 100 mg to 50 mg, because it was hypothesized that lowering the dose of the progestogen component will protect against mammary cancer; however, the reduction in the dose of P4 may not protect the uterus from excessive estrogen exposure. Therefore, melatonin was added to this therapy to provide additional protection against mammary cancer and to prevent excessive endometrial proliferation that could occur with an unbalanced E2 plus P4 therapy. Melatonin was added to the drinking water during the hours of darkness because previous studies using nocturnal, and not daytime, administration of melatonin via drinking water demonstrated effectiveness in preventing chemically- (i.e., dimethylbenzanthracene) and non-chemically-induced mammary carcinogenesis in rodents [88, 117].

Our experimental design utilized non-ovariectomized MMTV/unactivated *Neu* mice to mimic HRT usage in perimenopausal women who maintain ovarian function throughout this stage of their life and who would be ideal candidates for HRT. Also, in this mouse model, E2 is essential for tumor development [117, 145-147] as well as to maintain PR expression in the mammary gland [148-151]. The mice were maintained on an isoflavone-free diet because exposure to isoflavones has been demonstrated to affect tumorigenesis in these mice. Specifically, low-dose dietary isoflavones abrogated tamoxifen-associated mammary tumor prevention; high-dose dietary isoflavones fed to tamoxifen-treated mice resulted in longer tumor latency or no tumor formation by 60 weeks [118]. Also, isoflavones in the diet may affect endogenous E2 levels because women with a diet rich in soy foods have significantly lower E2 serum concentrations [152, 153] through possible suppression of aromatase enzyme activity [154].

EPMRT, as well as the other treatments, in this study had no effect on the body weight of the mice. In contrast, Anisimov V.N. et al. 2003 reported that melatonin (nightly, 20 mg/L), given in drinking water for 30 days, slowed down body weight gain in MMTV/activated *Neu* mice (i.e., over-express the *Neu* oncogene) [117]. Daily food consumption was not monitored in our study; however, the mice in our study consumed about 3.5 mL of water per night consistent with reported consumption of 3.4 ± 1.0 mL of water per night for melatonin-treated MMTV/activated *Neu* mice [117]. Therefore, our results suggest that the treatments had no effect on weight gain as well as on feeding and drinking habits of the mice.

The assessment of serum levels of E2 and P4 is imperative to gain information about the hormone exposures of the mice. Changes in the hormonal levels, specifically in circulating E2 and P4, may influence ductal differentiation and gene expression in the mammary gland as well as proliferation in the uterus. EPMRT and the other treatments did not impact serum hormone levels of E2 and P4 during estrus compared to Control. It was hypothesized that the treatments could decrease endogenous levels of E2 and P4 via inhibition of the gonadotropic axis and/or inhibition of aromatase activity in the ovary. Perhaps the exogenous administration of E2 and P4 via the food pellets masked any changes in endogenous serum E2 and P4 levels and vice versa with endogenous changes masking the supplemented levels. Another possibility was the changes in levels with the added hormones were not large enough to observe because of the normal variations in levels between individual mice. Melatonin increased P4 production, decreased E2 biosynthesis in ovarian granulosa cells [103-107], and inhibited aromatase expression and activity [71, 155]. Based on our RT-PCR results, the addition of melatonin to E2 plus P4 attenuated low dose P4 (25 mg)-induced *Cyp19a1* expression, the gene encoding aromatase, in the ovary possibly through its actions on aromatase promoters (Appendix, Figure 20).

Specific Aim 2 discussion

Even though there were no significant changes in the serum levels of E2 and P4 following administration of the treatments, other sensitive physiological process (i.e., estrous cycling, uterine epithelial height, proliferation, and ERα and PRA expression) regulated by E2 were examined. An assessment of estrous cycling using cytological techniques was conducted to elucidate if the treatments altered normal cycling. The length of the mouse estrous cycle is approximately four to five days and consists of four stages: 1) proestrus, 2) estrus, 3) metestrus, and 4) diestrus (see Figure 1) [129]. During the stages, E2 and P4 levels fluctuate. During proestrus, E2 production increases with elevated levels persisting throughout estrus before production reduces with levels remaining relatively unchanged during metestrus and diestrus. However, the level of P4 begins to increase after estrus due to the secretion of P4 by the newly formed corpus lutea [129, 156, 157].

Increasing levels of estrogen and an increase in duration of exposure in the mammary gland and uterus to estrogen may stimulate mammary carcinogenesis and excessive endometrial proliferation, respectively. Therefore, assessing alterations to the reproductive cycle may help to explain the protective actions of EPMRT as demonstrated in the tumor study. The pre-tumor study revealed that EPRT and EPMRT increased the number of days the mice spent in estrus over 30 days; however, the length and number of estrous cycles did not change over the same period of time. These results were similar to Anisimov V.N. et al. 2003 who reported an average length of an estrous cycle of 5.5 ± 0.31 days for Control mice and 6.38 ± 0.35 days for Melatonin-treated mice over 30 days. In our pre-tumor study, the Control and Melatonin mice had an average length of an estrous cycle of 6.10 ±1.28 days and 5.90 ± 1.18 days, respectively,

One difference between our study and that of Anisimov V.N. et al. 2003 was the percentage of days each mouse spent in estrus per estrous cycle for Control and Melatonin. In our study, the Control and Melatonin-treated mice were in estrus 36.1% and 34% of the time, respectively. However, Anisimov V.N. et al. 2003 reported values of 45% for Control and 51% for Melatonin-treated mice [117]. These minor variations may be attributed to the different dose of melatonin (i.e., 15 mg/L versus 20 mg/L used by Anisimov et al.), the diets, or the housing conditions.

The results indicated that Melatonin did not modify overall estrous function. This was an unexpected finding because melatonin has been implicated in the seasonal reproductive behavior of some animals (e.g., sheep and hamsters) [158], that is dependent upon the environmental conditions [159]. Moreover, melatonin has been demonstrated to regulate the estrous cycle in felines [160] and has been tested for use as a birth control in women [161]. If melatonin was inhibiting estrogen synthesis and stimulating P4 levels in the ovary, the days in estrus was hypothesized to decrease while the time in diestrus was hypothesized to increase. This effect was not observed in this study. However, EPMRT and EPRT increased the days in estrus and per estrous cycle, but did not affect the length and number of estrous cycles. The observed increase in the number of days in estrus induced by EPRT may explain the overall increase in uterine wet weight observed in the tumor study possibly due to an increase in exposure of the endometrium to estrogens. The addition of melatonin to E2 plus P4 did not attenuate the EPRT-induced increase in days in estrus indicating that melatonin did not have an inhibitory effect within 30 days. Thus, the 30-day treatment period may not have been long enough to produce any measureable effects in the uterus.

Even though no change in uterine wet weight was observed, the treatments may have affected uterine cell hypertrophy and/or proliferation. To assess for changes in epithelial cell hypertrophy, the height of the luminal columnar epithelial cells was measured following immunohistochemical staining of uterine tissue cross-sections. No observable or measurable changes in the height of these cells were detected across the treatments suggesting that the treatments, especially EPRT, did not induce hypertrophy of the luminal epithelium beyond what occurs in mice during in estrus.

Although no treatment effects occurred on epithelial cell hypertrophy, the treatments, especially EPRT, may have increased endometrial proliferation. Therefore, the expression of Ki67 in the luminal epithelium and the stroma, regions comprising the endometrium, was measured; an increase in Ki67 indicates a transition from G1 to the S phase of the cell cycle. No changes in the expression levels of Ki67 in the luminal epithelium and the stroma occurred among the treatments suggesting that the treatments did not increase cellular proliferation.

Even though there were no detectable changes in uterine weight, epithelial height, and proliferation by the treatments within 30 days, changes in the cellular ERα and PRA expression within the uterus may have occurred. Therefore, if given enough time, the changes in ERα and PRA expression may have altered the sensitivity of uterine tissues to these hormones to result in the observed increases in the uterine wet weight in the tumor study. Therefore, ERα and PRA levels in the uterus were assessed by western blot analysis. Mice treated with Melatonin had significantly increased nuclear expression of ERα and cytosolic expression of PRA; however, the cytosolic expression of PRA remained elevated in mice treated with EPMRT. Perhaps the increase in PRA expression in the uterus induced by melatonin underlies, in part, the protective actions of chronic EPMRT on uterine proliferation. Progestogens, acting via PRs, inhibit E2-induced increases in uterine cell hypertrophy and proliferation [1].

Specific Aim 1 discussion

In the mammary gland, the oncostatic effects of E2 and its metabolites include tumor initiation and promotion, regulatory control of genes, and cell proliferation. Estrogens regulate cancer-associated genes like *Erbb2* (i.e., *Neu*) [162, 163] or induce transcriptional up-regulation, synthesis, and secretion of heregulin (HRG), epidermal growth factor (EGF), amphiregulin, and the EGFR [164-167]. An increase in cell proliferation enhances the probability of genotoxic events that produce genetic mutations [168-172]. Because E2 is known to influence tumorgenesis in this model, it was hypothesized that melatonin, through its anti-estrogen actions, would attenuate tumorigenesis induced either by endogenous estrogens or through EPRT by initiating differentiation, by repressing genes in the mammary gland known to be involved in mammary cancer, and by inducing genes known to be involved in mammary ductal differentiation.

The process of mammary ductal development is a complex, tightly regulated orchestration of growth, proliferation, and other cellular process in the course of a few weeks to create an adult ductal network. In mice, this process begins at approximately at four weeks of age and concludes by eight weeks of age. During this time, the mammary ducts develop from a rudimentary tree, through elongation of the ducts into the mammary fat pad, to be become a branched network of ducts. Ductal elongation into the mammary fat pad occurs via the proliferation and differentiation of the epithelial progenitor cells in the terminal end buds located on the leading edge of the elongating ducts. This process is mediated by E2 actions at ERα because mammary glands lacking ERα demonstrated impaired ductal growth [134-136].

Ductal elongation in MMTV/unactivated *Neu* mice mammary glands may also be mediated by EGF signaling through ERBB1 receptors as evidenced by implantation of pellets containing EGF into estrogen-depleted mice initiated ductal growth [173]. The ERBB receptors influence cell proliferation, differentiation, development, and survival as well as being implicated with breast cancer tumorigenesis [174, 175]. The ERBB receptor belongs to the receptor protein tyrosine kinase superfamily that include ERBB1 (i.e., EGFR), ERBB2 (i.e., NEU), ERBB3, and ERBB4. Unlike the other family members, ERBB2 is an orphan receptor with no known endogenous ligand to initiate intracellular signaling. For example, ERBB3 and ERBB4 bind heregulin (HRG) while ERBB1 binds EGF, TGF-α, and amphiregulin [176, 177].

Amphiregulin is an EGFR/ERBB1 ligand that exists as a type 1 transmembrane protein in epithelial cells and extracellular cleavage produces the soluble ligand [178, 179]. Ectodomain shedding of the protein is important for control of ligand availability and activation of the EGFR [180]. The shedding allows amphiregulin to activate EGFR through paracrine and autocrine signaling. Even in the absence of shedding, the membrane bound amphiregulin may activate the EGFR through juxtacrine signaling [177].

Estrogens are important activators of amphiregulin expression because estrogen, through ERα, induced amphiregulin expression. This occurred through ERα binding to EREs on the gene [166] thus resulting in estrogen-induced expression in the breast [181]. Amphiregulin has been demonstrated to be important during ductal growth where inactivation of the *Areg* gene in mice delays pubertal ductal elongation [179]. Levels of *Areg* mRNA increased in mammary glands of FVB mice between two to five weeks of age and remained elevated past five weeks. Furthermore, these levels remained elevated into early pregnancy and then decrease sharply and remained low throughout lactation and involution [182]. Pregnancy, a time of increased mammary gland differentiation, may reduce the expression of amphiregulin. For example, *in situ* hybridization studies revealed reduction of *Areg* expression in parous mammary epithelia [182]. Also, the expression of *Areg* was reduced after the first pregnancy in rats and was correlated with reduced tumorigenecity [182, 183].

Elevated levels of *AREG* mRNA has been implicated in the pathogenesis of breast cancer, and the protein is over-expressed in 35-50% of breast cancers [184-186]. Hyperplastic enlarged lobular units (HELUs) are a common abnormality in breast tissue of adult women [187, 188]. Lee S. et al. 2007 reported an increase in *AREG* expression with a concomitant decrease in EGF expression in HELUs relative to terminal duct lobular units (TDLUs). These results suggested that a reactivation of embryonic development and a suppression of terminal differentiation could occur by switching EGFR ligand expression. This switching of ligand expression could lead to different functional consequences [189]. Lastly, amphiregulin expression was increased in mammary tumors of transgenic mice over-expressing the *Erbb2* oncogene [190].

We wanted to investigate if any of the treatments altered ductal elongation into the mammary fat pad because E2 is known to increase ductal elongation and melatonin, having anti-estrogenic properties, was hypothesized to decrease this process. To explore this question, a quantitative assessment of ductal elongation was performed in carmine alum stained mammary glands. The results revealed no significant differences on ductal elongation. This result was in agreement with Mukjerjee S. et al. 2000 who reported that ductal elongation in MMTV/unactivated *Neu* mice was 93.3% ± 6.0 of the fat pad at 10 to 15 weeks of age [151] similar to our results where ductal elongation in Control mice was 86.6% ± 7.2 of the fat pad and 79.8% ± 7.7 to 92.7% ± 1.6 for the other treatments at 12 weeks. These data suggest that ductal elongation was concluded by the time of treatment exposure. These results were also interesting because the levels of *Areg* mRNA were decreased in EPMRT-treated mice compared to Control. Even though there were no significant differences in overall elongation among the treatments, the decrease in the levels of *Areg* mRNA by EPMRT may indicate a termination of ductal elongation, at the genetic level, thereby reducing the overall proliferative capacity of the ductals earlier than EPRT. The decrease in levels of *Areg* mRNA at this time point by EPMRT may be contributing to the anti-tumor effects.

Differentiation of the mammary ducts in women contributes to the long-term decrease in breast cancer risk [137]. Melatonin induced differentiation in various cells lines expressing melatonin receptors and through MAPK pathways [58, 59, 66, 78]; therefore, the addition of melatonin to E2 plus P4 may enhance the induction of ductal differentiation through these mechanisms. However, melatonin may also induce ductal differentiation through effects on P4 and P4-mediated processes. Once ductal elongation is complete, the ducts begin to arborize through development of tertiary side-branches, an early stage of mammary differentiation, with P4 signaling through PRA being necessary for this process [136, 138-140]. Specifically, PR-deficient mice have less extensive tertiary branching [191] while over-expression of PRA increased tertiary-side branching by 10 to 14 weeks of age [192]. P4-induced activation of signal transducer and activator of transcription 5a (STAT5a) may be important for induction of tertiary side-branching because mammary glands of STAT5a-/- mice demonstrate defects in tertiary side-branching suggesting that Stat5a regulates this process [193].

To assess if the treatments induced tertiary side-branching, the number of tertiary side-branches in a given area were quantified in carmine alum stained post-pubertal mammary glands. The mammary glands of the EPMRT and Melatonin groups demonstrated enhanced tertiary side-branching suggesting an overall melatonin effect because EPRT had no effect compared to Control. Melatonin may be inducing tertiary side-branching through melatonin receptors and associated signaling cascades and/or through actions of melatonin on P4 synthesis and P4-mediated processes.

Regarding melatonin and melatonin receptors, melatonin binding sites have been detected in the mouse mammary gland [67] and other studies have demonstrated melatonin- and melatonin receptor-mediated effects on mammary gland development [133, 194] may be influenced by fluctuating melatonin levels. In the MMTV/unactivated

Neu mouse, a diurnal rhythm of melatonin secretion exists [195]. Thus, the rise in melatonin during the hours of darkness and the persistence for at least eight hours may regulate the melatonin receptors in a way that promotes cellular differentiation through β-arrestin scaffolds and MEK/ERK 1/2 activation [57, 59, 60]. Therefore, it was important to detect melatonin receptor binding sites and confirm the type of melatonin receptor in the mammary gland to provide support for the hypothesis of a melatonin receptor-dependent mechanism. To assess for melatonin specific binding sites in the mammary glands, radioligand binding analysis on mammary glands from Control mice was performed. The mammary glands were found to express melatonin receptors at 7.8 ± 2.8 fmol/mg protein.

Real-time RT-PCR was performed to assess for levels of melatonin receptor mRNA. The determination of melatonin receptor protein expression by western blot analysis or tissue distribution (i.e., epithelial or adipose) by immunohistochemisty could not be performed due to lack of a well-characterized and field-accepted primary antibodies for these receptors. The results of the real-time RT-PCR analysis indicated that MT_2 receptor mRNA was detected in the mammary tissue in four of the six mice tested; however, no MT_1 receptor mRNA was detected. The microarray analysis suggested the presence of *Mtnr1a* mRNA, but this was not confirmed by the real-time RT-PCR analysis. These data indicate that the relative expression of the melatonin receptors was low, and, in the mammary glands, the MT_2 receptor is the primary melatonin receptor subtype expressed. However, the possibility of MT_1 receptor expression was not excluded. The results suggested that the protective actions of EPMRT on mammary tumorigenesis and the effects of melatonin on mammary differentiation may be attributed, in part, to the actions of melatonin at MT_2 receptors in the mammary gland. We further suggest that the effects of melatonin are not receptor independent because there was no change in tumor incidence in the tumor study which was hypothesized to have occurred if melatonin was acting as a free radical scavenger.

In contrast to our results, Xiang S. et al. 2012 reported that in transgenic B6SJLF2 mice over-expressing the MT_1 receptor (i.e., MT1-mOE) significant reductions in branching occurred at 12 weeks of age. Also, nightly melatonin administration (25 µg/day i.p. 1 hr before lights off) for four weeks attenuated the E2 (0.1 mg pellet) plus P4 (10mg pellet)-induced increase in ductal branching in both B6SJLF2 and MT1-mOE mice by eight weeks of age. Moreover, the elevated MT_1 expression in mammary glands of pregnant and lactating MT1-mOE mice was associated with reduced lobuloalveolar development as well as reduced mammary expression of phospho-STAT5, a protein involved with inducing tertiary side-branching [194]. These conflicting findings could be explained by the time of administration of these treatments. For example, the administration of these treatments at the beginning of puberty, which is a critical time for mammary ductal growth, delays the induction of ductal differentiation while administration of our treatments post-pubertal enhances the initiation of ductal differentiation. Therefore, the timing of drug exposure, especially melatonin, may be an important factor that needs to be further scrutinized.

Melatonin may be enhancing mammary gland differentiation through increasing P4 synthesis, PRA expression, and P4-mediated pathways. P4 has been demonstrated to induce tertiary side-branching through actions at PRA [136, 138-140]. Thus, it was hypothesized that melatonin would induce ductal differentiation by increasing PRA expression in the mammary gland of mice treated with Melatonin and EPMRT. The levels of *Pgr(A)* mRNA were significantly decreased in the mammary tissues from mice treated with Melatonin and EPMRT.

The differences between the results of the tertiary branching analysis and the real-time RT-PCR analysis seem to be contradictory. The tertiary branching results suggest that melatonin may be promoting P4 actions in the mammary gland while the real-time RT-PCR results revealed a reduction in levels of *Pgr(A)* mRNA. For example, in rat gonadotropes and mouse mammary glands, E2 through actions at ERα, demonstrated increased expression of PRs [196-198]. Therefore, melatonin may be reducing E2 actions thereby inhibiting E2-induced PRA expression as observed in the real-time RT-PCR results. However, PRA expression levels in the mammary glands were not assessed by western blot or immunohistochemistry analyses. Therefore, future studies will need to assess if the decrease in *Pgr(A)* mRNA relates to changes in PRA expression. Also, the increase in tertiary branching may indicate that melatonin is stimulating tertiary branching without the need for increasing PRA expression. As the process of tertiary branching may have already been completed, the mRNA results may not reflect the changes that occurred in the developing gland undergoing this initial stage of differentiation. In conclusion, the effects through PRA are unlikely to be solely responsible for the melatonin-induced tertiary side-branching in the Melatonin and EPMRT groups.

To further characterize the progression of mammary differentiation, lobuloalveolar development, an indicator of a fully differentiated mammary duct, was assessed. Lobuloalveolar development is characterized by extensive expanding of the mammary ducts that fills the stroma, and this event occurs during pregnancy to prepare the ducts for lactation. Collectively, none of the mammary glands of any treatment displayed lobuloalveolar development (data not shown). The assessment of lobuloalveolar development was important to further characterize the type of PR expressed in the mammary gland. Pregnancy induces the expression of PRB and P4 actions at PRB drive lobuloalveolar growth in mice. Therefore, we conclude that P4 signaling in virgin glands of the treated mice occurred mostly through PRA. Overall, melatonin induced the initial stage of differentiation (i.e., tertiary side-branching) in the mammary gland, and this may have contributed to the reduced tumor formation by EPMRT through initiating ductal differentiation earlier in these mice.

The hypothesis that genetic expression changes or mutations are involved in cancer development especially in genes that control cell growth, survival, and/or differentiation is generally accepted and supported. Results from randomized clinical trials suggest that estrogen plus progestogen therapies increase the risk of breast cancer unlike estrogen alone therapies [1]. These findings suggest that the mitogenic actions of progestogens increase the likelihood of developing new mutations [1, 199, 200]. However, the mitogenic actions of progestogens are controversial, and it is believed that the type of progestogen may be crucial to the risk of breast cancer [1]. In addition to progestogens, estrogen may also have a role as estrogen is required to induce tumorigenesis in the MMTV/unactivated mouse model.

E2-induced mammary tumorigenesis in MMTV/unactivated *Neu* mice was independent of MMTV activity, and the tumors were characterized by having an increased proliferative rate, higher histologic grade, an increase in multiplicity, and a shorter latency of development [147]. Higher proliferative rates were observed in mammary tumor-derived cell lines taken from E2 exposed mice [145, 146]. The timing of E2 exposure may be important because short-term E2 exposure during the early reproductive period promoted mammary tumorigenesis with a peak window of risk between 8 to 16 weeks of age [145]. Also, ovariectomies performed at six weeks of age in the mice resulted in a reduction of both abnormal terminal end buds and hyperplastic ducts as compared to intact mice suggesting that proliferation of terminal end buds and ducts was ovarian dependent and associated with ERα-positive cells [124]. Subsequent investigations with mammary tumor-derived cell lines demonstrated that E2 induces HRG, a ligand for the ERBB3 receptor, resulting in heterodimer formation with ERBB2. The dimerization activated the ERBB2 leading to the activation of MAPK and PI3K/AKT pathways. This E2-induced cell proliferation was inhibited by ICI-182,780 (Fulvestrant), an ER antagonist that down-regulates ERs; AG825, an ERBB2 tyrosine kinase inhibitor; and by siRNA to reduce ERBB3 expression [147]. Moreover, short-term exposure with tamoxifen, an ER antagonist, abolished tumorigenesis in a high percentage of these mice [118].

To investigate if the protective actions of EPMRT on mammary tumorigenesis may occur through alterations in gene expression, microarray analysis was performed to identify those genes uniquely modulated in the mammary gland following EPMRT treatment. EPMRT resulted in differential expression of hundreds more genes compared to the other groups with more genes being repressed than induced (713 versus 204). Interestingly, Melatonin and EPRT induced 14 and 123 genes, respectively, and repressed

16 and 10 genes, respectively. Therefore, melatonin in combination with E2 plus P4 synergistically altered gene expression in the mammary gland.

To further identify those genes with expression uniquely altered by EPMRT, a Venn diagram was created. EPMRT altered exclusively 827 genes and co-regulated 69 and 13 genes with EPRT and Melatonin, respectively. Before beginning the real-time RT-PCR analysis of candidate genes, the RNA samples were analyzed for the epithelial cell marker, *Krt18*, to ensure equal amounts of epithelial tissue amongst the groups. Also, it was important to ensure the sampling was obtained from an epithelial-enriched area as opposed to an adipose-enriched area. Samples were also analyzed for lymph node contamination by assessing for *Ms1a4*, the gene encoding B-lymphocyte antigen CD20. Finally, levels of rat *Erbb2* (*Neu*) mRNA were assessed to ensure no treatment effects on gene transcription. No significant differences were detected among the groups suggesting the tissue samples expressed similar levels of rat *Erbb2*, *Krt18*, and *Ms4a1* mRNA among the groups. The tissues selected for all groups contained high levels of epithelial mRNA. Also, the samples contained very low levels, if any, of *Ms1a4*, the gene encoding B-lymphocyte antigen CD20, suggesting an absence of lymph node tissue. Therefore, this suggests that the mRNAs in the sample were not being diluted by mRNAs from the cells located in the lymph node. These findings also suggest that alterations in transcription of the candidate genes were due to the treatments and not due to different amounts of epithelial tissue between groups or lymph node contamination.

The finding that the transcription of the rat *Neu* transgene was not significantly different among the groups, $p = 0.25$ was also important because altered expression of the transgene would suggest regulation of the MMTV promoter by the treatments thereby influencing *Erbb2* gene and subsequent receptor expression and possibly tumor development. The MMTV promoter is active in virgin mice with activity increased by pregnancy. The MMTV promoter contains the Long Terminal Repeat (LTR) that has hormone-responsive elements which control the transcription of genes. Even though the MMTV promoter does not contain an ERE and was not modulated following E2 exposure [201], the promoter was responsive to glucocorticoids, prolactin, androgens, and P4 [201-205]. Specifically, the promoter was induced by the binding of an activated PR to a cluster of five hormone responsive elements (HREs) [206]. In contrast to our study, Baturin D.A. et al. 2001 reported that constant nightly melatonin exposure (20 mg/L) in MMTV/activated *Neu* mice resulted in a 2.5-fold reduction in levels of rat *Erbb2* mRNA in mammary tumors suggesting a decrease of *Erbb2* gene transcription [207]. Some factors that could have contributed to the lack of regulation of the transgene in our pre-tumor study include the fact that the mice were euthanized in estrus (i.e., state of high E2 and low P4 levels), and the serum levels of P4 were not increased by any of the treatments.

In the long-term tumor study, mice treated with EPMRT had improved tumor outcomes. One of the goals of this study was to identify candidate genes underlying the protective effects of EPMRT on tumorigenesis. Therefore, to confirm the results of the microarray, we performed real-time RT-PCR analysis on the selected candidate genes. These candidate genes were selected based on the following criteria: hormone regulated, growth promoting, related to epithelial cell differentiation, or involved in tumorigenesis. To further explore the biological functions of these selected candidate genes, a DAVID analysis was performed. The genes were grouped into seven clusters with the largest cluster involving mammary gland development and morphogenesis. Also, the analysis revealed that some of candidate genes were involved with signaling or transcription regulation. We performed an initial screening of these genes in mice given EPMRT for 30 days compared to Control. The results revealed significant decreases in levels of *Areg*, *Ido1*, and *Pgr(A)* mRNA, genes that are hormone-regulated, involved with growth promotion, or involved in tumorigenesis. Moreover, a trend nearing significance was detected for *Csn1s2a*, ($p = 0.06$), a marker of mammary ductal differentiation. These data suggest that expression of *Csn1s2a* mRNA may be increased due to increased ductal differentiation after EPMRT treatment. Based on the results of the initial screening, which identified three candidate genes, we expanded the real-time RT-PCR analysis to include mammary tissue exposed to Melatonin or EPRT.

The finding that the levels of *Areg* mRNA were significantly decreased by EPMRT, as well as by Melatonin, indicated a possible reduction of the EGFR (ERBB1) ligand. The reduction of mRNA levels may be a result of the anti-estrogenic actions of melatonin because the *Areg* gene contains an ERE [166] and gene transcription was induced by E2 [181]. Therefore, melatonin may be reducing the binding of the E2-ERα complex to the ERE [79] thereby attenuating gene transcription that may lead to decreased amphiregulin protein production which would decrease ERBB1 receptor activation and decrease mammary epithelial cell proliferation. Because amphiregulin does not bind and activate ERBB2, but does activate ERBB1, then transactivation of ERBB2 by ERBB1 or heterodimer formation between ERBB1 and ERBB2 may be occurring in the mammary tissue leading to mammary tumorigenesis. Heterodimer formation between the transgene ERBB2 and endogenous ERBB1 is probably not occurring because these heterodimers were not detected in the presence of EGF in tumor cell lines derived from MMTV/unactivated *Neu* mice [125]. Also Muller W.J. et al. 1996 failed to detect ERBB1/ERBB2 heterodimers in tumor tissues from bigenic (i.e., expressing both the unactivated *Neu* and TGF-α transgenes) or parental mouse strains (MMTV/unactivated *Neu* and MMTV-TGF-α). Their results suggested that ERBB2 and TGF-α may cooperate in tumorigenesis through ERBB1 and ERBB2 transactivation and not through heterodimerization. Specifically, tumor formation in these mice was associated with ERBB2 tyrosine phosphorylation and c-SRC recruitment to the complex [208]. Because amphiregulin is a ligand for the ERBB1, we suggest that a reduction amphiregulin may reduce activation of the ERBB1 resulting in a decrease in the transactivation of ERBB2. Therefore, a reduction in transgenic signaling through a reduction of amphiregulin by EPMRT would support our tumor study findings where EPMRT increased tumor latency beginning at 28 weeks and reduced overall tumor incidence.

Even though heterodimers of ERBB1/ERBB2 have not been detected in tumor-derived cells from MMTV/unactivated *Neu* mice, heterodimerization of the transgenic ERBB2 with ERBB3 may be occurring. For example, analyses of tumor-derived tissues demonstrated an elevated expression of activated ERBB2 and ERBB3 receptors, but ERBB3 did not co-immunoprecipitate with ERBB2 [209] suggesting a transient interaction. However, in another study, immunoprecipitation analysis revealed an interaction between these receptors [125]. Moreover, ERBB2/ERBB3 has a greater proliferative signal compared to other combinations of ERBB receptors [210].

Indoleamine 2, 3-dioxygenase (IDO1) is an immunoregulatory enzyme that is expressed in various cells types including fibroblasts and immune cells (e.g., macrophages, monocytes, and dendritic cells). IDO1 is induced by virus, lipopolysaccharide, cyclooxygenase 2 (COX-2) through prostaglandin E2, and interferon-γ (i.e., a pro-inflammatory cytokine) [211, 212]. IDO1 is responsible for catalyzing the rate-limiting step in the degradation of tryptophan into N-formylkynurenine. This enzyme-meditated tryptophan depletion resulted in the suppression of antigen-dependent T-cell activation, induced T-cell apoptosis, and promoted the differentiation of naïve T-cells into regulatory T-cells [213]. Therefore, increasing the activity of this enzyme impairs antigen-dependent T-cell activation; this contributes to immune tolerance by providing the tumor cells a mechanism of escape from the immune system.

In breast cancer, IDO1 is implicated in promoting tumor tolerance [214] and produces effects on the immune system [215, 216]. In patients with breast cancer, IDO1 expression is increased in the primary tumor and serum [217]. Simultaneous gene expression of *IDO1* and *FOXP3*, a marker of regulatory T-cells, is associated with sentinel lymph node metastases in breast cancer [218]. Also, over-expression of IDO1 is associated with poor prognosis in ovarian and colon cancer [212]. COX-2 activity modulates IDO1 expression levels. For example, in animal models of cancer, blockade of COX-2 resulted in down-regulation of IDO1 at tumor sites suggesting that IDO1 was downstream of COX-2[219]. Interestingly, E2 induced IDO1 expression on monocyte-derived dendritic cells (DC) obtained from multiple sclerosis patients [220]. Use of IDO1 inhibitors [1-methyl-DL-tryptophan (1MT) and methyl-thiohydantion-tryptophan (MTH-trp)] in combination with paclitaxel, brassinin (a phytoalexin), and 5-bromobrassinin induced regression of mammary tumors in MMTV/unactivated *Neu* mice [215, 221].

In our study, EPMRT significantly decreased expression of *Ido1* mRNA. Crabtree et al. 2006 reported an increase of *Ido1* mRNA expression in the presence of E2 that was suppressed by co-administration of E2 with P4 in the mammary glands of ovariectomized C57BL6 mice after 21 days of treatment. They also demonstrated that the mRNA expression was a dose-responsive marker of P4 and was independent of treatment duration [222]. Our results did not demonstrate a significant decrease of mRNA expression with EPRT suggesting our dose of P4 was not high enough to result in a suppression of the mRNA. However, the addition of melatonin to E2 plus P4 resulted in a significant reduction of mRNA expression. Interestingly, melatonin alone did not significantly alter the mRNA expression suggesting an effect of melatonin in combination with E2 plus P4. Overall, the decrease in the expression of *Ido1* mRNA may suggest a reduction of enzyme levels that will then enable T-cell activity towards tumor cells.

In summary, the influence of estrogen-containing hormone therapies on the uterus needs to be considered when developing novel hormone therapies due to the potential of estrogen-induced endometrial hyperplasia [1]. Estrogens stimulate proliferation of the uterine endometrium while P4 inhibits these effects. Even though the P4 dose used in the tumor study was not enough to prevent an increase in uterine wet weight [15], melatonin was added to increase P4 actions and/or to reduce estrogen effects. We hypothesized that nocturnal melatonin supplementation will reduce estrogenic actions in the uterus as well as increase the sensitivity of the uterus to circulating P4 thereby maximizing the beneficial effects of our novel EPMRT. The effects of melatonin may be occurring through melatonin receptor-dependent pathways because melatonin receptors are expressed in the uterus [15]. Even though we postulated that EPRT would promote uterine stimulation, we did not find any evidence of this following 30 days of exposure, which is in contrast to its long-term treatment effects observed in the tumor study. Moreover, the addition of melatonin to this therapy did not produce any uterine effects different from the Control. Interestingly, our study revealed an increase in the number of days the mice were in estrus per estrous cycle and over a 30 day period suggesting an increase in estrogen activity; however, no difference in serum E2 levels occurred between groups. Therefore, after long-term treatment, we postulate that the addition of melatonin to the combination of E2 and P4 may be reducing E2 actions in the uterus via increased PRA expression as well as by its anti-estrogenic [15] and anti-aromatase actions (See Appendix).

The novel replacement therapy containing melatonin (i.e., EPMRT) induced differentiation of the mammary ducts as indicated by an increase in tertiary side-branching. This increase in tertiary side-branching was also evident by the increased expression of *Csn1s2a* mRNA, a marker of epithelial cell differentiation. Melatonin may have induced mammary ductal differentiation through actions on MEK/ERK 1/2 or by enhancing P4 actions in the gland. The results of the real-time RT-PCR analysis revealed that EPMRT decreased the levels of mRNA of genes that are hormone-regulated and that are involved in growth promotion and tumorigenesis while at the same time increasing the expression of a gene involved in epithelial cell differentiation. The decrease in transcription of growth promoting genes coupled with an induction of genes involved in cell differentiation is hypothesized to contribute to the protective actions of EPMRT on mammary carcinogenesis.

In these mice, we hypothesize that a potential mechanism involved in tumorigenesis is due to E2 signaling through the non-classical ERα signaling pathway resulting in the activation of SRC which then activates matrix metalloproteinases (MMPs). The activation of MMPs enables cellular shedding of amphiregulin which can activate ERBB1 resulting in transactivation of the transgenic ERBB2 leading to the induction of tumorigenesis. Additionally, through the classical pathway, E2-ERα complex formation may be inducing transcription of the *Areg* gene through binding to the ERE. The subsequent enhancement of amphiregulin expression may increase ERBB1 signaling that results in transactivation of the ERBB2 leading to tumorigenesis. Furthermore, we hypothesize that E2 induces immune tolerance to tumors by increasing IDO1 expression through induction of *Ido1* gene transcription. Melatonin, added in combination with E2 plus P4, is mostly likely inhibiting the effects of E2 by blocking the binding of the E2-ERα complex to the ERE thereby blocking the aforementioned pathways from being initiated. Specifically, we suggest that melatonin in combination with E2 plus P4 blocks the activated E2-ERα-mediated cellular shedding of amphiregulin thereby inhibiting activity of amphiregulin at ERBB1; this ultimately reduces transactivation of ERBB2 leading to the reduction of tumorigenesis. Furthermore, melatonin addition may inhibit the E2-ERα complex binding to ERE located on the *Areg* gene thereby reducing gene transcription ultimately leading to a decrease in amphiregulin expression and a decrease in epithelial cell proliferation. Finally, we hypothesize that melatonin may decrease the expression of *Ido1* mRNA through inhibition of E2 actions (See Diagram 1).

Overall, these findings provide important insight into the protective actions of EPMRT on *Neu*-induced mammary cancer. Future studies will assess the role the proteins predicted to interact with amphiregulin and indoleamine 2, 3-dioxygenase may have in the protective actions of EPMRT. Therefore, the results described herein may help to explain the protective actions of EPMRT on mammary tumorigenesis and against excessive uterine proliferation in order to advance the future use of EPMRT in women experiencing menopausal symptoms while providing protective actions on the breast and the uterus.

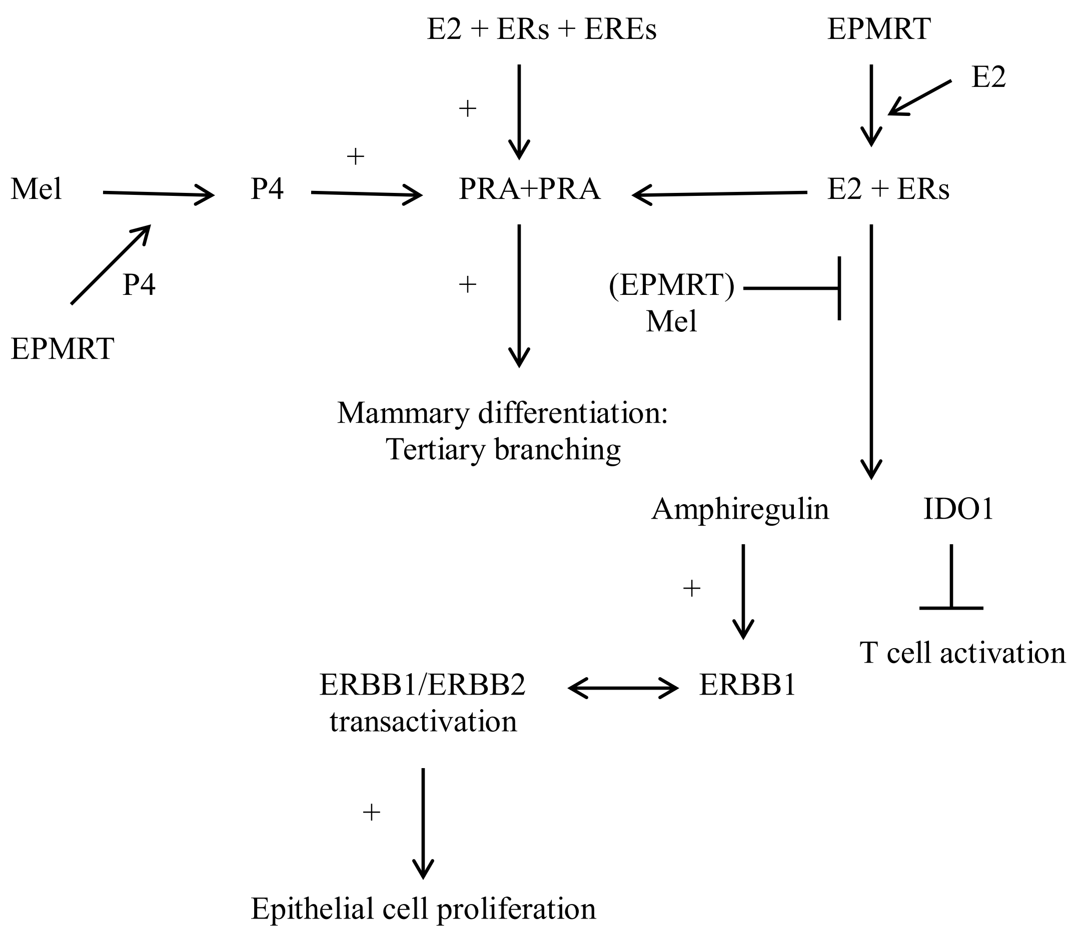

Diagram 2. Proposed actions of EPMRT with regards to its protective effects on mammary tumorigenesis.

APPENDIX

THE EFFECT OF PROGESTERONE AND MELATONIN ON OVARIAN AROMATASE mRNA EXPRESSION IN A MOUSE MODEL OF BREAST CANCER

INTRODUCTION

Aromatase

Melatonin and E2 have an inverse relationship, that is, when melatonin levels are low, E2 levels are high and when melatonin levels are high, E2 levels are low. The mechanisms underlying this relationship may be through the inhibitory effects of melatonin on the aromatase enzyme. Aromatase is a cytochrome P450 enzyme complex consisting of two components: the aromatase cytochrome P450 and a flavoprotein NADPH-cytochrome P450 reductase [223]. Aromatase is responsible for the biosynthesis of estrone (E1) and E2 from androstenedione and testosterone, respectively [224-226]. Aromatase is encoded by the *CYP19A1* gene which contains at least 10 promoters capable of being activated by different ligands in different tissues [227]. Aromatase expression, activity and mRNA expression was higher in breast cancer tissue than non-malignant breast tissue [225, 226, 228]. This increase in aromatase expression may be through an induction of mRNA expression via its promoters. For example, in MCF-7 cells as well as in adipose tissue taken from tumor-bearing breasts, aromatase expression was increased by cAMP acting on promoters I.3 and II. However, in stromal fibroblasts of adipose tissue taken from non-tumor bearing breasts, aromatase expression was low; and it is thought that this reduced expression of aromatase was due to the inhibitory actions of glucocorticoids and interleukin 6, 11 on promoter I.4 [227, 229-231]. In normal mammary tissue, the activities of 17β-hydroxysteroid dehydrogenase type 2, that converts E2 to E1, and estrone sulfotransferase, that inactivates E2 and E1, were higher than aromatase [82]; this difference in expression patterns of these enzymes is thought to reduce the E2-stimulated actions on mammary tissue.

Aromatase inhibitors

One of the strategies used to treat certain types of breast cancer is to reduce local synthesis of E2 in the breast by use of aromatase inhibitors in pre- and postmenopausal women [224]. Aromatase inhibitors are classified into steroidal and non-steroidal inhibitors. Steroidal inhibitors are androgen analogs that interfere with the substrate binding site of the enzyme while non-steroidal inhibitors inhibit the electron transfer of the cytochrome P450 group. Examples of the steroidal inhibitors are testolactone (first generation), formestane (second generation), exemestane, and atamestane (third generation). Examples of non-steroidal inhibitors are aminoglutethimide (first generation), fadrozole (second generation), anastrozole and letrozole (third generation) [225]. Aminoglutethimide is a competitive (i.e., reversible) aromatase inhibitor that binds to the heme moiety on aromatase thereby reducing activity without direct effect on mRNA expression [232].

Melatonin has been demonstrated to inhibit mRNA expression and activity of aromatase. For example, after 24 hours of incubation, melatonin at physiological (1 nM) and supraphysiological (10 μM) doses attenuated cAMP- and cortisol-induced aromatase activity [71]. Moreover, the expression of aromatase mRNA decreased following 90 minute melatonin (1 nM) incubation [71]. Melatonin, acting through MT_1 receptors which are Gi protein coupled receptors, decreases cAMP levels. This reduction of cAMP is thought to regulate negatively promoters I.3 and II to reduce mRNA expression [155] translating to tumor inhibitory actions in vivo. The reduction in tumorigenesis by inhibiting aromatase with melatonin is supported, in part, by a study in female Sprague-Dawley rats. In this study, it was demonstrated that melatonin supplementation via drinking water (500 µg/day) inhibited the growth of DMBA-induced tumors in female Sprague-Dawley rats through an inhibition of tumor aromatase activity [233].

The focus of this mini-study was to assess melatonin, EPRT, and EPMRT effects on mRNA expression of *Cyp19a1* in the ovaries of MMTV/unactivated *Neu* mice. The results of this mini-study will provide evidence that melatonin is a transcriptional inhibitor of aromatase and is an anti-estrogenic compound, in part, through its actions on expression of *Cyp19a1* mRNA.

METHODS

The expression of *Cyp19a1* mRNA was assessed in ovarian tissue taken from female mice exposed to vehicle, melatonin, and combinations of melatonin, E2, and P4 where the dose of P4 was varied (see Table 5 for all groups) by real time RT-PCR. It was hypothesized that the groups containing the lowest dose of P4 (i.e., 25 mg) would have the highest levels *Cyp19a1* mRNA, and the addition of melatonin would block these increases.

	Isoflavone-free Diet (Continuous)	Isoflavone-free Diet containing 0.5 mg E2 + 25 mg P4 (Continuous)	Isoflavone-free Diet containing 0.5 mg E2 + 50 mg P4 (Continuous)	Isoflavone-free Diet containing 0.5 mg E2 + 100 mg P4 (Continuous)
Water containing Vehicle (Night Only)	**Control**	**EP_LRT**	**EP_MRT**	**EP_HRT**
Water containing Melatonin (Night Only)	**Melatonin**	**EP_LMRT**	**EP_MMRT**	**EP_HMRT**

Table 5. Treatment groups

The treatments used to study the anti-aromatase effects of melatonin in the ovary are described in Table 5. At postnatal day 60 (i.e., two months of age), the mice began exposure to the treatment conditions. Depending on the experimental group, nocturnal melatonin supplementation (final concentration of 15 mg/L) was delivered in the drinking water during the hours of darkness. This supplementation was prepared daily by dissolving melatonin in 95% ethanol and then diluting this stock solution with water to a final concentration of 15 mg/L. Mice in the melatonin group were given melatonin in the drinking water between the hours of 18:00 to 06:00 (i.e., 6 p.m. to 6 a.m.) each day for 30 days. Each mouse is estimated to consume approximately 52.5 µg of melatonin per period of darkness based on the measured mean nightly consumption of 3.5 mL of water.

The melatonin dose is approximately equivalent to 5 mg of melatonin consumed by an adult woman per night. Mice not consuming the nocturnal melatonin supplementation were provided water containing a final ethanol concentration of 0.03% (i.e., vehicle water).

Depending on the experimental group, mice were provided a combination of 17β-estradiol (E2) and progesterone (P4) in the isoflavone-free diet. The hormones were blended into the diet by the supplier. The isoflavone-free diet containing the hormones was provided, *ad libitum,* to the EPRT and EPMRT groups beginning at postnatal day 60 and continuing until postnatal day 90, or after, until the mouse was in estrus, as confirmed by visualization of the vaginal smear. The dose of E2 (0.5 mg) or P4 925 mg, 50 mg, or 100 mg) was added to 1800 kcal of diet, the average daily caloric intake of a woman [128], to account for the metabolic differences between mice and humans. Therefore, the final daily hormonal doses consumed by the mice eating 18 kcal of diet would be 5 μg of E2 and 250 μg, 500 μg and 1000 μg of P4. Following completion of the experimental time-line, the mice were euthanized by carbon dioxide inhalation. Ovaries were collected, frozen immediately in liquid nitrogen, and stored at -80^{o}C.

Real-time RT-PCR

As conducted by Dr. Emilio Jose Sanchez-Barcelo's laboratory

Following the manufacturer's instructions, total cellular RNA from the ovaries was purified with TRI-Reagent (Sigma). Purity was determined by calculating the absorbance ratio (i.e., 260/280 nm), and all preparation were greater than 1.9. Gel electrophoresis, using ethidium bromide-stained 1.2% agarose-Tris-borate EDTA gels, was performed to determine RNA integrity. RNA was denatured at 65º C for ten minutes prior to being reverse transcribed using the cDNA Synthesis Kit (Bioline, London, UK) in the presence of 500ng of oligo(dT) 12-18 primer for 50 minutes at 45º C (total volume of 20μL). Next, QPCR was conducted (in triplicate) in three independent experiments to ensure reproducibility using Brilliant SYBR®Green PCR Master Mix (Stratagene) in an Mx3005p (Stratagene) (final volume of 25μL). Cycling parameters were 10 minutes at 95º C followed by 45 seconds at 95º C (denaturing step), then one minute at 57º C (annealing step) and finally 45 seconds at 72º C (extension step).

When designing the primers, the coding sequence between the two PCR primer sites was interrupted by at least one intron. This was done to ensure that the amplification was from cDNA and not genomic DNA. All primers were purchased from Sigma Genosys Ltd., (Cambridge, UK). Primer sequence for *Cyp19a1* (aromatase) *F*: 5'-GAAGTGCCTGCAACTACTAC - 3' and *R*: 5'- GCATGCCGATGCACTGCAGC - 3'. Ribosomal subunit 14s was used as a reference gene in order to normalize RNA expression variation. Primer sequence for *Rps14* (ribosomal protein S14) *F*: 5' – TCACTGCCCTGCACATCAAAC – 3' and *R*: 5'- TTTCTTCGAGTGCTATCAGAG – 3'. Single product amplifications were verified by performing melt curves by using dissociation curves.

Transcription efficiencies between the primers resulted in no significant differences. The change in threshold cycle (ΔCt) was calculated for each sample, and aromatase gene expression for each sample was normalized to the relative expression of *Rps14*. The fold change of expression was determined by the $2^{-\Delta\Delta Ct}$ method [132].

RESULTS

Low dose P4 increased expression of Cyp19a1 mRNA that was abolished by increasing doses of P4 and by addition of melatonin

Aromatase is an enzyme that converts androgens to estrogens, specifically testosterone to E2 and androstenedione to E1. An increase in mRNA expression may suggest an increase in the conversion of androgens to estrogens, thereby influencing the hormone environment of the mice. To determine whether or not the treatments, especially those containing P4 and melatonin, altered the expression of *Cyp19a1* mRNA, real-time RT-PCR analysis was performed on ovarian tissue. To investigate the effects of P4, we assessed the expression of *Cyp19a1* mRNA using low (25 mg), mid (50 mg), and high (100 mg) doses of P4 (each in 1800 kcal diet). Figure 20 displays a dose-dependent inhibition of *Cyp19a1*expression by P4 whereby the lowest dose of P4 (i.e., 25 mg) exhibited the highest expression of *Cyp19a1* mRNA, and this effect was attenuated by higher doses of P4 (i.e., 50 and 100 mg). The addition of melatonin to the E2 plus P4 containing the low dose P4 (25 mg) abolished the 25 mg P4-induced increase in expression of *Cyp19a1* mRNA. These data support a role for melatonin as an inhibitor of ovarian aromatase mRNA expression perhaps leading to a subsequent decrease in the synthesis of ovarian estrogens.

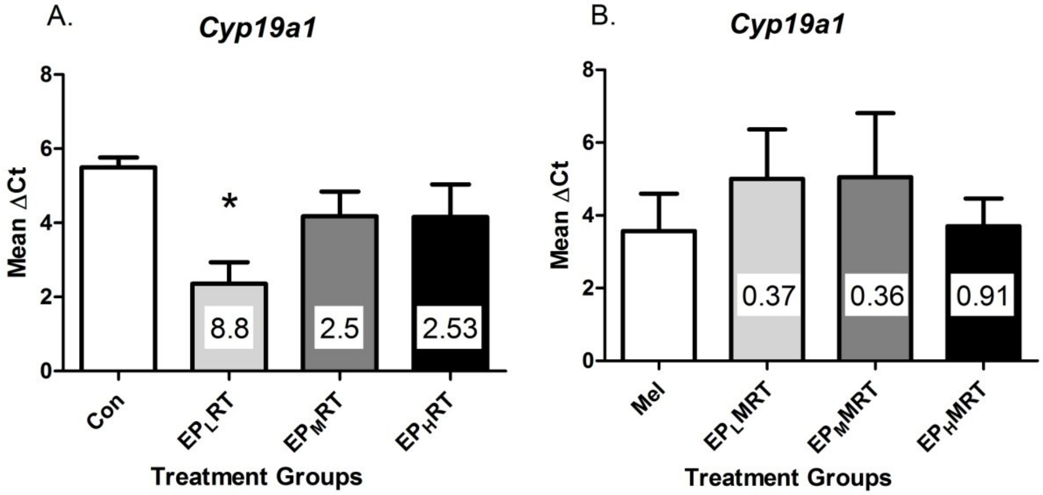

Figure 20. Dose-dependent effects of P4 on expression of *Cyp19a1* mRNA in the ovary. (A) A dose-dependent inhibition of *Cyp19a1*expression occurred with increasing doses of P4 compared to Control. (B) The addition of melatonin to the low dose P4 abolished the increase in mRNA expression. Each bar represents the mean ΔCt ± SEM values from n = 3-4 mice per treatment group. Value inside the bar represents fold change of expression as determined by the $2^{-\Delta\Delta Ct}$ method. Data were analyzed by one-way ANOVA followed by Newman-Keuls post-hoc test where significance was defined as $p < 0.05$ with (*) = $p < 0.05$ as compared to Control. Lower mean ΔCt indicates higher expression.

Abbreviations:
Con = Control; mice exposed to isoflavone-free diet and vehicle water
EP_LRT = mice exposed to 0.5mg E2 + 25mg P4 and vehicle water
EP_MRT = mice exposed to 0.5mg E2 + 50mg P4 and vehicle water
EP_HRT = mice exposed to 0.5mg E2 + 100mg P4 and vehicle water
Mel = Melatonin; mice exposed to melatonin water during the hours of darkness
EP_LMRT = mice exposed to 0.5mg E2 + 25mg P4 and melatonin water during the hours of darkness
EP_MMRT = mice exposed to 0.5mg E2 + 50mg P4 and melatonin water during the hours of darkness
EP_HMRT = mice exposed to 0.5mg E2 + 100mg P4 and melatonin water during the hours of darkness

DISCUSSION

Aromatase is responsible for the biosynthesis of E1 and E2 from androstenedione and testosterone, respectively [224-226]. Aromatase expression, activity and mRNA expression was higher in breast cancer tissue than non-malignant breast tissue [225, 226, 228]. In normal mammary tissue, the activities of the enzymes 17β-hydroxysteroid dehydrogenase type 2 and estrone sulfotransferase that convert E2 to E1 and inactivates E2 and E1, respectively, were higher than aromatase [82]. In this study, melatonin, added in combination with E2 and 25mg P4, attenuated the induction of *Cyp19a1* expression by E2 and 25 mg of P4. Melatonin has been shown in numerous studies to decrease the mRNA expression and activity of aromatase [71, 84, 232, 234]. Like melatonin, P4 is also known to inhibit aromatase mRNA expression. For example, in human-derived adipose fibroblasts, P4 (10 nM-10 μM) inhibits glucocorticoid-dependent aromatase induction via competition for the glucocorticoid receptor and not the progesterone receptor [235]; thus, the dose-dependent inhibition of expression of *Cyp19a1* mRNA by P4 may be occurring through this process in ovaries of MMTV/unactivated *Neu* mice. Because melatonin inhibits dexamethasone-induced increases in mRNA expression through promoter I.4 [227, 230, 231, 236], modulation of the promoter by melatonin to reduce gene transcription may be another possibility. Melatonin can modulate the promoters through cAMP-dependent mechanisms. Melatonin, acting through MT_1 melatonin receptors, inhibited adenylyl cyclase activity following activation of Gi protein. The resulting reduction of cAMP by melatonin may regulate negatively promoters I.3 and II to reduce aromatase expression because cAMP is an inducer of aromatase expression through promoters I.3 and II [227, 229-231] with melatonin being more potent at reducing promoter II activity [155]. Another way may be through actions of melatonin on P4 synthesis and release from the ovarian granulosa cells [103-107]. The increase in P4 induced by melatonin can inhibit the transcription of the aromatase gene through competition with glucocorticoids for binding to the glucocorticoid receptors [237]. Overall, our results suggest that melatonin in combination with E2 and P4 may attenuate both mammary epithelial cell and endometrial epithelial and stromal cell proliferation through anti-aromatase actions; reductions in estrogen and estrogen-mediated actions by melatonin may underlie the protective actions on the mammary gland and uterus.

BIBLIOGRAPHY

1. Santen, R.J., D.C. Allred, S.P. Ardoin, et al. Postmenopausal hormone therapy: an Endocrine Society scientific statement. *J Clin Endocrinol Metab*. 2010;95(7 Suppl 1):s1-s66.
2. Kotlarczyk, M.P., H.C. Lassila, C.K. O'Neil, et al. Melatonin osteoporosis prevention study (MOPS): a randomized, double-blind, placebo-controlled study examining the effects of melatonin on bone health and quality of life in perimenopausal women. *J Pineal Res*. 2012;52(4):414-26.
3. Chlebowski, R.T., G.L. Anderson, M. Gass, et al. Estrogen plus progestin and breast cancer incidence and mortality in postmenopausal women. *JAMA*. 2010;304(15):1684-92.
4. Rossouw, J.E., G.L. Anderson, R.L. Prentice, et al. Risks and benefits of estrogen plus progestin in healthy postmenopausal women: principal results From the Women's Health Initiative randomized controlled trial. *JAMA*. 2002;288(3):321-33.
5. Chlebowski, R.T., S.L. Hendrix, R.D. Langer, et al. Influence of estrogen plus progestin on breast cancer and mammography in healthy postmenopausal women: the Women's Health Initiative Randomized Trial. *JAMA*. 2003;289(24):3243-53.
6. Chlebowski, R.T. and G.L. Anderson. Changing concepts: Menopausal hormone therapy and breast cancer. *J Natl Cancer Inst*. 2012;104(7):517-27.
7. Fournier, A., F. Berrino, and F. Clavel-Chapelon. Unequal risks for breast cancer associated with different hormone replacement therapies: results from the E3N cohort study. *Breast Cancer Res Treat*. 2008;107(1):103-11.
8. Lyytinen, H., E. Pukkala, and O. Ylikorkala. Breast cancer risk in postmenopausal women using estradiol-progestogen therapy. *Obstet Gynecol*. 2009;113(1):65-73.
9. Wood, C.E., T.C. Register, C.J. Lees, et al. Effects of estradiol with micronized progesterone or medroxyprogesterone acetate on risk markers for breast cancer in postmenopausal monkeys. *Breast Cancer Res Treat*. 2007;101(2):125-34.
10. Anderson, G.L., M. Limacher, A.R. Assaf, et al. Effects of conjugated equine estrogen in postmenopausal women with hysterectomy: the Women's Health Initiative randomized controlled trial. *JAMA*. 2004;291(14):1701-12.
11. Stefanick, M.L., G.L. Anderson, K.L. Margolis, et al. Effects of conjugated equine estrogens on breast cancer and mammography screening in postmenopausal women with hysterectomy. *JAMA*. 2006;295(14):1647-57.
12. Bachmann, G.A., M. Schaefers, A. Uddin, et al. Lowest effective transdermal 17beta-estradiol dose for relief of hot flushes in postmenopausal women: a randomized controlled trial. *Obstet Gynecol*. 2007;110(4):771-9.
13. Fournier, A., A. Fabre, S. Mesrine, et al. Use of different postmenopausal hormone therapies and risk of histology- and hormone receptor-defined invasive breast cancer. *J Clin Oncol*. 2008;26(8):1260-8.
14. Fournier, A., S. Mesrine, M.C. Boutron-Ruault, et al. Estrogen-progestagen menopausal hormone therapy and breast cancer: does delay from menopause onset to treatment initiation influence risks? *J Clin Oncol*. 2009;27(31):5138-43.

15. Dodda, B.R. An evaluation of the effects of a novel estrogen, progesterone, and melatonin hormone therapy on mammary cancer development, progression and uterine protection in the mmtv-*neu* mouse model. *Dissertation*. 2013.
16. Kleinsmith L.J., K.V.M., Principles of Cellular and Molecular Biology 2nd Edition ed. 1995, New York: HarperCollins. College Publishers pp. 810.
17. NationalCancerInstitute. www.cancer.gov/cancertopics/pdq/treatment/breast/Patient. *Accessed: April 28, 2013*.
18. AmericanCancerSociety. www.cancer.org/aes/groups/cid/documents/webcontent/0030037-pdf.pdf. *Accessed: April 28, 2013*.
19. Jemal, A., R. Siegel, E. Ward, et al. Cancer statistics, 2008. *CA Cancer J Clin*. 2008;58(2):71-96.
20. National Cancer Institute http://seer.cancer.gov/statfacts/html/breast.html SEER Stat Fact Sheets: Breast.
21. Barlow, W.E., E. White, R. Ballard-Barbash, et al. Prospective breast cancer risk prediction model for women undergoing screening mammography. *J Natl Cancer Inst*. 2006;98(17):1204-14.
22. Chen, J., D. Pee, R. Ayyagari, et al. Projecting absolute invasive breast cancer risk in white women with a model that includes mammographic density. *J Natl Cancer Inst*. 2006;98(17):1215-26.
23. Davidson, N.E. Environmental estrogens and breast cancer risk. *Curr Opin Oncol*. 1998;10(5):475-8.
24. Rockhill, B., C.R. Weinberg, and B. Newman. Population attributable fraction estimation for established breast cancer risk factors: considering the issues of high prevalence and unmodifiability. *Am J Epidemiol*. 1998;147(9):826-33.
25. Bhatt, R.V. Environmental influence on reproductive health. *Int J Gynaecol Obstet*. 2000;70(1):69-75.
26. Harvey, P.W. and P. Darbre. Endocrine disrupters and human health: could oestrogenic chemicals in body care cosmetics adversely affect breast cancer incidence in women? *J Appl Toxicol*. 2004;24(3):167-76.
27. Lichtenstein, P., N.V. Holm, P.K. Verkasalo, et al. Environmental and heritable factors in the causation of cancer--analyses of cohorts of twins from Sweden, Denmark, and Finland. *N Engl J Med*. 2000;343(2):78-85.
28. Penuel, E., R.W. Akita, and M.X. Sliwkowski. Identification of a region within the ErbB2/HER2 intracellular domain that is necessary for ligand-independent association. *J Biol Chem*. 2002;277(32):28468-73.
29. Liu, E., A. Thor, M. He, et al. The HER2 (c-erbB-2) oncogene is frequently amplified in in situ carcinomas of the breast. *Oncogene*. 1992;7(5):1027-32.
30. Muss, H.B., A.D. Thor, D.A. Berry, et al. c-erbB-2 expression and response to adjuvant therapy in women with node-positive early breast cancer. *N Engl J Med*. 1994;330(18):1260-6.
31. Thor, A.D., D.A. Berry, D.R. Budman, et al. erbB-2, p53, and efficacy of adjuvant therapy in lymph node-positive breast cancer. *J Natl Cancer Inst*. 1998;90(18):1346-60.

32. Slamon, D.J., W. Godolphin, L.A. Jones, et al. Studies of the HER-2/neu proto-oncogene in human breast and ovarian cancer. *Science*. 1989;244(4905):707-12.
33. Davoli, A., B.A. Hocevar, and T.L. Brown. Progression and treatment of HER2-positive breast cancer. *Cancer Chemother Pharmacol*. 2010;65(4):611-23.
34. Bartlett, J.M., J.J. Going, E.A. Mallon, et al. Evaluating HER2 amplification and overexpression in breast cancer. *J Pathol*. 2001;195(4):422-8.
35. NCIDrugDictionary. www.cancer.gov/drugdictionary/. *Accessed: May 29, 2013*.
36. BreastCancer.org. www.breastcancer.org/treatment. *Accessed: April 28, 2013*.
37. Effects of hormone replacement therapy on endometrial histology in postmenopausal women. The Postmenopausal Estrogen/Progestin Interventions (PEPI) Trial. The Writing Group for the PEPI Trial. *JAMA*. 1996;275(5):370-5.
38. North American Menopause Society. Role of progestogen in hormone therapy for postmenaupausal women: position statement of the North American Menopause Society. *Menopause (New York, N.Y.)*. 2003; 10.2: 113-32.
39. Stampfer, M.J., G.A. Colditz, W.C. Willett, et al. Postmenopausal estrogen therapy and cardiovascular disease. Ten-year follow-up from the nurses' health study. *N Engl J Med*. 1991;325(11):756-62.
40. Nachtigall, L.E., R.H. Nachtigall, R.D. Nachtigall, et al. Estrogen replacement therapy I: a 10-year prospective study in the relationship to osteoporosis. *Obstet Gynecol*. 1979;53(3):277-81.
41. Chlebowski, R.T., G.L. Anderson, M. Gass, et al. Estrogen plus progestin and breast cancer incidence and mortality in postmenopausal women. *JAMA*. 2010;304(15):1684-92.
42. Chlebowski, R.T., L.H. Kuller, R.L. Prentice, et al. Breast cancer after use of estrogen plus progestin in postmenopausal women. *N Engl J Med*. 2009;360(6):573-87.
43. Beral, V. and C. Million Women Study. Breast cancer and hormone-replacement therapy in the Million Women Study. *Lancet*. 2003;362(9382):419-27.
44. Breast cancer and hormone replacement therapy: collaborative reanalysis of data from 51 epidemiological studies of 52,705 women with breast cancer and 108,411 women without breast cancer. Collaborative Group on Hormonal Factors in Breast Cancer. *Lancet*. 1997;350(9084):1047-59.
45. Magnusson, C., J.A. Baron, N. Correia, et al. Breast-cancer risk following long-term oestrogen- and oestrogen-progestin-replacement therapy. *Int J Cancer*. 1999;81(3):339-44.
46. Stahlberg, C., A.T. Pedersen, E. Lynge, et al. Increased risk of breast cancer following different regimens of hormone replacement therapy frequently used in Europe. *Int J Cancer*. 2004;109(5):721-7.
47. Bakken, K., E. Alsaker, A.E. Eggen, et al. Hormone replacement therapy and incidence of hormone-dependent cancers in the Norwegian Women and Cancer study. *Int J Cancer*. 2004;112(1):130-4.
48. Hersh, A.L., M.L. Stefanick, and R.S. Stafford. National use of postmenopausal hormone therapy: annual trends and response to recent evidence. *JAMA*. 2004;291(1):47-53.

49. Cogliano, V., Y. Grosse, R. Baan, et al. Carcinogenicity of combined oestrogen-progestagen contraceptives and menopausal treatment. *Lancet Oncol*. 2005;6(8):552-3.
50. Witt-Enderby, P.A., N.M. Radio, J.S. Doctor, et al. Therapeutic treatments potentially mediated by melatonin receptors: potential clinical uses in the prevention of osteoporosis, cancer and as an adjuvant therapy. *J Pineal Res*. 2006;41(4):297-305.
51. Reiter, R.J. The pineal and its hormones in the control of reproduction in mammals. *Endocr Rev*. 1980;1(2):109-31.
52. Zeitzer, J.M., J.F. Duffy, S.W. Lockley, et al. Plasma melatonin rhythms in young and older humans during sleep, sleep deprivation, and wake. *Sleep*. 2007;30(11):1437-43.
53. Berson, D.M., F.A. Dunn, and M. Takao. Phototransduction by retinal ganglion cells that set the circadian clock. *Science*. 2002;295(5557):1070-3.
54. Schomerus, C. and H.W. Korf. Mechanisms regulating melatonin synthesis in the mammalian pineal organ. *Ann N Y Acad Sci*. 2005;1057:372-83.
55. Lewy, A.J., T.A. Wehr, F.K. Goodwin, et al. Light suppresses melatonin secretion in humans. *Science*. 1980;210(4475):1267-9.
56. Morgan, P.J., P. Barrett, H.E. Howell, et al. Melatonin receptors: localization, molecular pharmacology and physiological significance. *Neurochem Int*. 1994;24(2):101-46.
57. Jarzynka, M.J., D.K. Passey, P.F. Ignatius, et al. Modulation of melatonin receptors and G-protein function by microtubules. *J Pineal Res*. 2006;41(4):324-36.
58. Radio, N.M., J.S. Doctor, and P.A. Witt-Enderby. Melatonin enhances alkaline phosphatase activity in differentiating human adult mesenchymal stem cells grown in osteogenic medium via MT2 melatonin receptors and the MEK/ERK (1/2) signaling cascade. *J Pineal Res*. 2006;40(4):332-42.
59. Bondi, C.D., R.M. McKeon, J.M. Bennett, et al. MT1 melatonin receptor internalization underlies melatonin-induced morphologic changes in Chinese hamster ovary cells and these processes are dependent on Gi proteins, MEK 1/2 and microtubule modulation. *J Pineal Res*. 2008;44(3):288-98.
60. Sethi, S., N.M. Radio, M.P. Kotlarczyk, et al. Determination of the minimal melatonin exposure required to induce osteoblast differentiation from human mesenchymal stem cells and these effects on downstream signaling pathways. *J Pineal Res*. 2010;49(3):222-38.
61. Iguichi, H., K.I. Kato, and H. Ibayashi. Age-dependent reduction in serum melatonin concentrations in healthy human subjects. *J Clin Endocrinol Metab*. 1982;55(1):27-9.
62. Micromedex2.0. http://www.micromedexsolutions.com. *Accessed: April 5, 2013*.
63. Witt-Enderby, P.A. and P.K. Li. Melatonin receptors and ligands. *Vitam Horm*. 2000;58:321-54.
64. Witt-Enderby, P.A., M.I. Masana, and M.L. Dubocovich. Physiological exposure to melatonin supersensitizes the cyclic adenosine 3',5'-monophosphate-dependent signal transduction cascade in Chinese hamster ovary cells expressing the human mt1 melatonin receptor. *Endocrinology*. 1998;139(7):3064-71.

65. Brydon, L., F. Roka, L. Petit, et al. Dual signaling of human Mel1a melatonin receptors via G(i2), G(i3), and G(q/11) proteins. *Mol Endocrinol*. 1999;13(12):2025-38.
66. Witt-Enderby, P.A., R.S. MacKenzie, R.M. McKeon, et al. Melatonin induction of filamentous structures in non-neuronal cells that is dependent on expression of the human mt1 melatonin receptor. *Cell Motil Cytoskeleton*. 2000;46(1):28-42.
67. Recio, J., D.P. Cardinali, and E.J. Sanchez-Barcelo. 2-[125I]iodomelatonin binding sites in murine mammary tissue. *Biol Signals*. 1994;3(2):85-90.
68. Li, P.-K., Witt-Enderby, P.A. Melatonin receptors as potential targets for drug discovery. *Drugs of the Future*. 2000;25(9):945-957.
69. Poeggeler, B., S. Saarela, R.J. Reiter, et al. Melatonin--a highly potent endogenous radical scavenger and electron donor: new aspects of the oxidation chemistry of this indole accessed in vitro. *Ann N Y Acad Sci*. 1994;738:419-20.
70. Karbownik, M., A. Lewinski, and R.J. Reiter. Anticarcinogenic actions of melatonin which involve antioxidative processes: comparison with other antioxidants. *Int J Biochem Cell Biol*. 2001;33(8):735-53.
71. Cos, S., C. Martinez-Campa, M.D. Mediavilla, et al. Melatonin modulates aromatase activity in MCF-7 human breast cancer cells. *J Pineal Res*. 2005;38(2):136-42.
72. Cini, G., B. Neri, A. Pacini, et al. Antiproliferative activity of melatonin by transcriptional inhibition of cyclin D1 expression: a molecular basis for melatonin-induced oncostatic effects. *J Pineal Res*. 2005;39(1):12-20.
73. Sainz, R.M., J.C. Mayo, D.X. Tan, et al. Antioxidant activity of melatonin in Chinese hamster ovarian cells: changes in cellular proliferation and differentiation. *Biochem Biophys Res Commun*. 2003;302(3):625-34.
74. Cos, S., R. Verduga, C. Fernandez-Viadero, et al. Effects of melatonin on the proliferation and differentiation of human neuroblastoma cells in culture. *Neurosci Lett*. 1996;216(2):113-6.
75. Cini, G., M. Coronnello, E. Mini, et al. Melatonin's growth-inhibitory effect on hepatoma AH 130 in the rat. *Cancer Lett*. 1998;125(1-2):51-9.
76. Mayo, J.C., R.M. Sainz, H. Uria, et al. Inhibition of cell proliferation: a mechanism likely to mediate the prevention of neuronal cell death by melatonin. *J Pineal Res*. 1998;25(1):12-8.
77. Kadekaro, A.L., L.N. Andrade, L.M. Floeter-Winter, et al. MT-1 melatonin receptor expression increases the antiproliferative effect of melatonin on S-91 murine melanoma cells. *J Pineal Res*. 2004;36(3):204-11.
78. Bordt, S.L., R.M. McKeon, P.K. Li, et al. N1E-115 mouse neuroblastoma cells express MT1 melatonin receptors and produce neurites in response to melatonin. *Biochim Biophys Acta*. 2001;1499(3):257-64.
79. Rato, A.G., J.G. Pedrero, M.A. Martinez, et al. Melatonin blocks the activation of estrogen receptor for DNA binding. *FASEB J*. 1999;13(8):857-68.
80. Hill, S.M., T. Frasch, S. Xiang, et al. Molecular mechanisms of melatonin anticancer effects. *Integr Cancer Ther*. 2009;8(4):337-46.
81. Girgert, R., V. Hanf, G. Emons, et al. Membrane-bound melatonin receptor MT1 down-regulates estrogen responsive genes in breast cancer cells. *J Pineal Res*. 2009;47(1):23-31.

82. Gonzalez, A., S. Cos, C. Martinez-Campa, et al. Selective estrogen enzyme modulator actions of melatonin in human breast cancer cells. *J Pineal Res*. 2008;45(1):86-92.
83. Jones, M.P., M.A. Melan, and P.A. Witt-Enderby. Melatonin decreases cell proliferation and transformation in a melatonin receptor-dependent manner. *Cancer Lett*. 2000;151(2):133-43.
84. Gonzalez, A., V. Alvarez-Garcia, C. Martinez-Campa, et al. Melatonin promotes differentiation of 3T3-L1 fibroblasts. *J Pineal Res*. 2012;52(1):12-20.
85. Tamarkin, L., M. Cohen, D. Roselle, et al. Melatonin inhibition and pinealectomy enhancement of 7,12-dimethylbenz(a)anthracene-induced mammary tumors in the rat. *Cancer Res*. 1981;41(11 Pt 1):4432-6.
86. Blask, D.E., S.M. Hill, K.M. Orstead, et al. Inhibitory effects of the pineal hormone melatonin and underfeeding during the promotional phase of 7,12-dimethylbenzanthracene-(DMBA)-induced mammary tumorigenesis. *J Neural Transm*. 1986;67(1-2):125-38.
87. Blask, D.E., R.T. Dauchy, and L.A. Sauer. Putting cancer to sleep at night: the neuroendocrine/circadian melatonin signal. *Endocrine*. 2005;27(2):179-88.
88. Cos, S., D. Mediavilla, C. Martinez-Campa, et al. Exposure to light-at-night increases the growth of DMBA-induced mammary adenocarcinomas in rats. *Cancer Lett*. 2006;235(2):266-71.
89. Mao, L., Q. Cheng, B. Guardiola-Lemaitre, et al. In vitro and in vivo antitumor activity of melatonin receptor agonists. *J Pineal Res*. 2010;49(3):210-21.
90. Yang, Q.H., J.N. Xu, R.K. Xu, et al. Inhibitory effects of melatonin on the growth of pituitary prolactin-secreting tumor in rats. *J Pineal Res*. 2006;40(3):230-5.
91. Cohen, M., M. Lippman, and B. Chabner. Role of pineal gland in aetiology and treatment of breast cancer. *Lancet*. 1978;2(8094):814-6.
92. Davis, S., D.K. Mirick, and R.G. Stevens. Night shift work, light at night, and risk of breast cancer. *J Natl Cancer Inst*. 2001;93(20):1557-62.
93. Hansen, J. Increased breast cancer risk among women who work predominantly at night. *Epidemiology*. 2001;12(1):74-7.
94. Schernhammer, E.S., F. Laden, F.E. Speizer, et al. Rotating night shifts and risk of breast cancer in women participating in the nurses' health study. *J Natl Cancer Inst*. 2001;93(20):1563-8.
95. Dickerman, B. and J. Liu. Does current scientific evidence support a link between light at night and breast cancer among female night-shift nurses? Review of evidence and implications for occupational and environmental health nurses. *Workplace Health Saf*. 2012;60(6):273-81; quiz 282.
96. Verkasalo, P.K., E. Pukkala, R.G. Stevens, et al. Inverse association between breast cancer incidence and degree of visual impairment in Finland. *Br J Cancer*. 1999;80(9):1459-60.
97. Coleman, M.P. and R.J. Reiter. Breast cancer, blindness and melatonin. *Eur J Cancer*. 1992;28(2-3):501-3.
98. Hahn, R.A. Profound bilateral blindness and the incidence of breast cancer. *Epidemiology*. 1991;2(3):208-10.
99. Lissoni, P., S. Barni, S. Meregalli, et al. Modulation of cancer endocrine therapy by melatonin: a phase II study of tamoxifen plus melatonin in metastatic breast

cancer patients progressing under tamoxifen alone. *Br J Cancer*. 1995;71(4):854-6.
100. Lissoni, P., A. Ardizzoia, S. Barni, et al. A randomized study of tamoxifen alone versus tamoxifen plus melatonin in estrogen receptor-negative heavily pretreated metastatic breast-cancer patients. *Oncol Rep*. 1995;2(5):871-3.
101. Seely, D., P. Wu, H. Fritz, et al. Melatonin as Adjuvant Cancer Care With and Without Chemotherapy: A Systematic Review and Meta-analysis of Randomized Trials. *Integr Cancer Ther*. 2012;11(4):293-303.
102. Webley, G.E. and F. Leidenberger. The circadian pattern of melatonin and its positive relationship with progesterone in women. *J Clin Endocrinol Metab*. 1986;63(2):323-8.
103. Webley, G.E. and M.R. Luck. Melatonin directly stimulates the secretion of progesterone by human and bovine granulosa cells in vitro. *J Reprod Fertil*. 1986;78(2):711-7.
104. Woo, M.M., C.J. Tai, S.K. Kang, et al. Direct action of melatonin in human granulosa-luteal cells. *J Clin Endocrinol Metab*. 2001;86(10):4789-97.
105. Wang, S.J., W.J. Liu, C.J. Wu, et al. Melatonin suppresses apoptosis and stimulates progesterone production by bovine granulosa cells via its receptors (MT1 and MT2). *Theriogenology*. 2012;78(7):1517-26.
106. Soares, J.M., Jr., M.J. Simoes, C.T. Oshima, et al. Pinealectomy changes rat ovarian interstitial cell morphology and decreases progesterone receptor expression. *Gynecol Endocrinol*. 2003;17(2):115-23.
107. Taketani, T., H. Tamura, A. Takasaki, et al. Protective role of melatonin in progesterone production by human luteal cells. *J Pineal Res*. 2011;51(2):207-13.
108. Cardiff, R.D., H.A. Bern, L.J. Faulkin, et al. Contributions of mouse biology to breast cancer research. *Comp Med*. 2002;52(1):12-31.
109. Taneja, P., D.P. Frazier, R.D. Kendig, et al. MMTV mouse models and the diagnostic values of MMTV-like sequences in human breast cancer. *Expert Rev Mol Diagn*. 2009;9(5):423-40.
110. Guy, C.T., M.A. Webster, M. Schaller, et al. Expression of the neu protooncogene in the mammary epithelium of transgenic mice induces metastatic disease. *Proc Natl Acad Sci U S A*. 1992;89(22):10578-82.
111. Sacco, M.G., S. Soldati, S. Indraccolo, et al. Combined antiestrogen, antiangiogenic and anti-invasion therapy inhibits primary and metastatic tumor growth in the MMTVneu model of breast cancer. *Gene Ther*. 2003;10(22):1903-9.
112. Taketo, M., A.C. Schroeder, L.E. Mobraaten, et al. FVB/N: an inbred mouse strain preferable for transgenic analyses. *Proc Natl Acad Sci U S A*. 1991;88(6):2065-9.
113. Mahler, J.F., W. Stokes, P.C. Mann, et al. Spontaneous lesions in aging FVB/N mice. *Toxicol Pathol*. 1996;24(6):710-6.
114. Rowse, G.J., S.R. Ritland, and S.J. Gendler. Genetic modulation of neu proto-oncogene-induced mammary tumorigenesis. *Cancer Res*. 1998;58(12):2675-9.
115. Lemoine, N.R., S. Staddon, C. Dickson, et al. Absence of activating transmembrane mutations in the c-erbB-2 proto-oncogene in human breast cancer. *Oncogene*. 1990;5(2):237-9.

116. Siegel, P.M., W.R. Hardy, and W.J. Muller. Mammary gland neoplasia: insights from transgenic mouse models. *Bioessays*. 2000;22(6):554-63.
117. Anisimov, V.N., I.N. Alimova, D.A. Baturin, et al. The effect of melatonin treatment regimen on mammary adenocarcinoma development in HER-2/neu transgenic mice. *Int J Cancer*. 2003;103(3):300-5.
118. Liu, B., S. Edgerton, X. Yang, et al. Low-dose dietary phytoestrogen abrogates tamoxifen-associated mammary tumor prevention. *Cancer Res*. 2005;65(3):879-86.
119. Siegel, P.M., D.L. Dankort, W.R. Hardy, et al. Novel activating mutations in the neu proto-oncogene involved in induction of mammary tumors. *Mol Cell Biol*. 1994;14(11):7068-77.
120. Siegel, P.M. and W.J. Muller. Mutations affecting conserved cysteine residues within the extracellular domain of Neu promote receptor dimerization and activation. *Proc Natl Acad Sci U S A*. 1996;93(17):8878-83.
121. Muthuswamy, S.K., P.M. Siegel, D.L. Dankort, et al. Mammary tumors expressing the neu proto-oncogene possess elevated c-Src tyrosine kinase activity. *Mol Cell Biol*. 1994;14(1):735-43.
122. Wolff, A.C., M.E. Hammond, J.N. Schwartz, et al. American Society of Clinical Oncology/College of American Pathologists guideline recommendations for human epidermal growth factor receptor 2 testing in breast cancer. *Arch Pathol Lab Med*. 2007;131(1):18-43.
123. Bershtein, L.M., I.N. Alimova, E.V. Tsyrlina, et al. Mammary tumors in HER-2/NEU mice are characterized by low content of estrogen receptors-alpha and absence of progesterone receptors. *Bull Exp Biol Med*. 2003;135(6):580-1.
124. Shyamala, G., Y.C. Chou, R.D. Cardiff, et al. Effect of c-neu/ ErbB2 expression levels on estrogen receptor alpha-dependent proliferation in mammary epithelial cells: implications for breast cancer biology. *Cancer Res*. 2006;66(21):10391-8.
125. Kim, A., B. Liu, D. Ordonez-Ercan, et al. Functional interaction between mouse erbB3 and wild-type rat c-neu in transgenic mouse mammary tumor cells. *Breast Cancer Res*. 2005;7(5):R708-18.
126. Young, C.D., E.C. Nolte, A. Lewis, et al. Activated Akt1 accelerates MMTV-c-ErbB2 mammary tumourigenesis in mice without activation of ErbB3. *Breast Cancer Res*. 2008;10(4):R70.
127. Davis, V.L., M.J. Jayo, A. Ho, et al. Black cohosh increases metastatic mammary cancer in transgenic mice expressing c-erbB2. *Cancer Res*. 2008;68(20):8377-83.
128. U.S. Department of Health and Human Services. National Health and Nutrition Examination Survey: Intake of Calories and Selected Nutrients for the United States Population, 1999-2000. 2000.
129. Caligioni, C.S. Assessing reproductive status/stages in mice. *Curr Protoc Neurosci*. 2009;Appendix 4:Appendix 4I.
130. Mettus, R.V. and S.G. Rane. Characterization of the abnormal pancreatic development, reduced growth and infertility in Cdk4 mutant mice. *Oncogene*. 2003;22(52):8413-21.
131. Gentleman, R.C., V.J. Carey, D.M. Bates, et al. Bioconductor: open software development for computational biology and bioinformatics. *Genome Biol*. 2004;5(10):R80.

132. Livak, K.J. and T.D. Schmittgen. Analysis of relative gene expression data using real-time quantitative PCR and the 2(-Delta Delta C(T)) Method. *Methods*. 2001;25(4):402-8.
133. Mediavilla, M.D., M. San Martin, and E.J. Sanchez-Barcelo. Melatonin inhibits mammary gland development in female mice. *J Pineal Res*. 1992;13(1):13-9.
134. Lyons, W.R., C.H. Li, and R.E. Johnson. The hormonal control of mammary growth and lactation. *Recent Prog Horm Res*. 1958;14:219-48; discussion 248-54.
135. Ferguson, D.J. Endocrine control of mammary glands in C3H mice. *Surgery*. 1956;39(1):30-6.
136. Bocchinfuso, W.P. and K.S. Korach. Mammary gland development and tumorigenesis in estrogen receptor knockout mice. *J Mammary Gland Biol Neoplasia*. 1997;2(4):323-34.
137. Russo, I.H. and J. Russo. Role of hormones in mammary cancer initiation and progression. *J Mammary Gland Biol Neoplasia*. 1998;3(1):49-61.
138. Shyamala, G. Roles of estrogen and progesterone in normal mammary gland development insights from progesterone receptor null mutant mice and in situ localization of receptor. *Trends Endocrinol Metab*. 1997;8(1):34-9.
139. Vonderhaar, B.K. Hormones and growth factors in mammary gland development. 1984:11-33.
140. Vonderhaar, B.K. and K. Plaut. Interdependence of hormones and growth factors in lobulo-alveolar development of the mammary gland and in tumorigenesis. *Breast Cancer: Biological and Clinical Progress*. 1992:59-80.
141. Dennis, G., Jr., B.T. Sherman, D.A. Hosack, et al. DAVID: Database for Annotation, Visualization, and Integrated Discovery. *Genome Biol*. 2003;4(5):P3.
142. Huang da, W., B.T. Sherman, and R.A. Lempicki. Systematic and integrative analysis of large gene lists using DAVID bioinformatics resources. *Nat Protoc*. 2009;4(1):44-57.
143. Franceschini, A., D. Szklarczyk, S. Frankild, et al. STRING v9.1: protein-protein interaction networks, with increased coverage and integration. *Nucleic Acids Res*. 2013;41(Database issue):D808-15.
144. Szklarczyk, D., A. Franceschini, M. Kuhn, et al. The STRING database in 2011: functional interaction networks of proteins, globally integrated and scored. *Nucleic Acids Res*. 2011;39(Database issue):D561-8.
145. Yang, X., S.M. Edgerton, S.D. Kosanke, et al. Hormonal and dietary modulation of mammary carcinogenesis in mouse mammary tumor virus-c-erbB-2 transgenic mice. *Cancer Res*. 2003;63(10):2425-33.
146. Jeruss, J.S., N.X. Liu, Y. Chung, et al. Characterization and chromosomal instability of novel derived cell lines from a wt-erbB-2 transgenic mouse model. *Carcinogenesis*. 2003;24(4):659-64.
147. Liu, B., D. Ordonez-Ercan, Z. Fan, et al. Estrogenic promotion of ErbB2 tyrosine kinase activity in mammary tumor cells requires activation of ErbB3 signaling. *Mol Cancer Res*. 2009;7(11):1882-92.
148. Aupperlee, M.D. and S.Z. Haslam. Differential hormonal regulation and function of progesterone receptor isoforms in normal adult mouse mammary gland. *Endocrinology*. 2007;148(5):2290-300.

149. Shyamala, G., W. Schneider, and D. Schott. Developmental regulation of murine mammary progesterone receptor gene expression. *Endocrinology*. 1990;126(6):2882-9.
150. Shyamala, G., W. Schneider, and M.C. Guiot. Estrogen dependent regulation of estrogen receptor gene expression in normal mammary gland and its relationship to estrogenic sensitivity. *Receptor*. 1992;2(2):121-8.
151. Mukherjee, S., S.G. Louie, M. Campbell, et al. Ductal growth is impeded in mammary glands of C-neu transgenic mice. *Oncogene*. 2000;19(52):5982-7.
152. Lu, L.J., K.E. Anderson, J.J. Grady, et al. Decreased ovarian hormones during a soya diet: implications for breast cancer prevention. *Cancer Res*. 2000;60(15):4112-21.
153. Kumar, N.B., A. Cantor, K. Allen, et al. The specific role of isoflavones on estrogen metabolism in premenopausal women. *Cancer*. 2002;94(4):1166-74.
154. Grube, B.J., E.T. Eng, Y.C. Kao, et al. White button mushroom phytochemicals inhibit aromatase activity and breast cancer cell proliferation. *J Nutr*. 2001;131(12):3288-93.
155. Martinez-Campa, C., A. Gonzalez, M.D. Mediavilla, et al. Melatonin inhibits aromatase promoter expression by regulating cyclooxygenases expression and activity in breast cancer cells. *Br J Cancer*. 2009;101(9):1613-9.
156. Parkening, T.A., T.J. Collins, and E.R. Smith. Plasma and pituitary concentrations of LH, FSH, and prolactin in aging C57BL/6 mice at various times of the estrous cycle. *Neurobiol Aging*. 1982;3(1):31-5.
157. Walmer, D.K., M.A. Wrona, C.L. Hughes, et al. Lactoferrin expression in the mouse reproductive tract during the natural estrous cycle: correlation with circulating estradiol and progesterone. *Endocrinology*. 1992;131(3):1458-66.
158. Tamarkin, L., C.J. Baird, and O.F. Almeida. Melatonin: a coordinating signal for mammalian reproduction? *Science*. 1985;227(4688):714-20.
159. Hernandez, X., L. Bodin, D. Chesneau, et al. Relationship between MT1 melatonin receptor gene polymorphism and seasonal physiological responses in Ile-de-France ewes. *Reprod Nutr Dev*. 2005;45(2):151-62.
160. Gimenez, F., M.C. Stornelli, C.M. Tittarelli, et al. Suppression of estrus in cats with melatonin implants. *Theriogenology*. 2009;72(4):493-9.
161. Silman, R.E. Melatonin: a contraceptive for the nineties. *Eur J Obstet Gynecol Reprod Biol*. 1993;49(1-2):3-9.
162. Grunt, T.W., M. Saceda, M.B. Martin, et al. Bidirectional interactions between the estrogen receptor and the cerbB-2 signaling pathways: heregulin inhibits estrogenic effects in breast cancer cells. *Int J Cancer*. 1995;63(4):560-7.
163. Read, L.D., D. Keith, Jr., D.J. Slamon, et al. Hormonal modulation of HER-2/neu protooncogene messenger ribonucleic acid and p185 protein expression in human breast cancer cell lines. *Cancer Res*. 1990;50(13):3947-51.
164. Keshamouni, V.G., R.R. Mattingly, and K.B. Reddy. Mechanism of 17-beta-estradiol-induced Erk1/2 activation in breast cancer cells. A role for HER2 AND PKC-delta. *J Biol Chem*. 2002;277(25):22558-65.
165. DiAugustine, R.P., P. Petrusz, G.I. Bell, et al. Influence of estrogens on mouse uterine epidermal growth factor precursor protein and messenger ribonucleic acid. *Endocrinology*. 1988;122(6):2355-63.

166. Britton, D.J., I.R. Hutcheson, J.M. Knowlden, et al. Bidirectional cross talk between ERalpha and EGFR signalling pathways regulates tamoxifen-resistant growth. *Breast Cancer Res Treat*. 2006;96(2):131-46.
167. Mukku, V.R. and G.M. Stancel. Regulation of epidermal growth factor receptor by estrogen. *J Biol Chem*. 1985;260(17):9820-4.
168. Nandi, S., R.C. Guzman, and J. Yang. Hormones and mammary carcinogenesis in mice, rats, and humans: a unifying hypothesis. *Proc Natl Acad Sci U S A*. 1995;92(9):3650-7.
169. Preston-Martin, S., M.C. Pike, R.K. Ross, et al. Increased cell division as a cause of human cancer. *Cancer Res*. 1990;50(23):7415-21.
170. Ethier, S.P. Growth factor synthesis and human breast cancer progression. *J Natl Cancer Inst*. 1995;87(13):964-73.
171. Fishman, J., M.P. Osborne, and N.T. Telang. The role of estrogen in mammary carcinogenesis. *Ann N Y Acad Sci*. 1995;768:91-100.
172. Cavalieri, E.L., D.E. Stack, P.D. Devanesan, et al. Molecular origin of cancer: catechol estrogen-3,4-quinones as endogenous tumor initiators. *Proc Natl Acad Sci U S A*. 1997;94(20):10937-42.
173. Snedeker, S.M., C.F. Brown, and R.P. DiAugustine. Expression and functional properties of transforming growth factor alpha and epidermal growth factor during mouse mammary gland ductal morphogenesis. *Proc Natl Acad Sci U S A*. 1991;88(1):276-80.
174. Voldborg, B.R., L. Damstrup, M. Spang-Thomsen, et al. Epidermal growth factor receptor (EGFR) and EGFR mutations, function and possible role in clinical trials. *Ann Oncol*. 1997;8(12):1197-206.
175. Olayioye, M.A., R.M. Neve, H.A. Lane, et al. The ErbB signaling network: receptor heterodimerization in development and cancer. *EMBO J*. 2000;19(13):3159-67.
176. Riese, D.J., 2nd and D.F. Stern. Specificity within the EGF family/ErbB receptor family signaling network. *Bioessays*. 1998;20(1):41-8.
177. Salomon, D.S., R. Brandt, F. Ciardiello, et al. Epidermal growth factor-related peptides and their receptors in human malignancies. *Crit Rev Oncol Hematol*. 1995;19(3):183-232.
178. Salomon, D.S., N. Normanno, F. Ciardiello, et al. The role of amphiregulin in breast cancer. *Breast Cancer Res Treat*. 1995;33(2):103-14.
179. Luetteke, N.C., T.H. Qiu, S.E. Fenton, et al. Targeted inactivation of the EGF and amphiregulin genes reveals distinct roles for EGF receptor ligands in mouse mammary gland development. *Development*. 1999;126(12):2739-50.
180. Sanderson, M.P., P.J. Dempsey, and A.J. Dunbar. Control of ErbB signaling through metalloprotease mediated ectodomain shedding of EGF-like factors. *Growth Factors*. 2006;24(2):121-36.
181. Wilson, C.L., A.H. Sims, A. Howell, et al. Effects of oestrogen on gene expression in epithelium and stroma of normal human breast tissue. *Endocr Relat Cancer*. 2006;13(2):617-28.
182. D'Cruz, C.M., S.E. Moody, S.R. Master, et al. Persistent parity-induced changes in growth factors, TGF-beta3, and differentiation in the rodent mammary gland. *Mol Endocrinol*. 2002;16(9):2034-51.

183. Blakely, C.M., A.J. Stoddard, G.K. Belka, et al. Hormone-induced protection against mammary tumorigenesis is conserved in multiple rat strains and identifies a core gene expression signature induced by pregnancy. *Cancer Res*. 2006;66(12):6421-31.
184. Harris, J.R., M.E. Lippman, U. Veronesi, et al. Breast cancer (2). *N Engl J Med*. 1992;327(6):390-8.
185. Panico, L., A. D'Antonio, G. Salvatore, et al. Differential immunohistochemical detection of transforming growth factor alpha, amphiregulin and CRIPTO in human normal and malignant breast tissues. *Int J Cancer*. 1996;65(1):51-6.
186. LeJeune, S., R. Leek, E. Horak, et al. Amphiregulin, epidermal growth factor receptor, and estrogen receptor expression in human primary breast cancer. *Cancer Res*. 1993;53(15):3597-602.
187. Nasser, S.M. Columnar cell lesions: current classification and controversies. *Semin Diagn Pathol*. 2004;21(1):18-24.
188. Lee, S., S.K. Mohsin, S. Mao, et al. Hormones, receptors, and growth in hyperplastic enlarged lobular units: early potential precursors of breast cancer. *Breast Cancer Res*. 2006;8(1):R6.
189. Lee, S., D. Medina, A. Tsimelzon, et al. Alterations of gene expression in the development of early hyperplastic precursors of breast cancer. *Am J Pathol*. 2007;171(1):252-62.
190. Kenney, N.J., G.H. Smith, I.G. Maroulakou, et al. Detection of amphiregulin and Cripto-1 in mammary tumors from transgenic mice. *Mol Carcinog*. 1996;15(1):44-56.
191. Lydon, J.P., F.J. DeMayo, O.M. Conneely, et al. Reproductive phenotpes of the progesterone receptor null mutant mouse. *J Steroid Biochem Mol Biol*. 1996;56(1-6 Spec No):67-77.
192. Shyamala, G., X. Yang, G. Silberstein, et al. Transgenic mice carrying an imbalance in the native ratio of A to B forms of progesterone receptor exhibit developmental abnormalities in mammary glands. *Proc Natl Acad Sci U S A*. 1998;95(2):696-701.
193. Santos, S.J., S.Z. Haslam, and S.E. Conrad. Signal transducer and activator of transcription 5a mediates mammary ductal branching and proliferation in the nulliparous mouse. *Endocrinology*. 2010;151(6):2876-85.
194. Xiang, S., L. Mao, L. Yuan, et al. Impaired mouse mammary gland growth and development is mediated by melatonin and its MT1 G protein-coupled receptor via repression of ERalpha, Akt1, and Stat5. *J Pineal Res*. 2012;53(3):307-318.
195. Witt-Enderby, P.A., J.P. Slater, N.A. Johnson, et al. Effects on bone by the light/dark cycle and chronic treatment with melatonin and/or hormone replacement therapy in intact female mice. *J Pineal Res*. 2012;53(4):374-84.
196. Haslam, S.Z. and G. Shyamala. Relative distribution of estrogen and progesterone receptors among the epithelial, adipose, and connective tissue components of the normal mammary gland. *Endocrinology*. 1981;108(3):825-30.
197. Haslam, S.Z. and M.L. Levely. Estrogen responsiveness of normal mouse mammary cells in primary cell culture: association of mammary fibroblasts with estrogenic regulation of progesterone receptors. *Endocrinology*. 1985;116(5):1835-44.

198. Turgeon, J.L., S.M. Van Patten, G. Shyamala, et al. Steroid regulation of progesterone receptor expression in cultured rat gonadotropes. *Endocrinology*. 1999;140(5):2318-25.
199. Preston-Martin, S., M.C. Pike, R.K. Ross, et al. Epidemiologic evidence for the increased cell proliferation model of carcinogenesis. *Environ Health Perspect*. 1993;101 Suppl 5:137-8.
200. Henderson, B.E. and H.S. Feigelson. Hormonal carcinogenesis. *Carcinogenesis*. 2000;21(3):427-33.
201. Otten, A.D., M.M. Sanders, and G.S. McKnight. The MMTV LTR promoter is induced by progesterone and dihydrotestosterone but not by estrogen. *Mol Endocrinol*. 1988;2(2):143-7.
202. Chalepakis, G., J. Arnemann, E. Slater, et al. Differential gene activation by glucocorticoids and progestins through the hormone regulatory element of mouse mammary tumor virus. *Cell*. 1988;53(3):371-82.
203. Darbre, P., C. Dickson, G. Peters, et al. Androgen regulation of cell proliferation and expression of viral sequences in mouse mammary tumour cells. *Nature*. 1983;303(5916):431-3.
204. Haraguchi, S., R.A. Good, R.W. Engelman, et al. Human prolactin regulates transfected MMTV LTR-directed gene expression in a human breast-carcinoma cell line through synergistic interaction with steroid hormones. *Int J Cancer*. 1992;52(6):928-33.
205. Parker, M.G., P. Webb, M. Needham, et al. Identification of androgen response elements in mouse mammary tumour virus and the rat prostate C3 gene. *J Cell Biochem*. 1987;35(4):285-92.
206. Vicent, G.P., R. Zaurin, C. Ballare, et al. Erk signaling and chromatin remodeling in MMTV promoter activation by progestins. *Nucl Recept Signal*. 2009;7:e008.
207. Baturin, D.A., I.N. Alimova, V.N. Anisimov, et al. The effect of light regimen and melatonin on the development of spontaneous mammary tumors in HER-2/neu transgenic mice is related to a downregulation of HER-2/neu gene expression. *Neuro Endocrinol Lett*. 2001;22(6):441-7.
208. Muller, W.J., C.L. Arteaga, S.K. Muthuswamy, et al. Synergistic interaction of the Neu proto-oncogene product and transforming growth factor alpha in the mammary epithelium of transgenic mice. *Mol Cell Biol*. 1996;16(10):5726-36.
209. Siegel, P.M., E.D. Ryan, R.D. Cardiff, et al. Elevated expression of activated forms of Neu/ErbB-2 and ErbB-3 are involved in the induction of mammary tumors in transgenic mice: implications for human breast cancer. *EMBO J*. 1999;18(8):2149-64.
210. Tzahar, E., H. Waterman, X. Chen, et al. A hierarchical network of interreceptor interactions determines signal transduction by Neu differentiation factor/neuregulin and epidermal growth factor. *Mol Cell Biol*. 1996;16(10):5276-87.
211. Maiwald, S., R. Wehner, M. Schmitz, et al. IDO1 and IDO2 gene expression analysis by quantitative polymerase chain reaction. *Tissue Antigens*. 2011;77(2):136-42.
212. Katz, J.B., A.J. Muller, and G.C. Prendergast. Indoleamine 2,3-dioxygenase in T-cell tolerance and tumoral immune escape. *Immunol Rev*. 2008;222:206-21.

213. Liu, X., R.C. Newton, S.M. Friedman, et al. Indoleamine 2,3-dioxygenase, an emerging target for anti-cancer therapy. *Curr Cancer Drug Targets*. 2009;9(8):938-52.
214. Friberg, M., R. Jennings, M. Alsarraj, et al. Indoleamine 2,3-dioxygenase contributes to tumor cell evasion of T cell-mediated rejection. *Int J Cancer*. 2002;101(2):151-5.
215. Muller, A.J., J.B. DuHadaway, P.S. Donover, et al. Inhibition of indoleamine 2,3-dioxygenase, an immunoregulatory target of the cancer suppression gene Bin1, potentiates cancer chemotherapy. *Nat Med*. 2005;11(3):312-9.
216. Travers, M.T., I.F. Gow, M.C. Barber, et al. Indoleamine 2,3-dioxygenase activity and L-tryptophan transport in human breast cancer cells. *Biochim Biophys Acta*. 2004;1661(1):106-12.
217. Sakurai, K., S. Amano, K. Enomoto, et al. [Study of indoleamine 2,3-dioxygenase expression in patients with breast cancer]. *Gan To Kagaku Ryoho*. 2005;32(11):1546-9.
218. Mansfield, A.S., P.S. Heikkila, A.T. Vaara, et al. Simultaneous Foxp3 and IDO expression is associated with sentinel lymph node metastases in breast cancer. *BMC Cancer*. 2009;9:231.
219. Cesario, A., B. Rocca, and S. Rutella. The interplay between indoleamine 2,3-dioxygenase 1 (IDO1) and cyclooxygenase (COX)-2 in chronic inflammation and cancer. *Curr Med Chem*. 2011;18(15):2263-71.
220. Zhu, W.H., C.Z. Lu, Y.M. Huang, et al. A putative mechanism on remission of multiple sclerosis during pregnancy: estrogen-induced indoleamine 2,3-dioxygenase by dendritic cells. *Mult Scler*. 2007;13(1):33-40.
221. Banerjee, T., J.B. Duhadaway, P. Gaspari, et al. A key in vivo antitumor mechanism of action of natural product-based brassinins is inhibition of indoleamine 2,3-dioxygenase. *Oncogene*. 2008;27(20):2851-7.
222. Crabtree, J.S., X. Zhang, B.J. Peano, et al. Development of a mouse model of mammary gland versus uterus tissue selectivity using estrogen- and progesterone-regulated gene markers. *J Steroid Biochem Mol Biol*. 2006;101(1):11-21.
223. Conley, A. and M. Hinshelwood. Mammalian aromatases. *Reproduction*. 2001;121(5):685-95.
224. Lonning, P.E., M. Dowsett, and T.J. Powles. Postmenopausal estrogen synthesis and metabolism: alterations caused by aromatase inhibitors used for the treatment of breast cancer. *J Steroid Biochem*. 1990;35(3-4):355-66.
225. Suzuki, T., Y. Miki, N. Ohuchi, et al. Intratumoral estrogen production in breast carcinoma: significance of aromatase. *Breast Cancer*. 2008;15(4):270-7.
226. Simpson, E., G. Rubin, C. Clyne, et al. Local estrogen biosynthesis in males and females. *Endocr Relat Cancer*. 1999;6(2):131-7.
227. Bulun, S.E., S. Sebastian, K. Takayama, et al. The human CYP19 (aromatase P450) gene: update on physiologic roles and genomic organization of promoters. *J Steroid Biochem Mol Biol*. 2003;86(3-5):219-24.
228. Bulun, S.E., K. Zeitoun, H. Sasano, et al. Aromatase in aging women. *Semin Reprod Endocrinol*. 1999;17(4):349-58.
229. Harada, N. Aberrant expression of aromatase in breast cancer tissues. *J Steroid Biochem Mol Biol*. 1997;61(3-6):175-84.

230. Zhou, D., P. Clarke, J. Wang, et al. Identification of a promoter that controls aromatase expression in human breast cancer and adipose stromal cells. *J Biol Chem*. 1996;271(25):15194-202.
231. Michael, M.D., L.F. Michael, and E.R. Simpson. A CRE-like sequence that binds CREB and contributes to cAMP-dependent regulation of the proximal promoter of the human aromatase P450 (CYP19) gene. *Mol Cell Endocrinol*. 1997;134(2):147-56.
232. Martinez-Campa, C., A. Gonzalez, M.D. Mediavilla, et al. Melatonin enhances the inhibitory effect of aminoglutethimide on aromatase activity in MCF-7 human breast cancer cells. *Breast Cancer Res Treat*. 2005;94(3):249-54.
233. Cos, S., A. Gonzalez, A. Guezmes, et al. Melatonin inhibits the growth of DMBA-induced mammary tumors by decreasing the local biosynthesis of estrogens through the modulation of aromatase activity. *Int J Cancer*. 2006;118(2):274-8.
234. Ryde, C.M., J.E. Nicholls, and M. Dowsett. Steroid and growth factor modulation of aromatase activity in MCF7 and T47D breast carcinoma cell lines. *Cancer Res*. 1992;52(6):1411-5.
235. Schmidt, M., C. Renner, and G. Loffler. Progesterone inhibits glucocorticoid-dependent aromatase induction in human adipose fibroblasts. *J Endocrinol*. 1998;158(3):401-7.
236. Kiefer, T.L., L. Lai, L. Yuan, et al. Differential regulation of estrogen receptor alpha, glucocorticoid receptor and retinoic acid receptor alpha transcriptional activity by melatonin is mediated via different G proteins. *J Pineal Res*. 2005;38(4):231-9.
237. Stocco, C. Aromatase expression in the ovary: hormonal and molecular regulation. *Steroids*. 2008;73(5):473-87.